INVESTIGATION OF THE POTENTIALITIES OF PHOTOCHEMICAL LASER SYSTEMS

PART 1 — SURVEY AND ANALYSIS

FINAL REPORT
CONTRACT NO. NAS 12-94

1 February 1966 through 31 January 1967

by

C. R. Giuliano, L. D. Hess, and J. D. Margerum

Hughes Research Laboratories
Malibu, California

prepared for

National Aeronautics and Space Administration
Electronic Research Center
Cambridge, Massachusetts

INVESTIGATION OF THE POTENTIALITIES OF PHOTOCHEMICAL LASER SYSTEMS

PART 1 — SURVEY AND ANALYSIS

by

C. R. Giuliano, L. D. Hess, and J. D. Margerum

TABLE OF CONTENTS

PART 1 — SURVEY AND ANALYSIS

TABLE OF CONTENTS

PART 2 – PRELIMINARY EXPERIMENTAL STUDIES

LIST OF ILLUSTRATIONS

PART 1 — SURVEY AND ANALYSIS

LIST OF ILLUSTRATIONS

PART 2 — PRELIMINARY EXPERIMENTAL STUDIES

LIST OF TABLES

PART 1 — SURVEY AND ANALYSIS

PART 2 — PRELIMINARY EXPERIMENTAL STUDIES

ABSTRACT

Photodissociative laser systems are proposed and evaluated with regard to their potential for conversion of solar radiation to monochromatic coherent emission. Spectroscopic and photochemical properties of several molecules which absorb light in the visible and near ultraviolet regions are reported, discussed, and compared with requirements for obtaining laser action. Additional mechanisms for achieving population inversions in these systems indirectly, such as Franck-Condon pumping and association processes stabilized by stimulated emission, are also discussed. Preliminary experimental studies are reported for methyl iodide and bromide, iodo- and bromocyanogen, iodine bromide, and nitrogen dioxide. Laser action was observed under a variety of experimental conditions from CF_3I and NOCl, but could not be detected in the initial studies conducted with other compounds. Chemical reversibility was demonstrated for the nitrosyl chloride system using mixtures of molecular chlorine and nitrosyl chloride.

SECTION I

INTRODUCTION AND SUMMARY

The objective of this study is to investigate the potentiality of photochemical systems for the conversion of solar radiation to coherent stimulated emission.

Prior to the initiation of this study, one photochemical gas laser with exceptionally high gain and peak powers of about 1 kW had been reported,[1,2] and it was predicted[3] that laser peak powers up to 100 kW would be attainable from alkyl iodide systems. These powers have been achieved, and the general potentialities of photochemical lasers as high gain, high power, sources of coherent radiation are presently under investigation in several laboratories. Photodissociative reactions producing molecular fragments in excited states are particularly interesting molecular laser sources. The development of photochemical systems for direct conversion of solar radiation to monochromatic coherent light may have distinct advantages over other methods because of their simplicity, broad band absorption, high gain, and power output. This is the basic motivation for our survey and analysis of photochemical processes as possible systems for solar pumped lasers.

A wide range of gas phase photochemical reactions and molecular excitation processes are reviewed as potential laser sources. However, special attention is given to reversible photochemical reactions which are initiated by the absorption of light in the visible and near ultraviolet spectral regions. Utilization of spontaneously reversible reactions would allow repeated use of the same material, thus reducing both storage requirements and problems of reaction product disposal. In general, photochemical reactions occur as a result of electronic transitions which are induced by visible or ultraviolet light. The wavelength distribution of solar radiation limits the photochemical reactions which can be considered for the efficient conversion of solar energy to those

which can be initiated by light in the 3000 to 8000 Å region. About 57% of the incident solar energy above the earth's atmosphere is distributed over these wavelengths; only 1% of the incident solar energy is in the active photochemical region below 3000 Å, while the 42% which falls above 8000 Å is not effective in the direct excitation of photochemical reactions.

General gain equations for photochemical lasers are presented and discussed in terms of optical pumping of materials, particularly those which photodissociate to produce excited state species. Both electronically and vibrationally excited species from photodissociative chemical reactions are potential laser sources; previous evidence for photochemical reactions of each type is reviewed. Several other types of possible excitation mechanisms for solar pumped molecular lasers are also considered and analyzed. One category is that of association processes which can be stabilized by emission. This includes the possibility of utilizing photochemical reactions in which the rate of recombination of products is enhanced by stimulated emission (i.e., radiative transitions giving vibrational deactivation of the recombination product). Population inversion of molecular vibrational states might also be achieved by Franck-Condon pumping. This type of excitation process is reviewed as a potential mechanism for optical pumping of molecular lasers. Chemical reactions are also considered as laser sources, particularly reactions resulting from solar initiated photochemical processes. Several possibilities for photochemically pumping a carbon dioxide laser are suggested.

Absorption spectra and potential energy diagrams are given and discussed for many photochemically active gaseous molecules which absorb in the solar region, (e.g., halogens, interhalogens, alkyl halides, nitrosyl halides, halogen oxides, nitrogen oxides, and many other compounds). The photochemical mechanisms and reaction kinetics of the products are reviewed in detail for the more interesting laser possibilities (e.g., nitrosyl chloride, iodine monochloride,

nitrogen dioxide, and studies on the deactivation of excited iodine atoms). Calculations are made of the solar pumping rates expected for the activation of excited species from these various photodissociative processes. Comparison with the lifetime of these species is made in order to estimate the approximate population of active species which might be expected with direct solar pumping. The most favorable estimates for solar pumped active species are obtained with iodine monochloride, nitrosyl chloride, chlorine monoxide, iodine monobromide, and nitrogen dioxide.

Although this investigation is primarily a review and analysis of literature data, a flash photolysis apparatus was built for preliminary studies of photochemical laser systems. Many of the most critical data are not available on actual or natural radiative lifetimes and collisional quenching rates of excited species. Operationally, the key factors are whether a particular photochemical system can produce laser action from intense pulsed optical excitation and whether critical parameters can be adjusted to produce oscillation from solar pumping. The apparatus described here answers the first of these questions for a variety of experimental conditions which can be used as an approximate basis for evaluation of solar operation. Photochemical laser results obtained with this apparatus are described for electronically excited iodine atoms (1.3 μ) obtained from the flash photolysis of trifluoromethyliodide and for vibrationally excited nitric oxide molecules (6 μ) from the photolysis of nitrosyl chloride (see Part 2 for details).

SECTION II

EXCITATION MECHANISMS

A. ELECTRONICALLY EXCITED PHOTODISSOCIATIVE SPECIES

Photodissociative reactions of the general type $AB + h\nu \rightarrow A^* + B$ are quite advantageous as possible photochemical laser sources, and it is primarily this type of reaction that is considered in this study. Many photochemical investigations have been carried out with radiation of shorter wavelength than is energetically necessary to achieve a particular chemical change. In some instances, this has been intentional; however, it has often been a case of experimental convenience with regard to the availability of light sources. The magnitude of this excess energy, the form in which it is carried and transferred by the primary fragments, and the special chemical properties it may confer on them are related to the attainment of the population inversion necessary to achieve laser action from a photochemical system.

Cases where atoms and diatomic or triatomic radicals are produced in electronically excited states have been known for many years.[4-7] These include halogen atoms from inorganic halides; the OH radical from water, methyl and ethyl alcohols, and formic and acetic acids; the CN radical from methyl cyanide, cyanogen, bromocyanogen, and iodocyanogen; the NH_2 radical from ammonia and hydrazine; and the NO molecule from nitrous oxide. In all these examples the parent compound was photolyzed with radiation in the Schumann ultraviolet region and the products were observed by their fluorescence emission. Under certain conditions, emission from the second vibrational level of the upper electronic state of OH ($A^2\Sigma^+$) and from the second and third levels of CN($B^2\Sigma^+$) was observed; the

bands also show high rotational temperatures. The prediction by Porret and Goodeve[8] in 1938 of electronically excited iodine atoms from irradiation of alkyl iodides in the 2500 Å region was first demonstrated when Kasper and Pimentel[1] observed laser action at 1.3 μ, which coincides with the allowed atomic transition ($^2P_{1/2} \rightarrow {}^2P_{3/2}$) for iodine.

$$CH_3I + h\nu \rightarrow CH_3\cdot + I\cdot\,(^2P_{1/2})$$

$$I\cdot\,(^2P_{1/2}) \rightarrow I\cdot\,(^2P_{3/2}) + h\nu'$$

The characteristics of this first photochemical laser have also been studied by other groups[9-11] and in our laboratory. The results of these studies are given in the photochemical and experimental sections of this report.

B. VIBRATIONALLY EXCITED PHOTODISSOCIATIVE SPECIES

Photochemical reactions which give vibrationally excited species have advantages similar to those discussed for electronically excited species, except that the stimulated emission usually occurs over a range of frequencies corresponding to a number of different vibrational-rotational transitions, each having a different characteristic gain. As early as 1932, Franck, et al., considered that it was theoretically possible that part of the excess excitation energy could appear in vibrational and rotational modes.[12] The exceptional reactivity of SO produced by photolysis of SO_2 was attributed to the presence of excess vibrational energy.[13] Unusual chemical reactivity of the methyl radical obtained from irradiation of methyl iodide[14, 15] and the methylene radical produced from diazomethane photolysis[16] has been observed recently and interpreted as vibrational excitation in these fragments.

Direct evidence for the presence of excess vibrational energy in photolysis products has been obtained from flash photolysis studies by Herzberg,[17] Basco and Norrish,[18] and Callear and Norrish,[19] although in one instance[19] the excitation of the fragment may have arisen directly from the flash. The distribution of the excess energy between the various possible modes is uncertain but it is clear that when the photon energy is much greater than the dissociation energy, as in the cases cited above, a large portion can appear in the form of vibrational energy. Molecules which can be dissociated by light in the visible region may be expected to yield vibrationally excited fragments when decomposed by irradiation in the near ultraviolet region. In favorable circumstances, dissociation in the visible may yield an electronically excited atom; irradiation in the near ultraviolet may give both an excited atom and a vibrationally excited molecular fragment.

Since this project began, a laser has been reported which utilizes vibrationally excited fragments produced by photodissociation. The photolysis of nitrosyl chloride[20] to give stimulated emission from vibrational-rotational transitions of nitric oxide is of particular interest to this study because NOCl absorbs strongly in the solar region and because the photolysis products react spontaneously to reform the starting material.

$$NOCl + h\nu \rightarrow NO^{*} + Cl$$

$$NO^{*} \rightarrow NO + h\nu'$$

$$Cl + NOCl \rightarrow Cl_2 + NO$$

$$2NO + Cl_2 \rightarrow 2\ NOCl$$

This was one of the photochemical reactions for which we had predicted laser action. Pollack's results[20] and our own experimental studies on nitrosyl chloride are discussed in subsequent sections.

C. LASER GAIN EQUATIONS

In order for a resonant cavity to sustain oscillation, the gain g of the active material must be larger than reflection and scattering losses. Gain is defined as the ratio of the number of photons leaving the active material to the number incident upon it and is related to transition probabilities in the following way.

$$g = e^{\sigma(\nu)[(m_1/m_2) N_2 - N_1] L} \tag{1a}$$

where

$\sigma(\nu)$ ≡ absorption cross section, cm^2

N_2, N_1 ≡ population density of upper and lower laser levels, cm^{-3}

m_2, m_1 ≡ degeneracies of upper and lower laser levels

L ≡ length of active material, cm.

Equation (1a) determines the single pass gain g. The total amplification obtained from multiple passes through the cavity is given by

$$G = R^n e^{n\alpha(\nu)L} \tag{1b}$$

where

R ≡ reflectivity of the mirrors

n ≡ number of passes

$\alpha(\nu)$ ≡ absorption coefficient, cm^{-1}, i. e.,

$$\alpha(\nu) = \sigma(\nu)\left(\frac{m_1}{m_2} N_2 - N_1\right) \quad .$$

Laser action occurs when the product of g and the reflection coefficient R exceeds unity.

$$R e^{\sigma(\nu)[(m_1/m_2)N_2 - N_1]L} > 1 \tag{2}$$

$$e^{\sigma(\nu)[(m_1/m_2)N_2 - N_1]L} > (1/R) \tag{3}$$

$$\sigma(\nu)\left(\frac{m_1}{m_2} N_2 - N_1\right) L > \ln(1/R) \tag{4}$$

For an atomic transition,

$$\sigma(\nu) = \frac{\lambda_o^2}{8\pi \tau_{21}} f(\nu) \tag{5}$$

where

$\lambda_o \equiv$ mean wavelength of the laser transition

$\tau_{21} \equiv$ natural lifetime of the upper level

$f(\nu) \equiv$ line shape function normalized so that

$$\int_{-\infty}^{\infty} f(\nu)\, d\nu = 1 \quad .$$

For a Lorenztian line shape,

$$\sigma(\nu) \cong \frac{\lambda_o^2}{4\pi^2 \tau_{21} \Delta\nu_L} \tag{6}$$

where $\Delta\nu_L \equiv$ line width at one-half absorption. Thus, the condition for laser action is expressed by

$$\frac{\lambda_o^2}{4\pi^2 \tau_{21} \Delta\nu_L} \frac{L}{\ln(1/R)} \left(\frac{m_1}{m_2} N_2 - N_1\right) > 1 \quad . \tag{7}$$

This inequality is favored for high reflectivity of the mirrors, long length of active material, short radiative lifetime and narrow spectral width of the transition, greater degeneracy of the lower level, and a large increase in population of the upper over the lower laser level. Threshold is reached when the combination of these quantities causes the left side of eq. (7) to equal unity. The factors determining the formation F_2, of N_2 in a photodissociative laser, are expressed by the relation

$$F_2 = C \int S(\nu)\, \epsilon(\nu)\, K(\nu)\, \phi_2(\nu)\, d\nu \tag{8}$$

where

$S(\nu) \equiv$ spectral distribution of the pumping source

$\epsilon(\nu) \equiv$ absorption coefficient of the laser material

$K(\nu) \equiv$ coupling coefficient between pumping source and laser tube; $K(\nu)\, S(\nu)$ represents the light intensity inside the laser tube

$\phi_2(\nu)$ ≡ quantum yield for formation of N_2

C ≡ concentration of laser material.

A similar relation may hold for N_1, but it is expected than in most cases $\phi_1(\nu)$ will be small compared with $\phi_2(\nu)$. $\phi_1(\nu)$ and $\phi_2(\nu)$ for the halogens will be equal in certain regions of ν, but examination of eq. (7) shows that laser action can still be achieved since $m_1 = 2m_2$ for the atomic $^2P_{1/2}$ and $^2P_{3/2}$ level of the halogens. It is apparent from eqs. (7) and (8) that the unique ability of photodissociative systems to absorb in a broad spectral region and produce excited species with narrow line emission is advantageous with respect to realization of laser action.

Photodissociative systems are expected to function as four-level lasers. Depletion of the two laser levels is most likely to occur by the usual secondary reactions encountered in photochemical studies. A discussion of processes and a detailed description of four-level systems will appear in Section V.

The approach most commonly used in a study of potential laser materials is to construct a cavity and laser tube of arbitrary size and attempt to observe coherent emission. This procedure suffers somewhat, however, because it gives little insight into the reasons for failure to observe laser emission when negative results are obtained.

An alternative approach is to determine the single pass gain g of a given laser material by measuring its total spontaneous emission power under conditions of population inversion. Knowledge of g yields quantitative relationships between the experimental parameters and hence the feasibility of the system as a laser. These relationships are outlined below.

Consider a cylindrical tube of material which has been pumped to an inverted state ($N_2 > N_1$). Each volume element Adx emits spontaneously at the rate

$$\frac{N_2 f(\nu) A dx}{\tau_{21} 4\pi} \text{ (photons/sec/solid angle/unit bandwidth)} \qquad (9)$$

where A is the cross-sectional area and the other quantities are as defined above.

The spontaneous emission from each volume element is amplified by stimulated emission processes as it travels down the tube. In the treatment the extent of amplification is assumed to be dependent only on the distance between the end of the tube and each volume element $(L - x)$. The amplification factor for each volume element is then $e^{\alpha(L-x)}$. The total spontaneous emission power per frequency interval, $P_{sp}(\nu)$, observed at the end of the tube is equal to the integral of the spontaneous emission of each volume element multiplied by the appropriate gain for each volume element as determined by its position x in the tube. The dimensions are related as shown below.

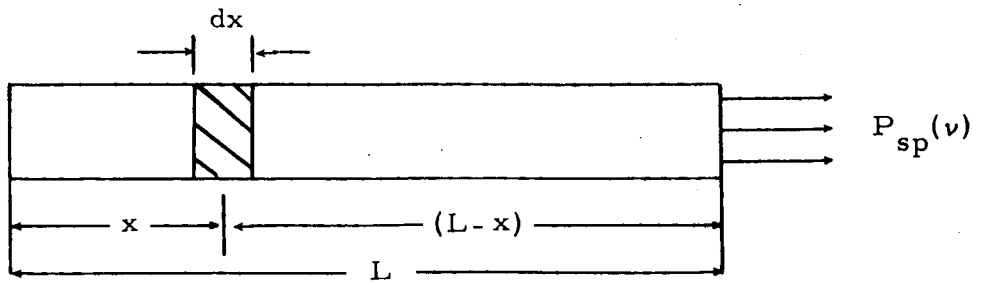

Thus,

$$\frac{P_{sp}(\nu)}{h\nu} = \int_0^L \frac{N_2 f(\nu) A}{4\pi \tau_{21}} e^{\alpha(L-x)} dx \qquad (10)$$

$P_{sp}(\nu)$ has units of energy/sec/solid angle/unit bandwidth.

$$\frac{P_{sp}(\nu)}{h\nu} = \frac{A N_2 f(\nu)}{4\pi \tau_{21} \alpha} (e^{\alpha L} - 1) \qquad (11)$$

Substitution for α gives

$$\frac{P_{sp}(\nu)}{h\nu} = \frac{A\, N_2\, f(\nu)}{4\pi\, \tau_{21}} \frac{(g-1)}{\sigma(\nu)\left(\frac{m_1}{m_2} N_2 - N_1\right)} \tag{12}$$

$$P_{sp}(\nu) = \frac{2A\, N_2}{\frac{m_1}{m_2} N_2 - N_1} \frac{h\nu_o^3}{c^2} (g-1) \quad . \tag{13}$$

The total spontaneous emission over the entire bandwidth of the transition is

$$P_{tot} = \int P_{sp}(\nu)\, d\nu \quad . \tag{14}$$

This integral is approximated by the product of the peak value of the integrand and the bandwidth at half-height.

$$P_{tot} \simeq P_{sp}\, \Delta\nu_L \tag{15}$$

Thus,

$$P_{tot} \simeq \frac{2A\, N_2}{\frac{m_1}{m_2} N_2 - N_1} \frac{h\nu_o^3\, \Delta\nu_L}{c^2} (g-1) \tag{16}$$

The total spontaneous power P_{tot} can be measured directly. Also, $N = N_1 + N_2$ may be known or can be determined experimentally. The single pass gain g is related to the measured quantity P_{tot} in the following way

$$\left[\frac{\sigma(\nu)\, LN}{\ln g} + 1 \right] (g - 1) = (1 + k)P' \qquad (17)$$

where

$$P' = \frac{P_{tot}\, c^2}{2A\, \Delta\nu_L\, h\nu_o^3}$$

and $k = m_1/m_2$. Thus an experimental determination of P', together with a knowledge of L, N, $\sigma(\nu)$ and k, yields a value (after numerical solution of (17)) for the single pass gain and hence provides a direct evaluation of the laser system.

D. ASSOCIATION PROCESSES STABILIZED BY STIMULATED EMISSION

The previous discussion has been concerned mainly with possible laser action from excited products formed by photodissociation. Although this appears to be the most favorable mechanism, other possibilities should be considered. The process of recombination of dissociation products is an important factor in the operation of dissociative laser systems; in addition, it has the potential for being another source of excited species which can also produce laser light. Stimulated emission may reduce the lifetimes of excited associated species sufficiently to increase substantially the over-all rate of formation of the stable recombined molecules. In this case the main route for recombination would be by stimulated emission, and the pumping source would serve the dual role of removing the ground state and of forming the photodissociative products for the laser recombination processes. Thus this mode may be comparable with other means of excitation.

Characteristically, radiation is only one of several competitive processes which lead to the destruction of excited atoms or molecules. As the radiative lifetime decreases, because of stimulated emission, competing loss processes become less important and the conversion of potential energy into specific radiation energy becomes more efficient. Especially when the major loss of excited species occurs by a process which is the inverse of their formation, the reduced radiative lifetime will increase the net formation rate. This situation is characteristic of atomic association and of other chemical reactions which produce excited products (chemiluminescence).

When the chemical processes create a population inversion large enough that stimulated emission can overcome cavity losses, the efficiency of energy conversion will be primarily determined by the rate at which species in the lower state are removed. Gas-phase free radical association reactions are known to populate highly excited states of the initially formed complex.[21] The simplest example is atomic association: $X + X + (M) \rightarrow X_2^* + (M)$ where M may or may not be necessary as a third collision partner to conserve energy and momentum, and X_2^* may be electronically and/or vibrationally excited. The rate at which X_2 is formed is determined primarily by energy transfer processes which remove sufficient energy from X_2^* to prevent the immediate reversal of the reaction. Since collisions between atoms occur in $\sim(10^{-8}/P_{mm})$ sec, few bimolecular collisions ($\sim 10^{25}\ P_{mm}$/sec) can be stabilized by termolecular collisions or spontaneous emission ($\sim 10^{-9}$ sec) at reasonable pressures of M. However, the radiative lifetime of X_2^* is shortened appreciably by stimulated emission since

$$-\frac{d\,X_2^*}{dt} = A_{21}X_2^* + B_{21}\,\rho(\nu)\,X_2^*$$

where A_{21} and B_{21} are the Einstein coefficients for spontaneous and induced emission from X_2^* and $\rho(\nu)$ is the radiation density

$$\left[\rho(\nu)(\text{photons/cm}^3) = \frac{4\pi}{c} I\,(\text{photons/cm}^2\text{-sec})\right] .$$

$$B_{21} = A_{21} \frac{c^3}{8\pi h \nu_{12}^3} = \frac{1}{\tau_o} \frac{\lambda^3}{8\pi h}$$

$$\frac{1}{\tau} = A_{21} + B_{21}\,\rho(\nu)$$

$$\frac{1}{\tau} = \frac{1}{\tau_o} + \frac{1}{\tau_o} \frac{\lambda^3}{8\pi h} 4\pi \frac{I}{c} = \frac{1}{\tau_o}\left(1 + \frac{\lambda^3 I}{2hc}\right)$$

Thus if the lower laser level could be removed rapidly enough (by photochemical or thermal dissociation, for example), the maximum laser intensity would be limited by the volume of active material and the collision frequency: $I \approx V\,Z_{11} \approx V\,10^{-10}\,(X)^2$ where Z_{11} is the bimolecular collision frequency per cubic centimeter, V is the volume, and (X) is the number of species X per cubic centimeter. For a pressure of 10 Torr ($10^{17}/\text{cm}^3$) and an effective mode volume of 100 cm^3, the potential intensity is $\sim 10^{26}$ photons/sec. Allowing for one collision per thousand to be effective, the intensity could be as high as 10^{23} photons/sec. However, the radiation may be distributed over a large wavelength range and the spontaneous intensity between any two particular levels may be insufficient to initiate laser oscillation. This situation is less likely if intersystem crossing or internal conversion to a metastable state occurs. A transition probability of 0.01 for this type of process reduces the maximum intensity to 10^{21} photons/sec. The initial spontaneous emission will in all likelihood still be distributed over a range of frequencies, but the chances for initial oscillation are increased since most of the radiation originates from the same upper level.

The minimum value of the rate constant for association reactions to produce laser action in this way can be estimated from consideration of the gain equation:

$$\frac{\lambda_o^2}{4\pi^2 \tau_{21} \Delta\nu_L} \quad \frac{L}{\ln(1/r)} \left(\frac{M_1}{M_2} N_2 - N_1 \right) = 1 \quad .$$

Thus the rate of excited state production R necessary for initial oscillation if the lower state is essentially unpopulated is

$$R = \frac{N_2}{\tau_{21}} = \frac{4\pi^2 \Delta\nu}{\lambda_o^2} \quad \frac{\ln(1/r)}{L}$$

$$R = 4\pi^2 c \, \frac{\Delta\tilde{\nu}}{\tilde{\nu}} \, \frac{\ln(1/r)}{L} \, \tilde{\nu}^3 = k(X)^2 \quad .$$

Hence

$$k = 4\pi^2 \, \frac{c}{(X)^2} \quad \frac{\Delta\tilde{\nu}}{\tilde{\nu}} \quad \frac{\ln(1/r)}{L} \quad \tilde{\nu}^3 \quad .$$

Substitution of the values $(X) = 10^{16}/cm^3$, $\Delta\tilde{\nu} = 0.08\ cm^{-1}$, $\tilde{\nu} = 2.5 \times 10^4\ cm^{-1}$, $r = 0.97$, and $L = 100$ cm gives $k = 2 \times 10^{-16}\ cm^3 - sec^{-1}$. Examples of associative reactions with this order of magnitude for the rate coefficient[22] are the formation of nitric oxide $N + O \rightarrow NO\ (C^2\pi) + h\nu$ and nitrogen $N + N \rightarrow N_2 + h\nu$. Although the specific rate constant has not been measured for formation of CN, the potential energy curves for CN and NO are similar; it is possible that a process similar to that exciting the $C^2\pi$ state of NO could produce laser radiation in the CN bands. Although not all of the necessary rate constants have been determined, the following association reactions are potentially useful as laser sources.

$$NO\ (^2\pi) + O(^3P) \rightarrow NO_2^*\ (^2A_1,\ ^2B_2 \text{ or } ^2B_1)$$

$$I(^2P_{3/2}) + Cl\ (^2P_{3/2}) \rightarrow ICl^*\ (^3\pi_1)$$

$$I(^2P_{3/2}) + Br\ (^2P_{3/2}) \rightarrow IBr^*\ (^3\pi_1)$$

It is possible that none of these particular examples is feasible, but they serve to illustrate another potentially useful mechanism for conversion of solar radiation to coherent emission. The probability per collision for the formation of halogen molecules as a result of recombination of the atoms and stabilization of the intermediate quasimolecule by emission of radiation was calculated by Terenin and Prilezhaeva[23] to be $\sim 10^{-6}$ using natural radiative lifetimes. Thus there are both experimental and theoretical indications that laser action can be obtained from association reactions.

A molecular system of this general type which might produce laser action from vibrational transitions is shown in Fig. 1. Absorption of visible or near ultraviolet radiation results in photodissociation of molecule AB to the fragments A and B, which are not necessarily electronically excited. Recombination of A and B to form AB in the excited electronic state II, from which emission is forbidden (spin), could result in sufficient population of the n^{th} vibrational level of state I to form a downward cascading infrared laser. Intersystem crossing from state ^{3}II to ^{1}I is expected to be dependent on collisional perturbations.

Thus, if a large population suddenly appears in the n^{th} vibration of the ^{1}I state, a burst of stimulated emission can take half of that population down to the n-1 vibrational level, and so on. The primary competition for this energy will be collisional transfer of the vibrational energy to translational energy. However, studies outlined by Kondrat'ev[21] based on sound dispersion measurements suggest that conversion of a vibrational quantum to translational energy occurs only on the order of once in thousands of collisions for many gases. Even smaller factors have been proposed by Zener.[24]

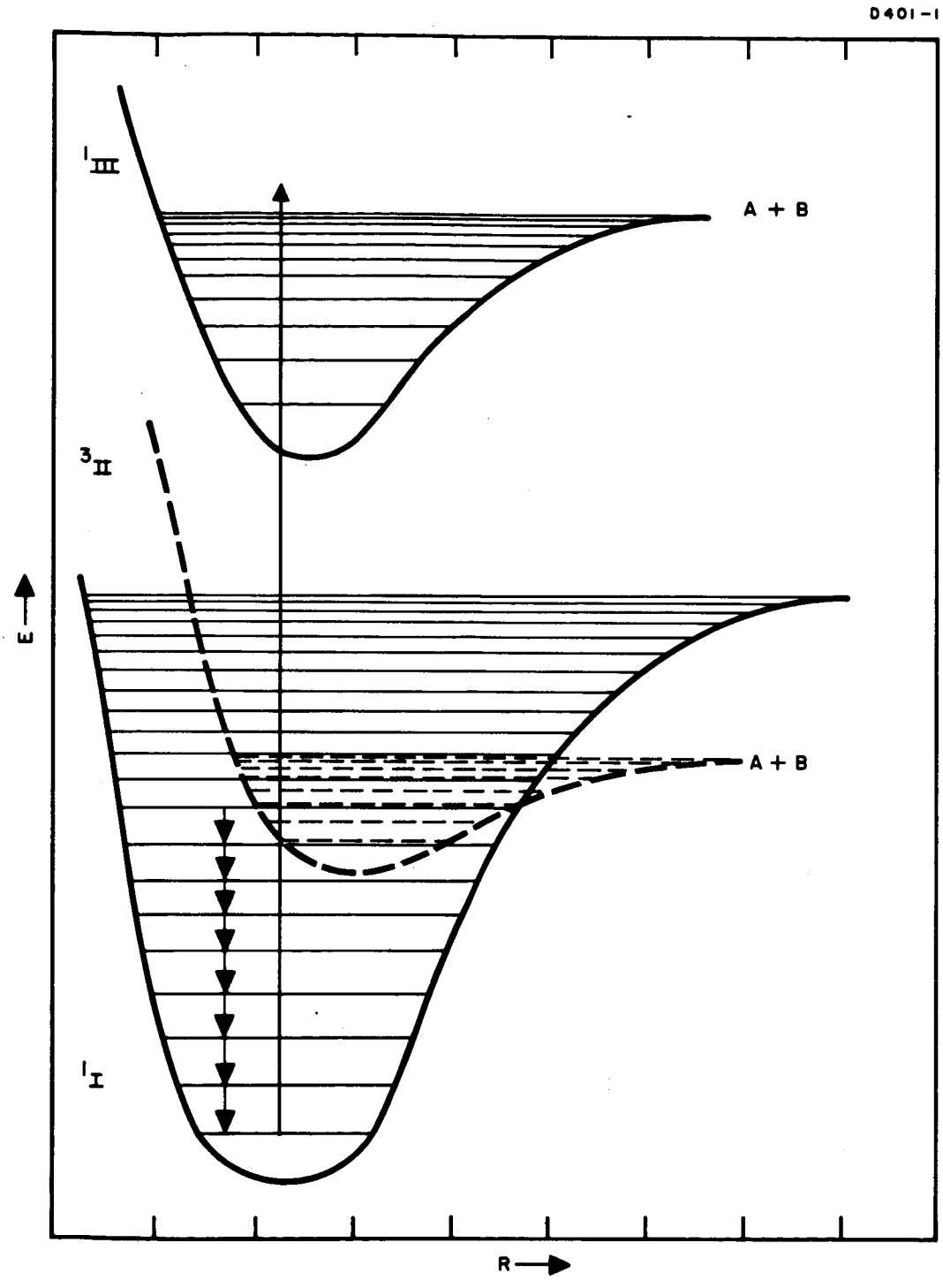

Fig. 1. Potential energy diagram for a photodissociative vibrational laser system.

Because of anharmonicity in the potential energy curves, the successive quantum jumps are shifted slightly so that the low vibrational transitions correspond to a slightly shorter wavelength than those from the upper levels. This allows the possibility of stimulated emission between two successive levels, which would not be possible for equal spacing, since in the latter case incident photons would be just as likely to induce absorption to the next highest level as emission to the adjacent lower level.

E. FRANCK-CONDON PUMPING — NONEQUILIBRIUM DISTRIBUTION OF MOLECULAR VIBRATIONAL STATES

A possible method for producing a population inversion between vibrational levels which we have not discussed in detail is Franck-Condon (FC) pumping. It is well known that the intensity distribution of vibration-rotation bands in molecular electronic spectra can be accounted for in detail by the FC principle. Since electronic transitions are several orders of magnitude faster than nuclear motions, the intensity distribution in a particular vibronic band is proportional to the overlap of the vibrational wave functions of the initial and final states of the band. This is illustrated in Fig. 2; the profile on the right side of the diagram illustrates the over-all absorption envelope when the equilibrium internuclear separation of the upper electronic state is greater than that of the ground state. Horizontal lines in the potential wells represent quantized vibrational levels, and the forms of the corresponding wave functions are superimposed on these levels. If the internuclear potentials of two electronic states are similar (i.e., the equilibrium force constants and configurations are similar), the vibrational components of the transition correspond to $\Delta v = 0$. However, when these potentials differ significantly, as in Fig. 2, each initial vibrational state gives rise to a long series of transitions whose maximum intensity coincides with the largest vibrational overlap integral and may occur for large values of Δv.

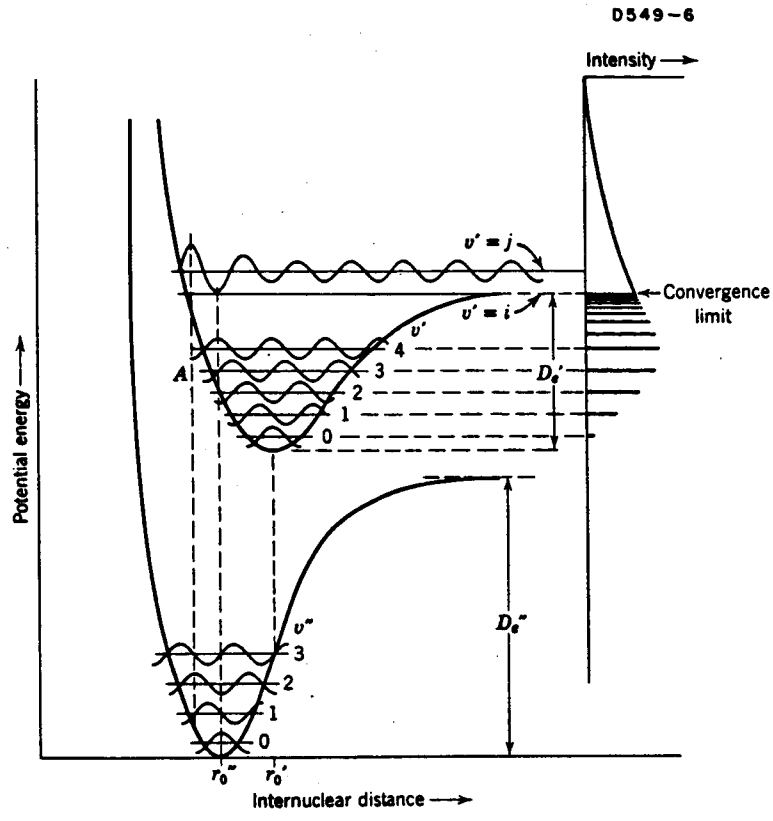

Fig. 2. The transitions between potential energy curves for an electronically excited and ground-state diatomic molecule (from Calvert and Pitts[25]).

When an ensemble of molecules which are initially in their lowest vibrational state is exposed to broad band radiation corresponding to an electronic transition, the population distribution of vibrational levels in the excited electronic state may be nonthermal because of differences in internuclear potentials of the two electronic states. The steady state population of electronically excited molecules in the vibrational levels v' is given by

$$N_{v'} = R_{v'} \tau_{v'} \tag{18}$$

where $R_{v'}$ and $\tau_{v'}$ are the rate of formation and lifetime of the vibrational state v', respectively. $R_{v'}$ is a product of the absorption coefficient, the radiation density, and the concentration of ground state molecules and consequently is directly proportional to the FC factor

$$X_{v'', v'} = \left| \int \phi_{v''}(r)\, \phi_{v'}(r) dr \right|^2 \tag{19}$$

where $\phi_{v''}$ and $\phi_{v'}$ are the vibrational wave functions of the electronic ground and excited states, and r represents the nuclear coordinates. Thus the distribution of electronically excited molecules among vibrational energy levels is nonthermal whenever the electronic transition involves changes in the nuclear equilibrium configuration; in suitable cases, it may produce population inversions.

In order for $N_{v'}$ to be large, the formation rate and lifetime must be large. For the usual allowed electronic optical transitions, these requirements are contradictory. However, the same considerations with regard to the FC principle apply for both emission and absorption, and a population inversion between vibrational levels in the ground electronic state may result from an absorption-emission cycle. The probability of this process is expressible as a sum of products of FC factors for absorption and emission by way of each accessible vibrational level of the upper state.

Thus

$$P_{v_i'', v_j''} \propto \sum_k X_{v_i'', v_k'} X_{v_k', v_j''} \tag{20}$$

where $P_{v_i'', v_j''}$ is the probability for a transition from the i^{th} vibrational level of the ground electronic state to the j^{th} level as a result of a broadband absorption emission cycle. If conditions are such that these cycles can be repeated many times before the effects of dissipative processes (collisional relaxation of vibrational excitation) are significant, a high degree of vibrational excitation may be built up in specific levels; this can result in population inversion and laser action if the critical inversion density is large enough to overcome cavity losses.

A mechanism of this type may be operative in the photolysis of cyanogen and the cyanogen halides. Initial decomposition yields the CN radical in its ground electronic state, which can then undergo a number of absorption-emission cycles. Population inversion between vibrational levels has been demonstrated in the photodecomposition of cyanogen ($(CN)_2$) by both flash photolysis[26] and laser techniques.[27] This mechanism may be very useful in obtaining coherent emission from molecules which absorb strongly in the long wavelength portion of the solar spectrum but do not dissociate.

The degree of inversion between vibrational levels obtained in this way can be calculated if the FC factor array is known. It is available in a limited number of cases and is calculable in principle for all molecules whose potential energy functions are known. The treatment of FC pumping given below has been outlined previously.[28]

P_{ij} is the probability that a molecule initially in vibrational level j of the electronic ground state absorbs a photon and ends up in level i of the electronic ground state as a result of a vibronic absorption-emission cycle.

$$P_{i \leftarrow j} = \sum_k P_{i \leftarrow k} P_{k \leftarrow j} \tag{21}$$

where k designates a vibrational level of an excited electronic state. The normalized probabilities p_{ik} and p_{kj} are given by

$$p_{k \leftarrow j} = \frac{\rho_{kj} |\mu_{kj}|^2}{\sum_k \rho_{kj} |\mu_{kj}|^2} \tag{22}$$

$$p_{i \leftarrow k} = \frac{(8\pi hc^{-3}\nu_{ik}^3 + \rho_{ik}) |\mu_{ik}|^2 + S_{ik}}{\sum_k \left[(8\pi hc^{-3}\nu_{ik}^3 + \rho_{ik}) |\mu_{ik}|^2 + S_{ik} \right]} \tag{23}$$

$\rho_{\ell m}$ is the radiation density in the system at the frequency of the transition ν_{lm}, μ_{lm} is the transition moment matrix element, and S_{ik} is the rate coefficient for nonradiative transitions. p_{kj} is the probability that a molecule initially in level j absorbs a photon and is transferred to level k; p_{ik} is the probability that a molecule in level k will go to level i by either spontaneous or induced emission or a nonradiative process. The rate constant for transitions from level j is given by

$$K_j = \sum_k \rho_{kj} B_{kj} \tag{24}$$

where B_{kj} is the Einstein coefficient for absorption. The product of K_j and P_{ij} is the rate constant for transitions from j to i. The net rate of change of the population N_i of level i is

$$\frac{dN_i}{dt} = \sum_j (P_{ij} K_j N_j - P_{ji} K_i N_i) \quad . \tag{25}$$

Since

$$\sum_j (P_{ij}K_jN_j - P_{ji}K_iN_i) = \sum_j (P_{ij} - \delta_{ij}) K_jN_j \qquad (26)$$

where

$$\delta_{ij} = \begin{cases} 0 \text{ for } i \neq j \\ 1 \text{ for } i = j \end{cases} , \qquad (27)$$

$$\frac{dN_i}{dt} = \sum_j (P_{ij} - \delta_{ij}) K_jN_j \quad ; \qquad (28)$$

in matrix notation

$$\frac{d\overline{N}}{dt} = (\overline{P} - \overline{I})\,\overline{K}\,\overline{N} \qquad (29)$$

where $\overline{I}$ is the unit matrix and $\overline{K}$ is a diagonal matrix with elements K_j. Integration of (12) gives

$$\overline{N}(t) = \overline{N}(o)\, e^{(\overline{P}-\overline{I})\,\overline{K}t} \quad . \qquad (30)$$

$\overline{N}(o)$ is the initial vibrational distribution before the pumping radiation is turned on.

The steady state solution of (29) is

$$(\overline{P} - \overline{I})\,\overline{K}\,\overline{N} = 0 \quad . \qquad (31)$$

Since the value of (31) is unchanged upon division by the constant $\rho(\nu)$, the steady state value of N_i is independent of light intensity; hence the inversion density between two levels is determined by the relative transition probabilities for these levels when dissipative effects are negligible. $\overline{N}(t)$ is obtained from (30) by ordinary computer methods when the elements of $\overline{P}$ and $\overline{K}$ are known.

As mentioned above, the collision-induced dissipative processes play a major role in determining the pumping power required to produce a given inversion density. In the absence of such collisions, the light intensity affects only the time scale of the approach to the steady state and does not otherwise influence the vibrational distribution. If relaxing collisions are effective, the pumping rate must be greater than the deactivation rate for the levels of interest.

Of the systems suggested to date for producing coherent emission from sunlight, the cases where the FC pumping mechanism is likely to occur are NO_2, N_2O_4, IBr, ICl, I_2, ICN, and $CO(CN)_2$ when they are irradiated with light of longer wavelength than that required for photodissociation. Thus several mechanisms for producing laser action may be operative in some of the suggested systems when they are exposed to the full spectrum of solar radiation.

F. COMBINATIONS OF SOLAR AND CHEMICAL PUMPING

Solar energy might be utilized in various indirect ways to achieve chemical laser action. Chemical reactions between photochemically produced active species and other molecules might lead to stimulated emission similar to those discussed above as association processes. For example, oxygen atoms produced from the photolysis of nitrogen dioxide or of ozone could react with carbon monoxide to form excited carbon dioxide:

$$CO + O(^3P) \rightarrow CO_2^* (^3\pi) \quad .$$

Emission has been observed from CO_2 formed from CO and oxygen atoms.

Many chemical reactions proceed at a high rate after initiation by ultraviolet radiation. Although the distribution of solar intensity in the ultraviolet region is relatively small, the intensity is probably adequate for initiation of chain reactions which may form sufficient concentrations of excited species to produce laser action. Examples

of this type are the reactions of molecular hydrogen with oxygen and halogens to form water and hydrogen halides:

$$H_2 + 1/2\ O_2 + h\nu \rightarrow H_2O$$

$$H_2 + X_2 + h\nu \rightarrow 2HX \quad .$$

The driving force for these reactions is the energy of the chemical bonds rather than an external source. Laser action from vibrationally excited HCl formed in a chain reaction has been reported by Kasper and Pimentel.[29] Solar energy could be utilized further in such systems by incorporating solar cells to produce electrical energy for conversion of the products formed in the chain reaction to the original starting material by electrolysis.

Solar energy could also be used to provide a high temperature source for thermal decomposition reactions that yield excited species. For example, the possibility of a laser system by thermal decomposition of dimethyl peroxide has been explored by Henderson and Muramoto.[30] Although these workers could not obtain a sufficient inversion density to support laser action on the 4231 Å vibronic band of formaldehyde, systems of this type may produce sufficient inversion between vibrational and rotational levels to produce an infrared laser. As pointed out by these investigators, one of the major difficulties in obtaining oscillation on molecular electronic bands is the large number of individual levels in the lower state to which transitions can occur. However, further experimental studies of thermal systems which utilize compounds such as the peroxides appear warranted because of the propects for discovering infrared laser materials.

Other systems such as

$$N_2O_3 \rightarrow NO_2 + NO$$

which dissociate both thermally and photochemically may produce molecular fragments in excited levels that could be inverted under proper conditions. An obvious advantage of such systems is the possibility of recycling the dissociation products by cooling. Solar power would then be utilized for production of the active material. Dimers and polymers such as paraformaldehyde may also be suitable for this type of laser system.

Another system which may be adaptable for conversion of solar energy to a laser beam has been described recently by Basov, Oraevskii, and Shcheglov.[31] In this application solar radiation would be used to thermally pump molecules with energy levels E_β and E_a such that the time of their radiative decay satisfies the conditions

$$\tau_\beta > \tau_a \tag{32}$$

$$E_\beta > E_a . \tag{33}$$

A nonequilibrium distribution of energy levels is brought about by allowing molecules to escape from a highly heated reservoir into a vacuum in which the equilibrium radiation is much smaller than $(E_\beta - E_a)/k$, where k is the Boltzmann constant. Spontaneous processes deplete the a level faster than the β level, as indicated by condition (32). The necessary condition for population inversion is

$$\tau_\beta > \left(1 + \frac{\tau_\beta}{\tau_{\beta a}}\right)\tau_a \tag{34}$$

or

$$k_a > (k_\beta + k_{\beta a}) \tag{35}$$

where k and τ are defined in the usual way, i.e., $k_\beta = \sum_i k_{\beta i}$ and $\tau_\beta = (1/k_\beta)$. The most practical wavelength region for operation of this type of system is from 3 to 20 μ. For shorter wavelengths, the

excited state lifetimes are too small; they are too large for longer wavelengths and would require large apparatus dimensions. Molecules which meet the necessary conditions are CO_2, N_2O, and HCN. These molecules could potentially operate on the transitions given in Table I.

TABLE I

Molecular Vibrational Transitions[32] for Laser Action by Thermal Pumping Techniques

Molecule	Transition	Wavenumber, cm^{-1}
CO_2	$20^00 \rightarrow 01^10$	2137
	$12^20 \rightarrow 01^10$	2094
	$10^00 \rightarrow 01^10$	720
	$02^20 \rightarrow 01^10$	668
	$02^00 \rightarrow 01^10$	618
	$01^10 \rightarrow 00^00$	667
N_2O	$02^20 \rightarrow 01^10$	578
HCN	$02^00 \rightarrow 01^10$	700

SECTION III

SPECTROSCOPY

A. ABSORPTION SPECTRA AND POTENTIAL ENERGY DIAGRAMS

The spectroscopy of gases that absorb light in the solar region ($\lambda > 3000$ Å) is reviewed in terms of their absorption spectra and potential energy diagrams. These spectra and diagrams are discussed with regard to the general requirements of a photochemical laser system. The importance of molecular processes such as internal conversion, intersystem crossing, and predissociation and their dependence on experimental parameters (temperature, pressure, and wavelength) are pointed out.

The distribution of absorption intensity between the various structured bands and continua within the absorption region are determined by the relative positioning of the potential energy surfaces which characterize the ground state and the excited electronic states of a molecule. The origin of band progressions (systems) is illustrated schematically by the energy level diagram for iodine shown in Fig. 3. In this case an appreciable fraction of the ground state molecules is in the second vibrational level, resulting in the presence of a weak second progression. The relative intensity of each component of these progressions is determined by the Franck-Condon principle. Since electronic transitions are at least two orders of magnitude faster than nuclear motions, the absorption distribution over vibrational bands can be obtained from comparison of the overlap between excited and ground state nuclear wave functions. This is shown in Fig. 4. The profile on the right side of Fig. 4 illustrates the over-all absorption envelope when the equilibrium internuclear separation of the upper electronic state is greater than that of the ground state; the horizontal lines in the potential wells represent quantized vibrational levels and the forms of the corresponding vibrational wave functions are superimposed on these levels.

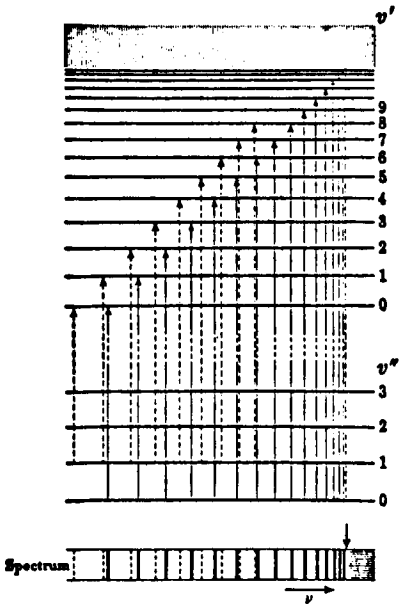

Fig. 3.
Energy level diagram for an absorption band system with convergence and continuum (schematic). The resulting spectrum is shown at bottom. The verticle arrow in the schematic spectrogram gives the position of the convergence limit. The transitions starting from v''= 1 at higher temperature are indicated by broken lines.

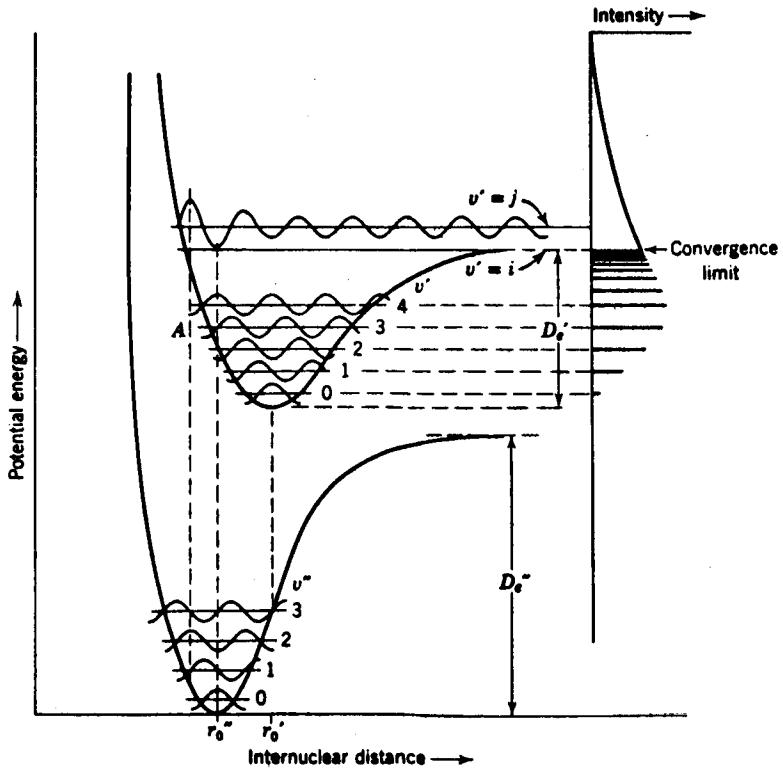

Fig. 4. The transitions between potential energy curves for an electronically excited and ground-state diatomic molecule (from Calvert and Pitts[25]).

A harmonic oscillator model is used except for $v' = j$, where r extends to infinity and the absorption spectrum becomes continuous as the molecule dissociates.

Photodissociation can also occur by another process called predissociation, which can take place when potential energy curves cross or are in close proximity so that rapid nonradiative transfers occur. This behavior is evidenced by broadened or blurred rotational components in a vibronic band when nonadiabatic transfer occurs in a time period comparable to the time of a molecular rotation. Potential energy curves for the ground and three excited states of diatomic sulfur are shown in Fig. 5. The high resolution absorption spectrum[33] shows a banded spectrum from 4100 to 2799 Å, corresponding to rotational structure superimposed on vibrational changes from $v'' = 0$ to $v' = 9$. At 2799 Å, the vibronic transition is to $v' = 10$ where the $^3\Sigma_u^-$ and $^1\Sigma_u^-$ curves intersect (point A). In the wavelength region 2799 to 2615 Å, the electronic transitions terminate at one of the vibrational levels $v' = 10$ to 17 of the $^3\Sigma_u^-$ state (A-B region). During the period of a vibration, when the nuclei reach the intersection at A, a radiationless transition to the $^1\Sigma_u^-$ state may occur. This transition would yield two ^3P sulfur atoms as photodissociative products. Nonradiative transitions of this type can be affected by collisional perturbations. In the case of S_2, the absorption lines in the region $v' = 10$ to 17 are sharp at low pressures, but at higher pressures they become blurred as a result of induced predissociation.

Excitation to $v' = 17$ or greater ($\lambda \leq 2615$ Å) can result in a radiationless transition at point C leading directly to dissociation into two normal sulfur atoms (^3P). Since this transition ($^3\Sigma_u^- \rightarrow {}^3\Pi_u$) is not forbidden by selection rules, the phenomenon is called spontaneous predissociation and is not pressure dependent; rotational blurring occurs at low pressures. The two types of predissociation discussed above for S_2 are illustrative of two general types of perturbations which may lead to indirect photodissociation of molecules. The relative probability for these processes can be inferred from the potential energy diagrams by the following criteria.[25,33] (1) The selection rules for allowed electronic transitions also apply to predissociation except

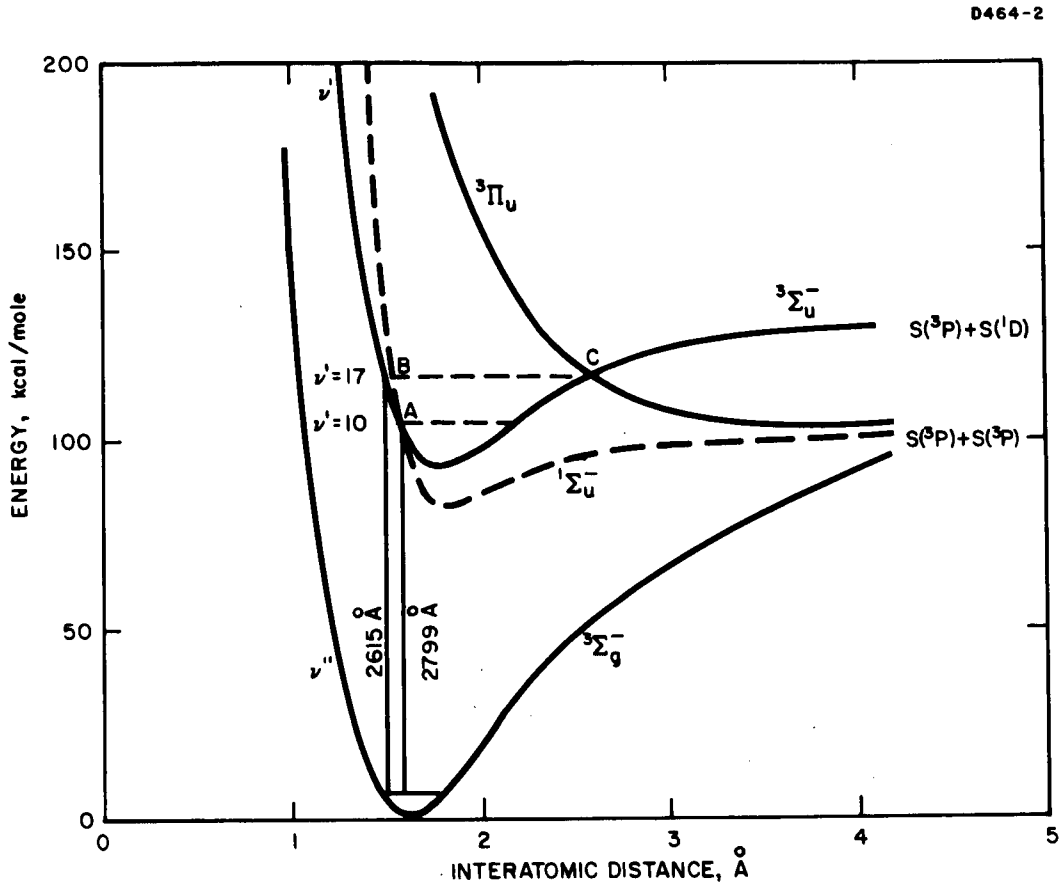

Fig. 5. Potential energy curves for the S_2 molecule (from Calvert and Pitts[25]).

that the g $\longleftrightarrow$ u and + $\longleftrightarrow$ - restrictions are reversed. (2) The transition probability depends on the shapes of the two curves at the crossover points. If they approach gradually over a long range of r, the transition probability is much greater than if they intersect at an acute angle. Other factors being comparable, a crossover at A (Fig. 5), would be more probable than at C. (3) Radiationless transition probabilities decrease with the increasing velocity of the system at the crossover point. For example, the nonradiative transition ($^3\Sigma_u^- \rightarrow {}^1\Sigma_u^-$) is more probable if excitation is to v' = 11 rather than to v' = 15 (Fig. 5), indicating the possibility of product selection at certain wavelengths. It should be noted that in the regions near curve-crossing points, the separability of electronic and nuclear energies breaks down, and the potential energy curves fade into ill-defined areas. Also, collisionally induced predissociation is thought to be a very important mechanism for internal energy transfer in polyatomic molecules.[25, 34]

B. HALOGENS

Dissociation of the halogens occurs with radiation in the continuum portion of the absorption spectrum and may also occur via predissociation in the banded region (see Fig. 6). The formation of excited atoms depends on the wavelength of the absorbed light.

Absorption in the banded region by iodine is comparable in intensity with that in the continuum and fluorescence is relatively easy to observe.[35] The failure to observe molecular fluorescence when absorption is in the continuum was the first substantial evidence that dissociation occurs at the onset and throughout the continuum. Direct evidence for photodissociation of iodine has been obtained by detection of atomic absorption lines when iodine is irradiated with light of wavelengths less than 4990 Å (Ref. 36).

A well-known band system beginning in the near infrared converges at 4989 Å, at which point one normal and one excited atom are produced (see Fig. 7). This process may be pressure dependent, however. After absorption to the $^3\Pi_{0u}^+$ state with light of wavelength

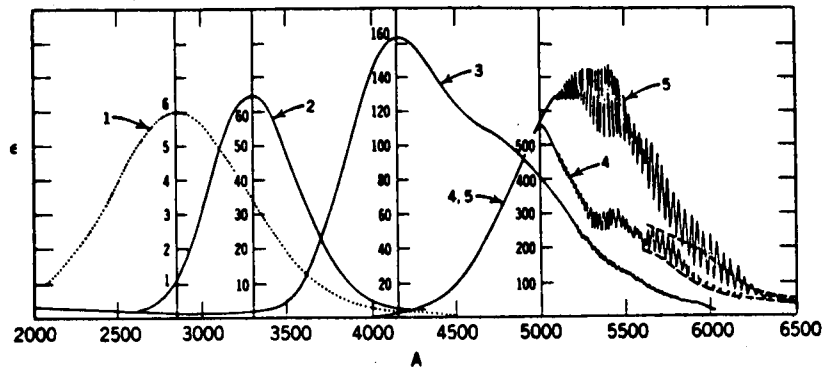

Fig. 6. Absorption spectra of the halogens. (1) $F_2(g)$, 25°C; (2) $Cl_2(g)$, 18°; (3) $Br_2(g)$, 25°; (4) $I_2(g)$ plus 1 atm air, 70-80°; the weak banded region in Cl_2 which converges to the continuum at 4785 Å is not visible with the scale chosen. (From Calvert and Pitts[25]).

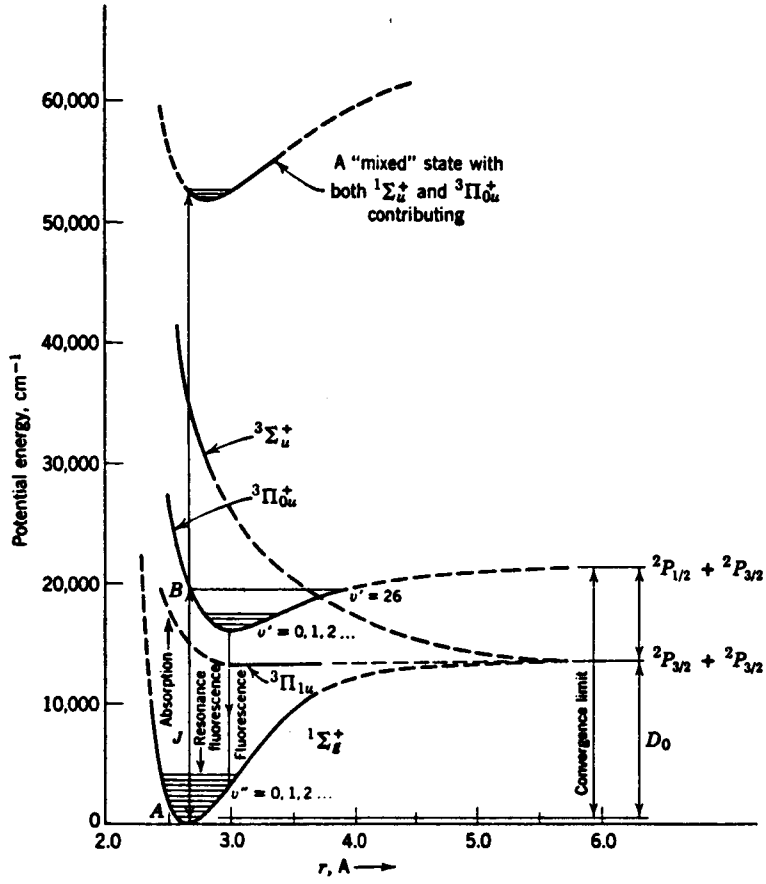

Fig. 7. Potential energy diagram for several states of the $I_2(g)$ molecule (from Calvert and Pitts[25]).

5000 Å (region near B in Fig. 7), a pressure induced transition to the repulsive $^3\sum_u^+$ state may occur resulting in formation of two ground state iodine atoms. Thus the inversion necessary for laser action from I_2 may be highly pressure sensitive in this excitation region and also at shorter wavelengths, but to a lesser degree.

Two band systems have also been observed for bromine. One converges to give two normal atoms and the other converges at 5100 Å to give one excited and one normal bromine atom (see Fig. 8). As with iodine, pressure dependent predissociation may also occur. As a result of collisional perturbations, a bromine molecule excited to the $^3\Pi_{0u}^+$ state may cross to the repulsive $^1\Pi_u$ state and dissociate into two $^2P_{3/2}$ atoms. Weak molecular fluorescence has been observed upon excitation in this region at low pressures, indicating that the nonadiabatic transition is somewhat less probable for bromine than iodine. Weak bands in the absorption spectrum of chlorine begin at 5760 Å and convergence is observed at 4785 Å where a normal and an excited atom are formed. As with the other halogens, another upper level converging to two normal atoms is known. Thus, in order to obtain laser action from the halogens, the excitation wavelengths should be less than the spectroscopic convergence limit, which yields an excited atom. In addition, the pressure should be maintained at a value consistent with maximum population density of excited atoms but low enough to avoid deleterious effects from predissociation, which leads to formation of ground state atoms. Although the number of atoms in the upper level ($^2P_{1/2}$) is not expected to exceed the number in the lower laser level ($^2P_{3/2}$), inversion is possible because of the increased degeneracy of the lower over the upper level (4:2).

C. INTERHALOGENS

Literature studies have yielded data[37] from which absorption curves of three interhalogens could be constructed. These spectra are shown in Figs. 9-11. The spectrum of IBr peaks near 5000 Å, where the solar spectral irradiance is greatest. Although the absorption

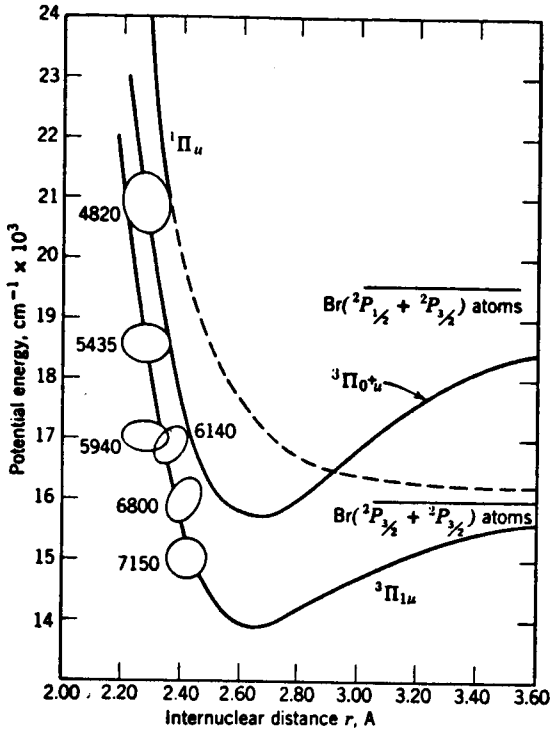

Fig. 8.
Potential energy diagram of the lowest excited states in the Br_2 molecule (from Calvert and Pitts[25]).

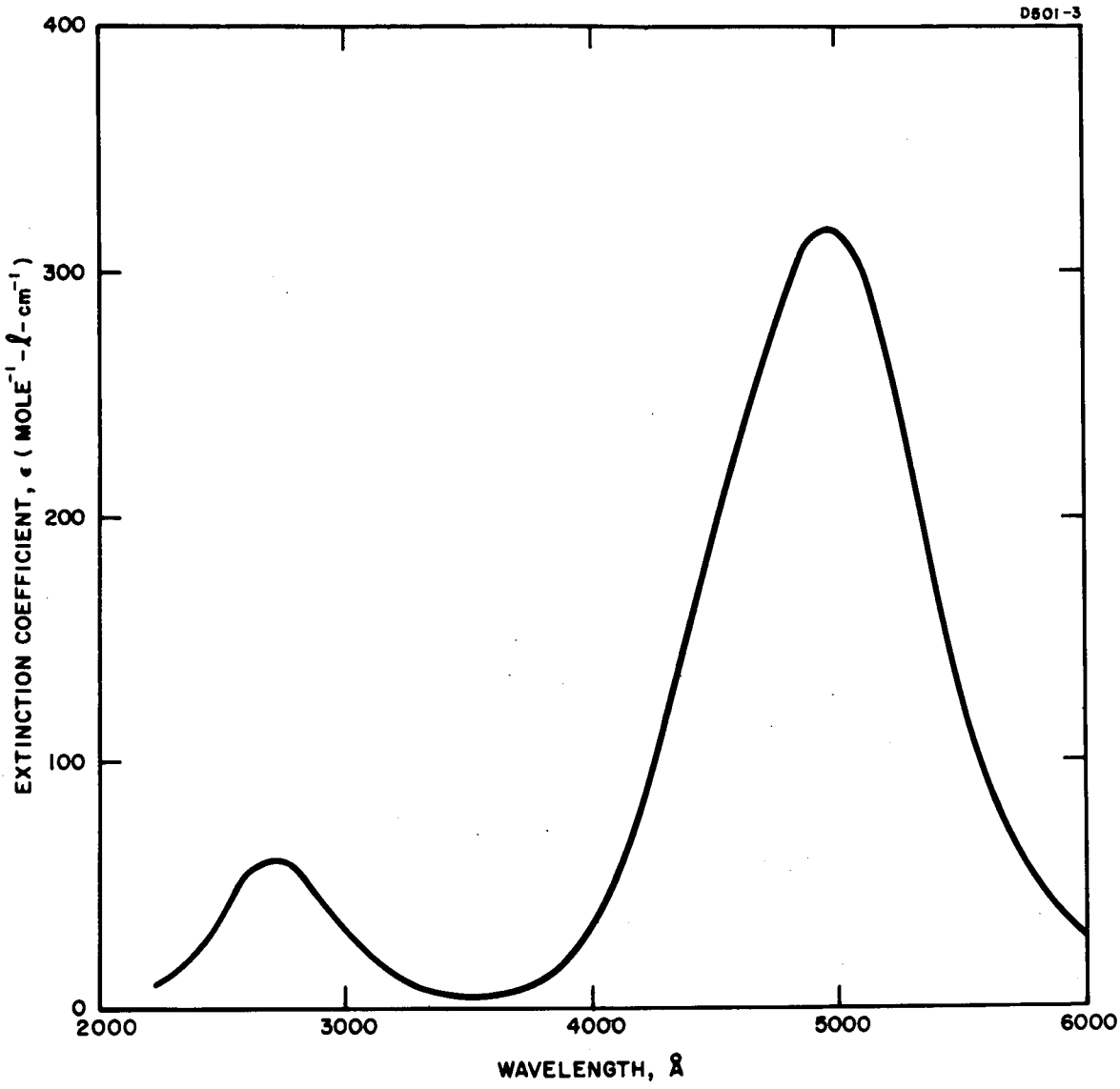

Fig. 9. Absorption spectrum of IBr in the vapor phase at 25°C.

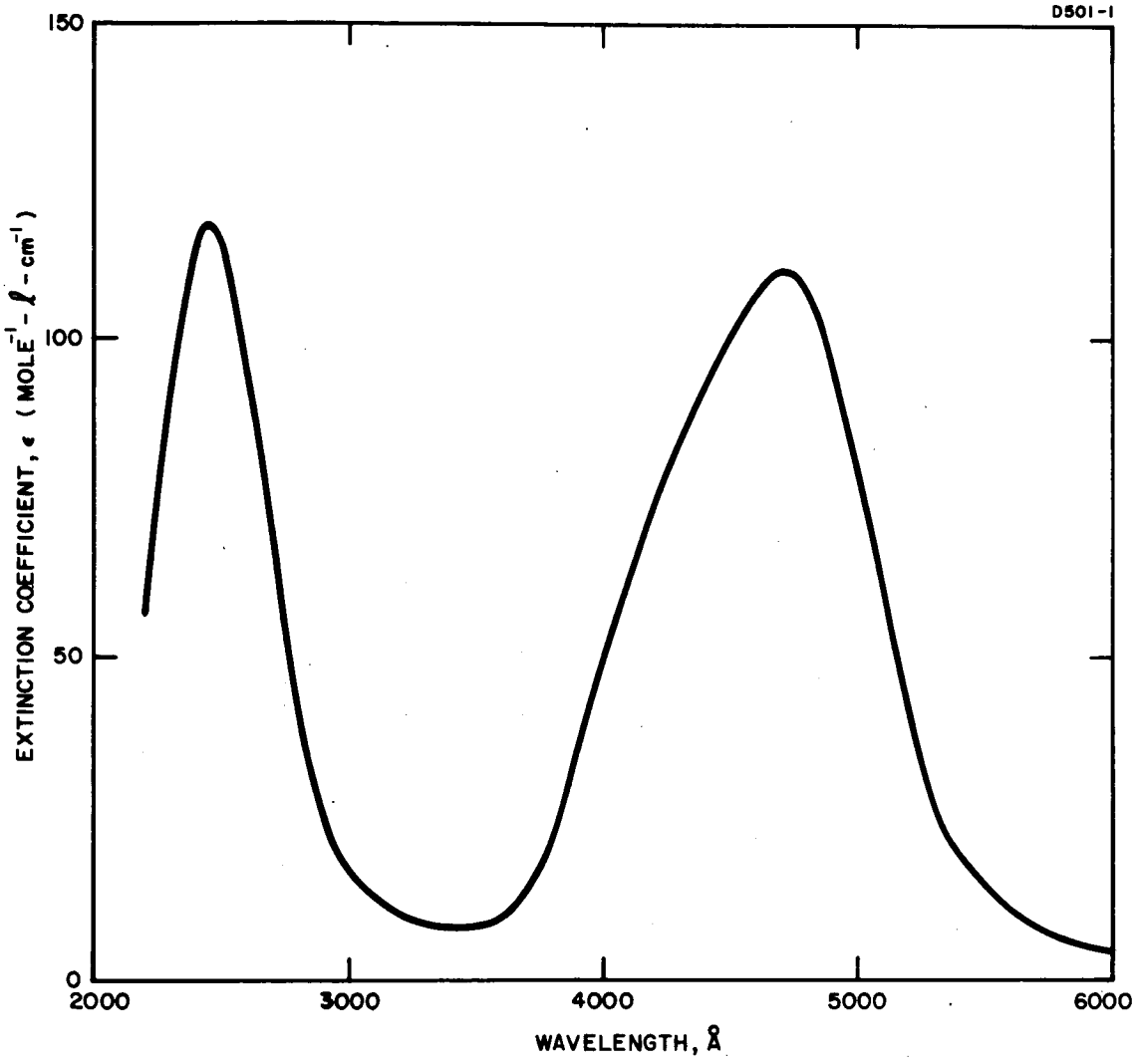

Fig. 10. Absorption spectrum of ICl in the vapor phase at 25°C.

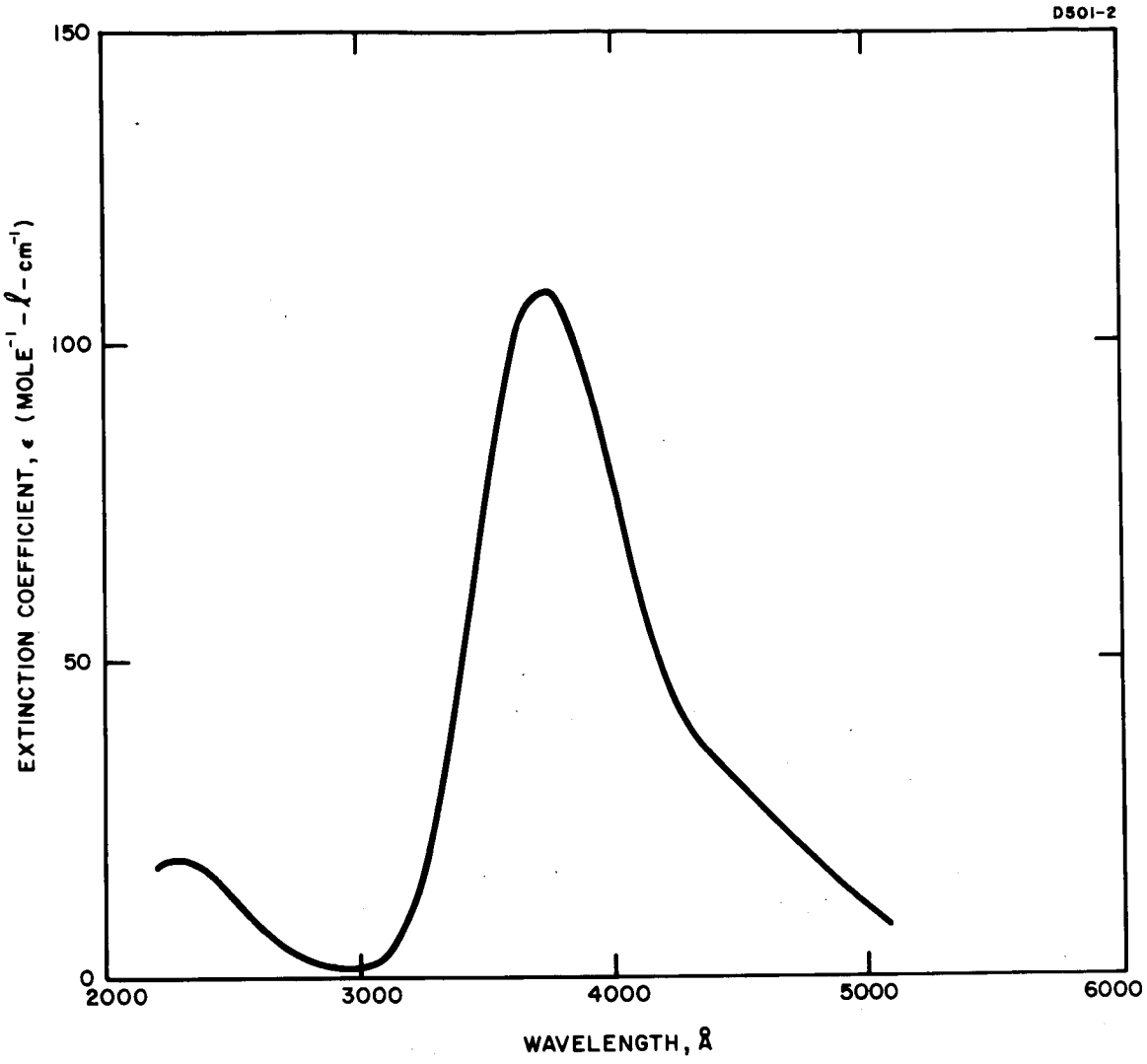

Fig. 11. Absorption spectrum of BrCl in the vapor phase at 25°C.

coefficient of ICl is about one-third that of IBr and the spectrum is blue-shifted, there is a strong overlap between its spectrum and that for solar emission. BrCl is less favorable because it is shifted farther to the ultraviolet, although there is considerable absorption in the 3900 Å region.

The potential energy diagram of iodine monochloride is shown in Fig. 12. The absorption spectrum of ICl, like the other halogens, consists of a number of band heads extending throughout the red and yellow. The $v'' = 0$ progression converges at 5755 Å where a broad band of continuous absorption begins and extends into the near ultraviolet with a maximum at 4700 Å (Ref. 38). The accurate thermodynamic data of Yost and McMorris[39] for the formation of ICl are in good agreement with the results calculated from band spectral data on the assumption that convergence at 5755 Å corresponds to dissociation into two normal atoms.[38] This assumption is consistent with extrapolations of rotational bands from vibronic systems whereas dissociation to an excited atomic state is clearly inconsistent for excitation at 5755 Å. Extrapolation of system I ($^1\sum^+ \rightarrow {}^3\Pi_1$) gives a ground state dissociation energy of 17,356 cm^{-1}. For the $v' = 2$ and 3 levels of system II ($^1\sum^+ \rightarrow {}^3\Pi_0^+$) extrapolation yields 18,270 cm^{-1}. The difference between these energies (905 cm^{-1}) corresponds to the energy separation of the first excited and ground states of the chlorine atom. Thus at wavelengths less than 5479 Å the photodissociation products of iodine monochloride expected from spectroscopic analysis clearly are excited chlorine atoms, $^2P_{1/2}$, and normal iodine atoms, $^2P_{3/2}$. Because of the relative internuclear equilibrium positions of the electronic states and the Franck-Condon principle, the transition $^1\sum \rightarrow {}^3\Pi_0^+$ is a more probable transition for the continuum at 4700 Å than the $^1\sum \rightarrow {}^3\Pi_1$ transition. The maximum for the latter process is thought to occur near the convergence limit (5755 Å), resulting in an intensity distribution similar to that of the visible iodine bands.

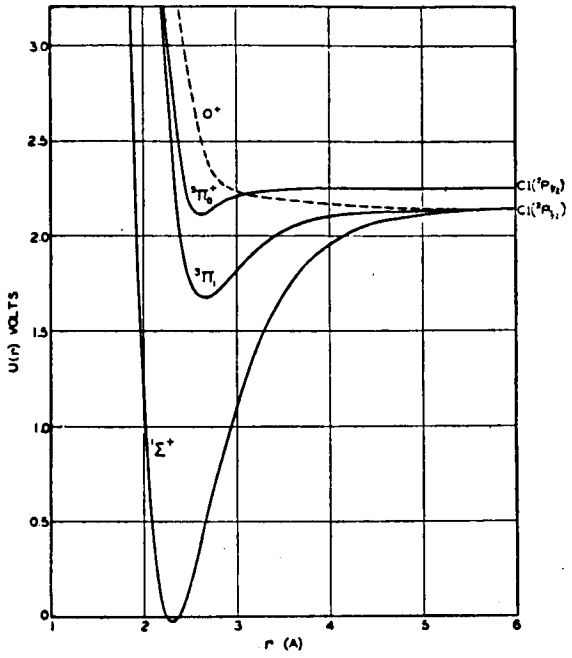

Fig. 12.
Potential energy curves for the $^1\pi$ (normal) and $^3\pi$ states of ICl. The $^3\pi_0^+$ state is shown here as derived from normal iodine and excited chlorine atoms, and crossed by a repulsive state derived from two normal atoms (from Brown and Gibson[38]).

Predissociation of ICl is observed at wavelengths around 5567 Å (Ref. 38). Figure 13 is an enlarged drawing of the upper electronic states of ICl. The repulsive O^+ state, derived from normal atoms, crosses the $^3\Pi_0^+$ state at 17,960 cm^{-1}. This interaction allows dissociation from the $^3\Pi_0^+$ state to two normal atoms rather than to an excited chlorine atom. The over-all spectroscopic implication is that the relative amounts of normal and excited chlorine atoms will depend on both excitation wavelength and pressure induced predissociation.

Potential energy curves for iodine monobromide are shown in Fig. 14. Vibrational analysis of the electronic absorption spectrum of IBr by W. G. Brown[40] yields an interpretation similar to that for ICl.[38] A set of bands in the near infrared are assigned to the $^1\Sigma \rightarrow {}^3\Pi_1$ transition. The $^1\Sigma \rightarrow {}^3\Pi_0^+$ system is observed as a faint set of bands in the red which show the same type of pressure dependent predissociation as the corresponding bands of ICl. Transitions to a state which originates at the maximum of the $^3\Pi_0^+$ state, where dissociation yields a normal iodine and excited bromine atom, are observed as a strong system of partially diffuse bands. The earlier assignment by Cordes[41] of these bands to two systems, one of which allows dissociation to excited iodine atoms, was not confirmed in the study by Brown.[40] The spectroscopic argument for dissociation to excited bromine and normal iodine atoms is based on the heat of dissociation of IBr.[42] Extrapolation of the vibrational bands of the $^3\Pi_0^+$ state gives a value of 18,345 cm^{-1} for the convergence limit of this electronic state. Subtraction of the excitation energy of $Br(^2P_{1/2})$, 3685 cm^{-1}, from this value gives 14,660 cm^{-1} for the heat of dissociation, which is in excellent agreement with the thermodynamic value. The O^+ state is analogous to that for ICl and leads to normal iodine and bromine atoms when crossover to the $^3\Pi_0^+$ state does not occur.

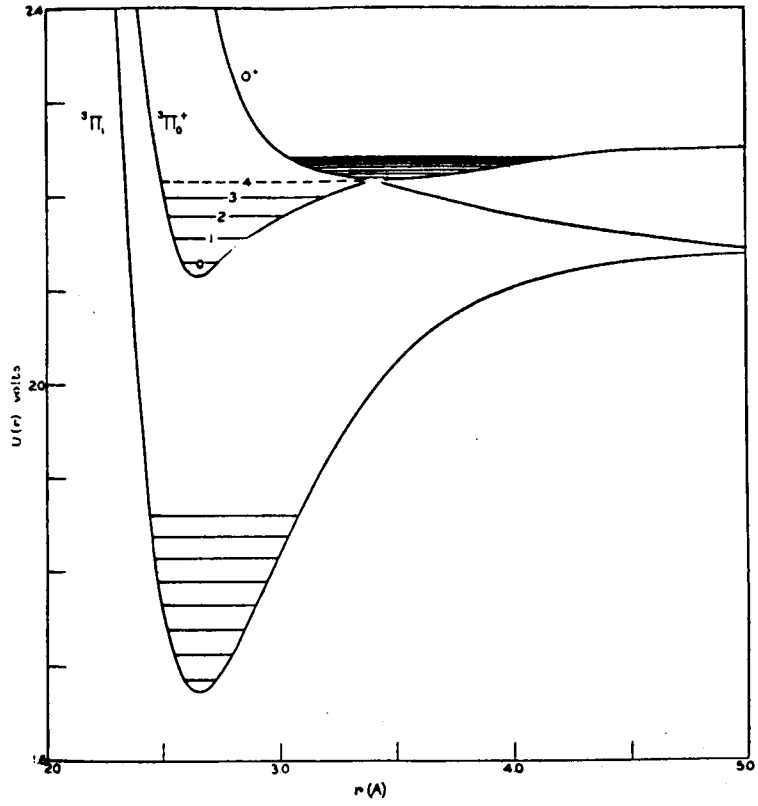

Fig. 13. Potential energy curves for the $^3\pi$ states (U(r) scale greatly increased over Fig. 12) showing how the $^3\pi_0^+$ state may predissociate above the level v = 3. The upper levels of system III are shown as a series of closely spaced levels above the point of predissociation (from Brown and Gibson[38]).

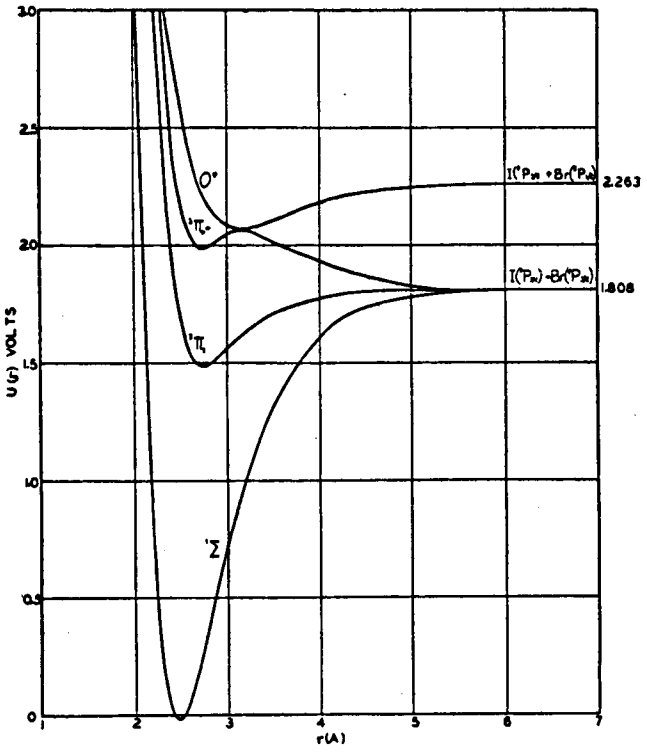

Fig. 14.
Approximate potential energy curves of IBr. The r_e value for the normal state is assumed to lie midway between those for I_2 and Br_2 (from Brown[40]).

In addition, the relative intensities of the $^1\sum \rightarrow {}^3\Pi_1$ and $^1\sum \rightarrow {}^3\Pi_0^+$ transitions are very much the same as for ICl when the Franck-Condon factors are taken into account. As shown in Fig. 14, the potential energy curves indicate that transitions from the lowest vibrational level of the $^1\sum$ state to the $^3\Pi_1$ state would be strongest in the region of the latter's discrete states at high vibrational quantum numbers. Transitions to the $^3\Pi_0^+$ state account for the strong absorption maximum at 4950 Å. The energy of this radiation is slightly more than enough to give excited bromine atoms; however, the path followed by the $^3\Pi_0^+$ state depends on the extent of interaction with the O^+ state, i.e., on the pressure of the system. The absorption maximum at 4050 Å is attributed to transitions to the O^+ state; this is in agreement with the observation that IBr does not exhibit a region of continuous absorption in the ultraviolet corresponding to that of ICl.[43]

D. ALKYL HALIDES

The alkyl halides have been studied extensively by both spectroscopic and photochemical means. Absorption, exhibiting band structure, occurs in the visible region and extends into the ultraviolet, where the structure merges into a continuum. The continuous absorption region of methyl iodide, first observed by Herzberg and Scheibe,[44] has been interpreted by Goodeve and Porret.[8]

Analysis of the absorption spectrum of methyl iodide (Figs. 15, 16) by Porret and Goodeve[8] shows the presence of two repulsive upper electronic states (Fig. 17). The corresponding absorption curves are shown by the dotted lines in Fig. 16. Thus, transitions to two separate upper states may occur in the same spectral region. This interpretation is in agreement with that for the inorganic halides.[45] Absorption in band A is expected to yield a methyl radical in its ground electronic state and an excited iodine atom ($^2P_{1/2}$) while absorption in the B band leads to electronically unexcited methyl radicals and iodine atoms ($^2P_{3/2}$). As shown in Fig 15, the alkyl bromides have an absorption spectrum similar to the iodides, except that the bromides are shifted

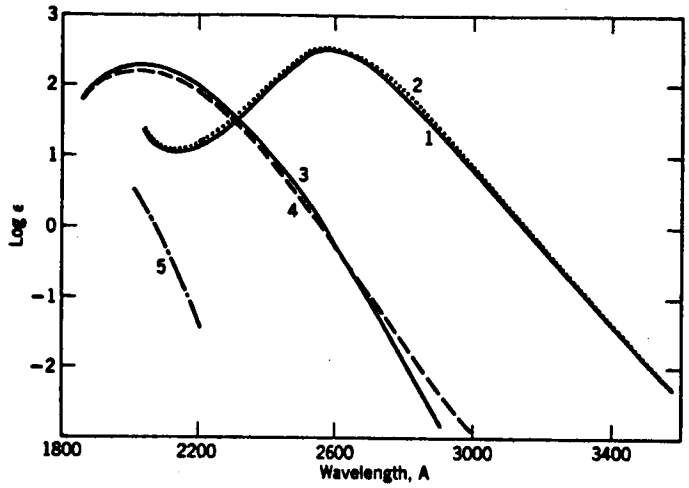

Fig. 15.
Absorption spectra of alkyl halides: (1) methyl iodide $CH_3I(g)$; (2) ethyl iodide $C_2H_5I(g)$; (3) methyl bromide $CH_3Br(g)$; (4) ethyl bromide $C_2H_5Br(g)$; (5) ethyl chloride (C_2H_5Cl) in alcohol solution (from Calvert and Pitts[25]).

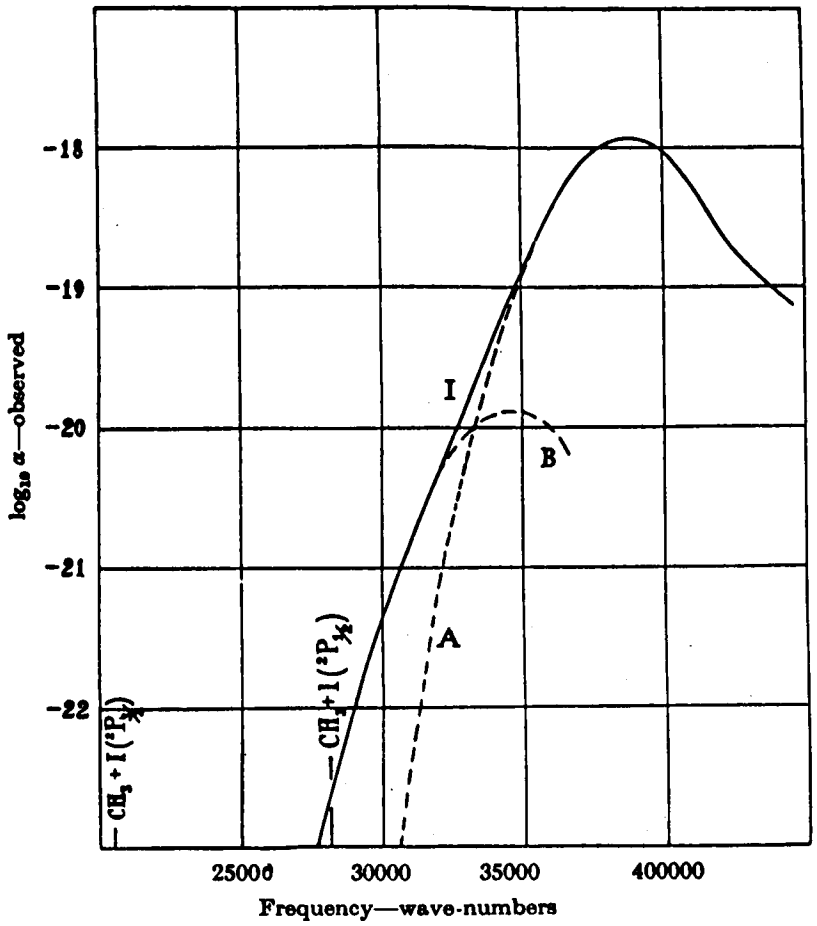

Fig. 16. The observed extinction coefficient curve of methyl iodide and the proposed resolution into two bands (from Porret and Goodeve[8]).

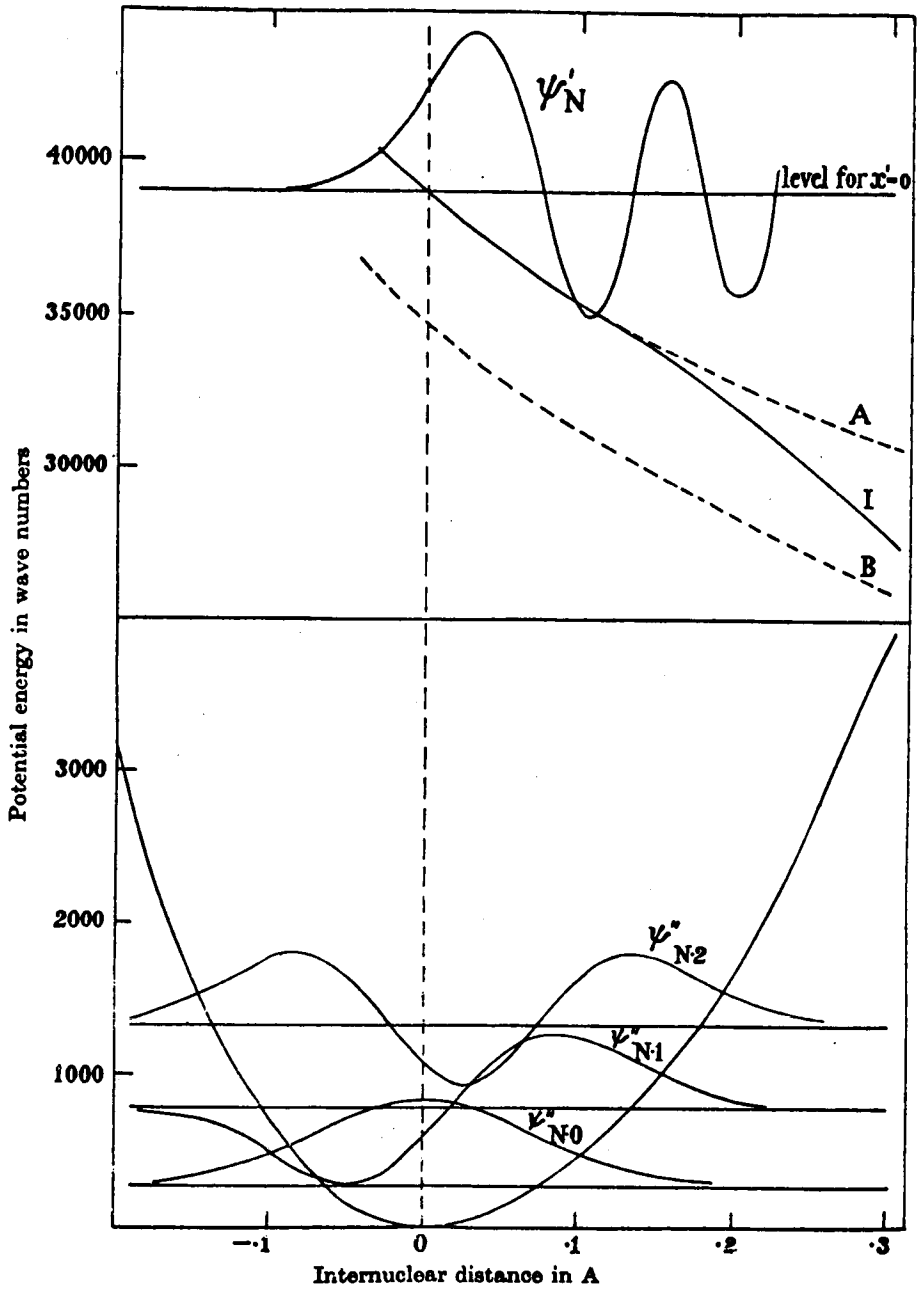

Fig. 17. The potential energy curves of the C-I link and the eigenfunction curves of some of the energy levels (from Porret and Goodeve[8]).

to shorter wavelengths. Also the absorption of either the iodides or bromides is little influenced by the size of the alkyl substituent, indicating that the absorption process is localized within the C-X band.

E. NITROSYL HALIDES

The absorption spectrum of nitrosyl chloride is shown in Fig. 18, and the potential energy diagram in Fig. 19. Absorption bands A, B, and D are broad and continuous, corresponding to electronic levels in which there is a repulsive force between some parts of the molecule.[46] From consideration of thermal and excited state energies, dissociation to NO and Cl is possible over the entire range of these bands but formation of NCl and O is possible only in band A. Since the N-O bond distance in nitric oxide is almost exactly equal to the N-O distance in nitrosyl chloride, NOCl can be considered, to a good approximation, as a diatomic molecule, ON-Cl. Curves A, B, and D were calculated[46] using this approach and 633 cm^{-1} as the vibrational frequency of the ON-Cl bond. Dissociation products from these states by extrapolation of the calculated curves are $NO(^2\Pi)$ and $Cl(^2P_{3/2, 1/2})$. The approximations do not allow a distinct choice between the $^2P_{1/2}$ and $^2P_{3/2}$ states of atomic chlorine. It was not possible to extrapolate the calculated section of curve A to the energy level of O and NCl as products without introducing a minimum at an unusually large internuclear separation or a discontinuity in curvature.[46] The bands E through L in the visible region arise from transitions to separate vibrational levels of one electronic state. The lower extinction coefficients in this region indicate a forbidden character (spin) to the transition. Predissociation is expected because of the indicated intersections of bound and continuous states (curves A-H). However, the rotational spacing (1.1 cm^{-1}) is beyond the resolution limit (3 cm^{-1}) of the instrument used by Goodeve and Katz[46] and has not yet been resolved. Thus predissociation is indicated but has not been verified spectroscopically. The upper state, corresponding to dissociation

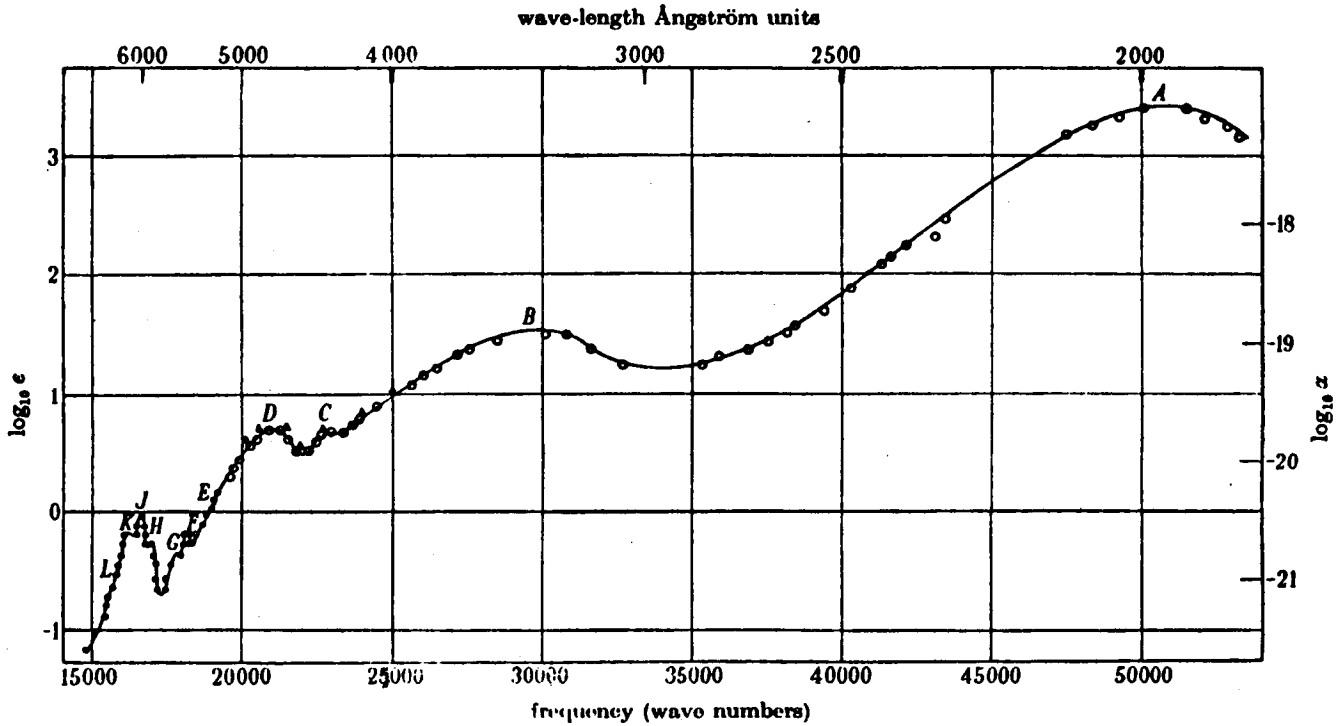

Fig. 18. Absorption spectrum of NOCl vapor at room temperature showing the 11 bands (from Goodeve and Katz[46]).

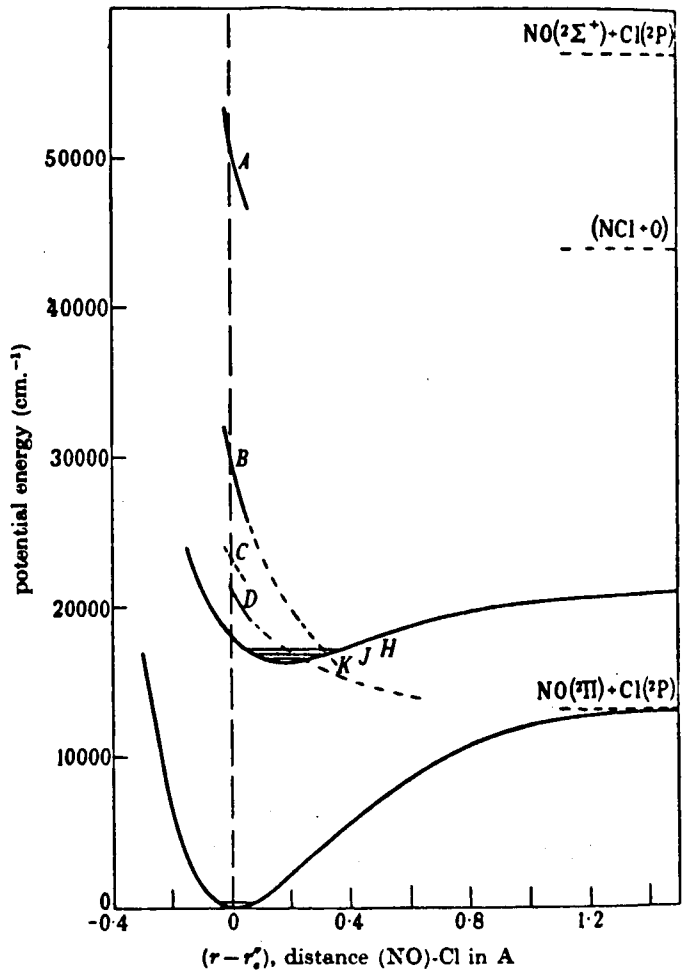

Fig. 19. Potential energy diagram of the NOCl molecule as a function of (NO)-Cl distance (from Goodeve and Katz[46]).

to NO($^4\Pi$) and Cl($^2P_{1/2, 3/2}$), was postulated by Goodeve and Katz from indirect evidence and later by Basco and Norrish[47] who studied NOCl and NOBr by flash photolysis techniques. The absorption spectrum of NOBr has not been studied in detail. Basco and Norrish indicate that it is similar to that of NOCl, but is somewhat more intense and extends more toward the red.

F. ALKYL NITROSO COMPOUNDS

The long wavelength absorption band of alkyl nitroso compounds (R-NO) occurs in the red and is most likely an $n \rightarrow \pi^*$ transition. The spectra of trifluoronitrosomethane (CF_3NO) and 2-nitroso-2-methylpropane [$(CH_3)_3CNO$] are shown in Fig. 20. The alkylnitroso compounds have fairly high, long wavelength absorption coefficients for gases: CF_3NO has an absorption maximum at ~6920 Å with $\epsilon \cong 24$ and C_3F_7NO has its maximum at 6840 Å with $\epsilon = 22.7$. They photochemically decompose[48] in red light with quantum yields of near unity for the primary dissociation process into NO and alkyl radicals:

$$CF_3N = O + h\nu \rightarrow CF_3^{\cdot} + NO$$

$$CF_3CF_2CF_2N = O + h\nu \rightarrow C_3F_7^{\cdot} + NO \quad .$$

G. NITROGEN OXIDES

The vapor phase spectra of nitrogen dioxide (NO_2) and its dimer, dinitrogen tetroxide (N_2O_4), are shown in Fig. 21. Liquid phase spectra of dinitrogen trioxide (N_2O_3) are shown in Fig. 22. At room temperature the vapor of the latter is largely dissociated into nitric oxide and nitrogen dioxide:

$$N_2O_3 \rightleftharpoons NO + NO_2 \quad .$$

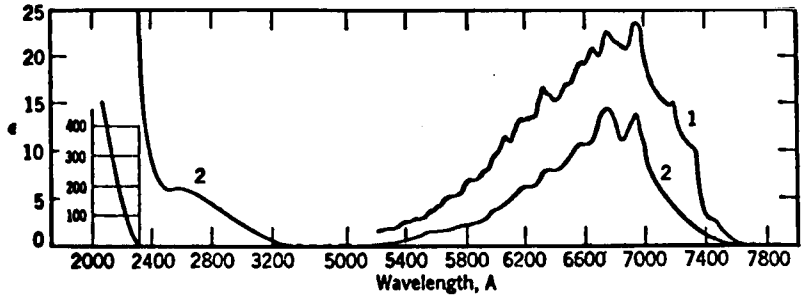

Fig. 20. Absorption spectra. (1) Trifluoronitrosomethane [$CF_3NO(g)$. (2) 2-nitroso-2-methylpropane [$(CH_3)_3CNO(g)$], 25°C. From Calvert and Pitts.[25]

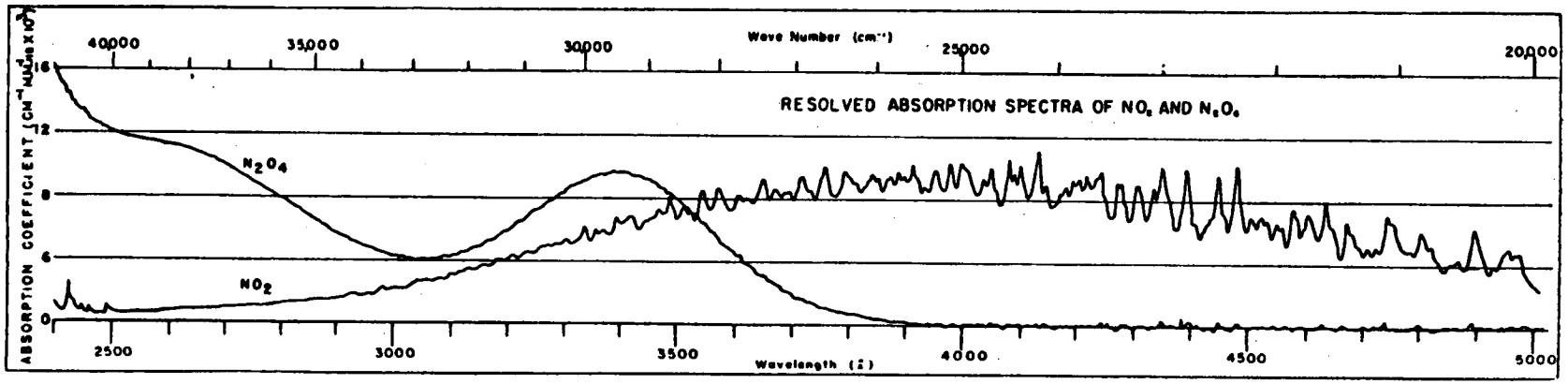

Fig. 21. Absorption spectra $(1/pl \log_{10} I_o/I)$ of NO_2 and N_2O_4 versus wavelength and wave number, measured at 25°C. (From T. C. Hall, Jr., and F. E. Blacet, J. Chem. Phys. 20, 1745 (1952)).

A potential energy diagram illustrating the electronic states thought to be involved in the photolysis of NO_2 in the visible and near ultraviolet regions is shown in Fig. 23. The orbital energies, calculated by Green and Linnett,[49] are shown diagrammatically in Fig. 24. These energy levels place the following allowed transitions in the visible and near ultraviolet regions.

(1) $4a_1\ ^2A_1 \longrightarrow 2b_1\ ^2B_1$ (7600 Å)

(2) $3b_2\ ^2A_1 \longrightarrow 4a_1\ ^2B_2$ (4600 Å)

(3) $4a_1\ ^2A_1 \longrightarrow 5a_1\ ^2A_1$ (<4100 Å)

H. CHLORINE OXIDES

The absorption spectrum of chlorine monoxide (Cl_2O) has been studied by Goodeve and Wallace[50] and Finkelnburg, et al.,[51] (Fig. 25); its extinction coefficient was measured over the range 6200 to 2200 Å. The entire band is continuous but is apparently composed of three independent bands defined by the limits 16,000 to 20,000 cm^{-1}, 20,000 to 26,000 cm^{-1}, and 26,000 to 45,000 cm^{-1} (Ref. 50). The analysis does not allow a clear decision as to the excitation of the dissociation products, but a ClO fragment and an excited chlorine atom are expected at wavelengths less than 5300 Å.

$$Cl_2O + h\nu \rightarrow ClO\cdot + Cl\cdot \quad .$$

The spectrum of chlorine dioxide (ClO_2) in carbon tetrachloride solution is shown in Fig. 26 along with that of other chlorine oxides. Chlorine dioxide has absorption maxima at 3550 and 3750 Å, and absorbs on the long wavelength side out to about 4400 Å. Lifscomb, Norrish, and Porter[52] studied the flash photolysis of ClO_2 vapor and concluded that the primary photolysis reaction is:

$$ClO_2 + h\nu \rightarrow ClO\cdot + O\cdot \quad .$$

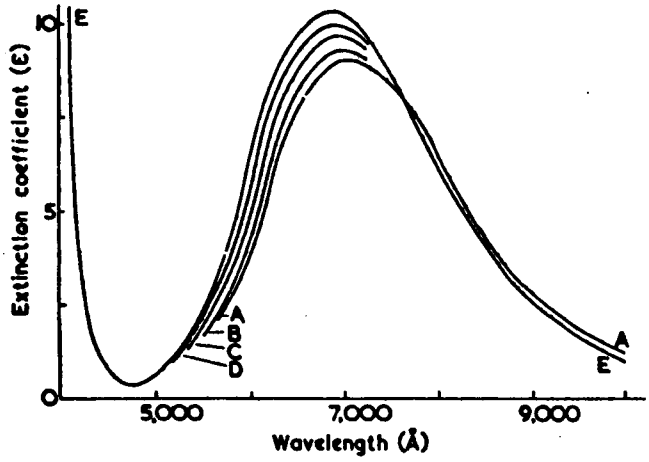

Fig. 22.
The extinction coefficients of dinitrogen trioxide at different liquid compositions, at 10°C. (A, liquid composition $x_1 = 1.946$; B, $x_1 = 1.896$; C, $x_1 = 1.823$; D, $x_1 = 1.789$; E, $x_1 = 1.735$). (From A. J. Vosper, J. Chem. Soc. 1760.)

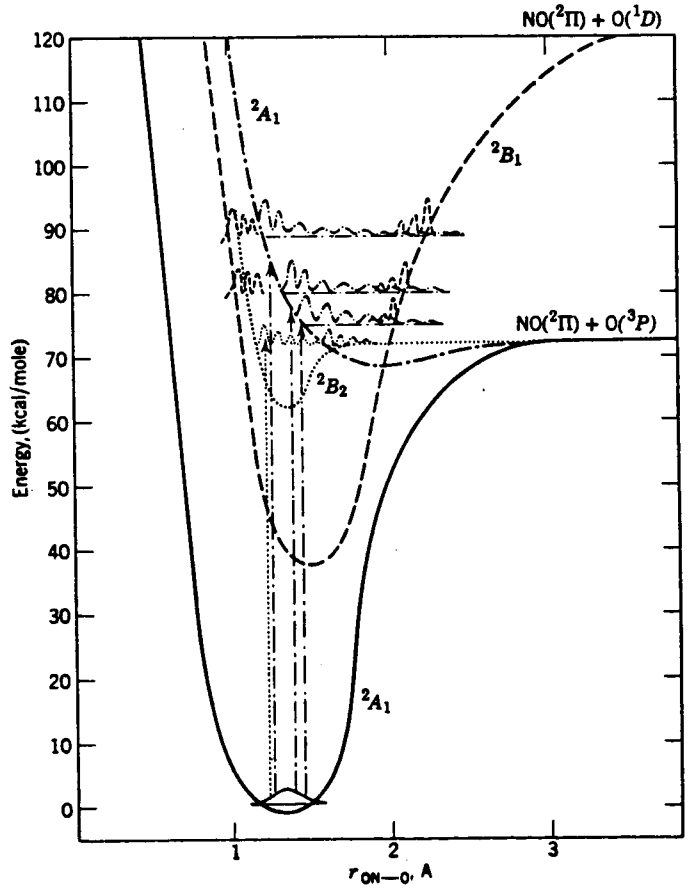

Fig. 23.
Approximate potential energy diagram for some probable electronic states of NO_2. (From J. N. Pitts, J. H. Sharp, and S. J. Chan, J. Chem. Phys. 40, 3655 (1964).

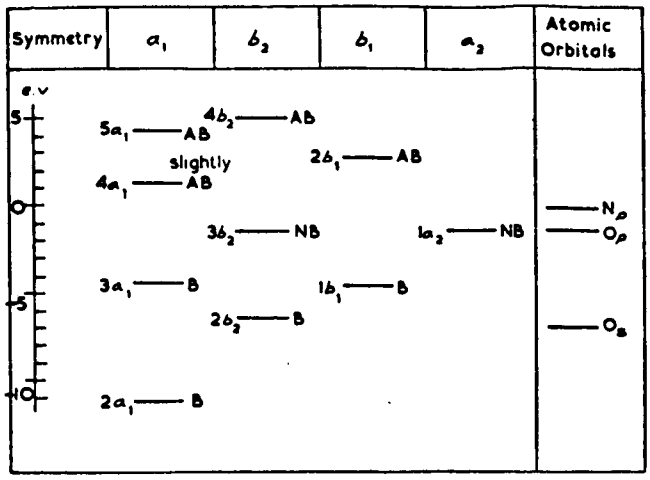

Fig. 24.
Orbital energies in NO_2 relative to a nitrogen p orbital. B, bonding; NB, non-bonding; AB, anti-bonding.

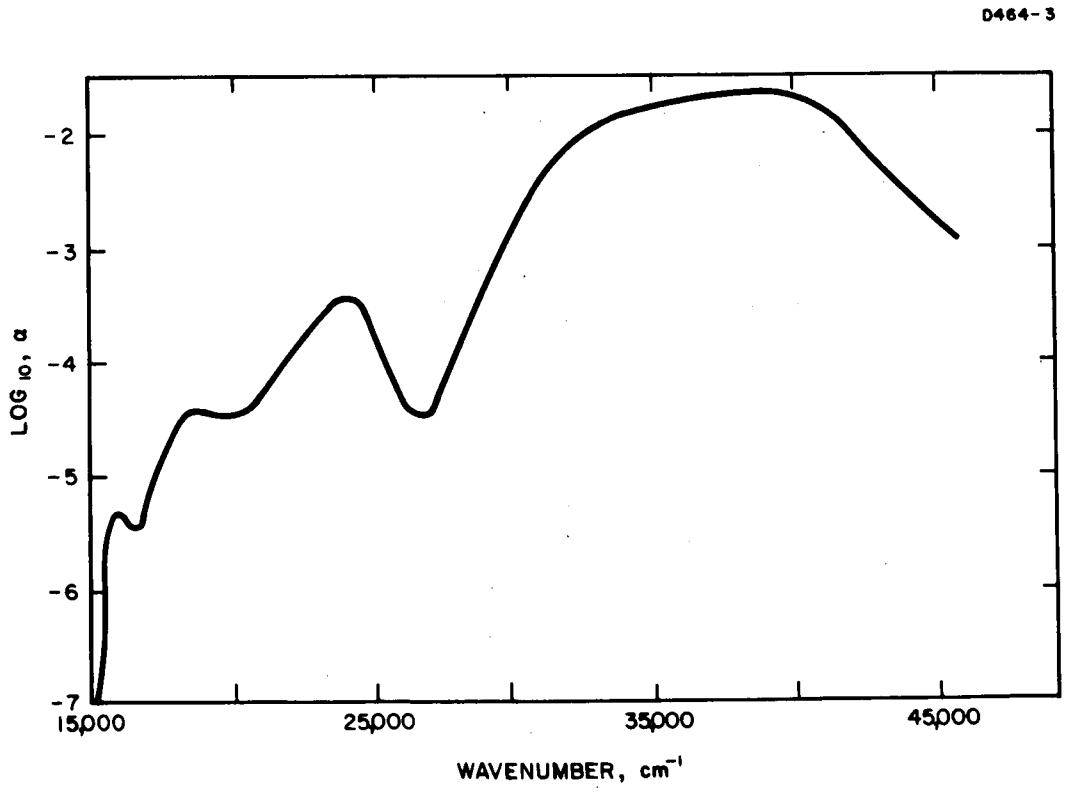

Fig. 25. Absorption spectrum of Cl_2O; a = 1/P (mm) (cm) log I_o/I (from Finkelnburg, et al.,[51]).

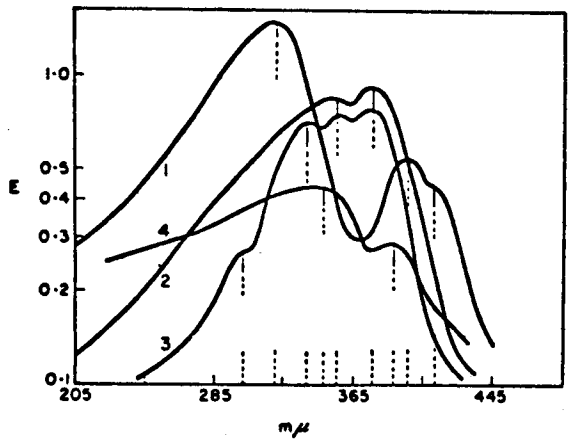

Fig. 26. Absorption spectra of chlorine oxides dissolved in carbon tetrachloride. (1) $Cl_2 + Cl_2O$. (2) ClO_2. (3) $ClO_2 + Cl_2O_6$. (4) Cl_2O_7 (from Z. Spurny, Talanta 9, 885 (1962)).

I. CYANIDES

The potential energy diagrams for iodine cyanide[53] (ICN) and the cyanyl radical[54] are shown in Figs. 27 and 28. Operation of the ICN system by solar pumping is likely to be marginal, since the onset of absorption occurs at 3100 Å. However, fluorescence has been observed from the $B^2\Sigma^+$ excited state of the CN radical during both flash photolysis[56] and continuous irradiation studies of ICN.[57-59] No fluorescence from $CN(^2\Sigma)$ was reported for continuous photolyses carried out with radiation of wavelengths greater than 1864 Å, although the possibility of emission from the $A^2\pi$ state of CN does not seem to have been investigated under these conditions.

Since the bond dissociation energy[56] of ICN is 64 kcal/mole, the energy of the radiation absorbed at the longest wavelength (~ 3100 Å) is sufficient to produce excited dissociation fragments. The flash photolysis studies show that although appreciable populations of vibrationally excited CN states are attained in the system, they result from secondary electronic absorption by CN which is initially produced in the $X^2\Sigma'$ (v = 0) state. This result implies that the iodine atom may be formed in the electronically excited $^2P_{1/2}$ level as in the alkyl halides. However, if the potential energy diagram for ICN (Fig. 27) is correct, excited iodine atoms would not be expected with radiation of wavelengths greater than 2400 Å.

The absorption spectra of carbonyl cyanide, $CO(CN)_2$, is given in Fig. 29, and a schematic representation of the potential energy of carbonyl cyanide as a function of the $\theta_{c\text{-}c\text{-}c}$ angle for the dissociative state and for different vibrational levels of the A_2 state is given in Fig. 30.

The energy levels and electronic transitions of formaldehyde are illustrated in Fig. 31 for reference. These states and transitions are analogous to those for carbonyl cyanide. Rotational and vibrational analysis of the absorption spectra shows that formaldehyde has a pyrimidal structure in the first excited state, while the excited state configuration of unsaturated aldehydes is planar.[62-64] In the case of carbonyl cyanide the rotational structure has not been resolved, but

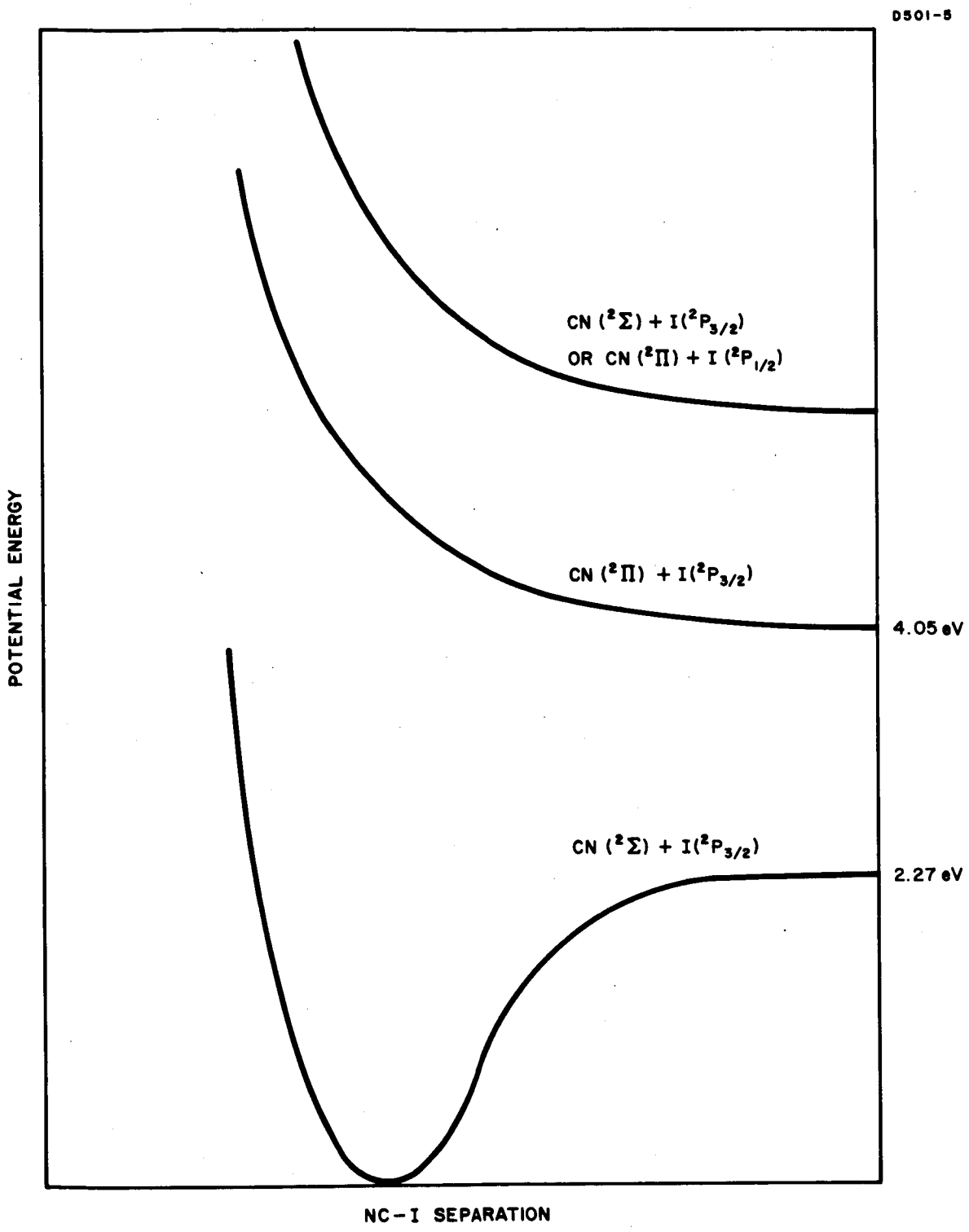

Fig. 27. Approximate potential energy curves showing the potential energy of the ICN molecule as a function of the carbon-iodine separation, for three electronic states (from Badger and Woo[53]).

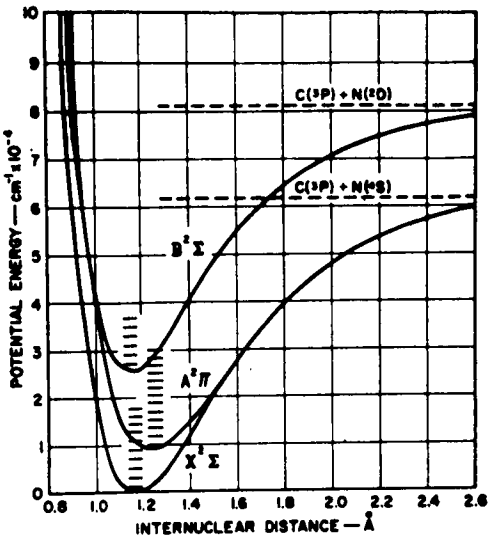

Fig. 28.
The potential energy diagram for CN (from Young[55]).

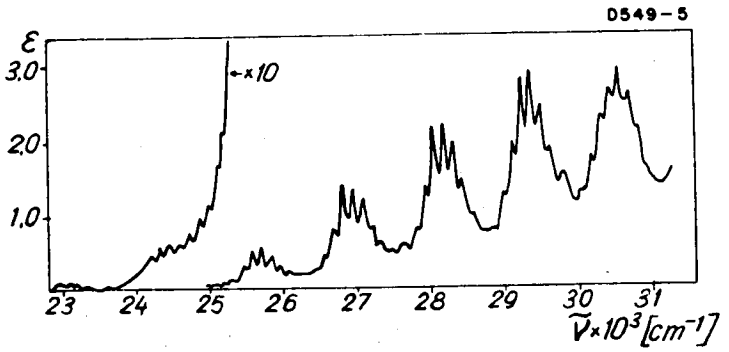

(a)

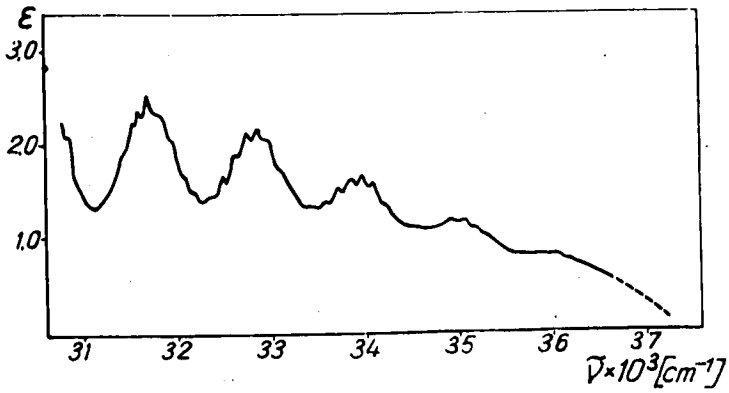

(b)

Fig. 29.
Absorption spectrum of $CO(CN)_2$ vapor (from Prochorow[60]).

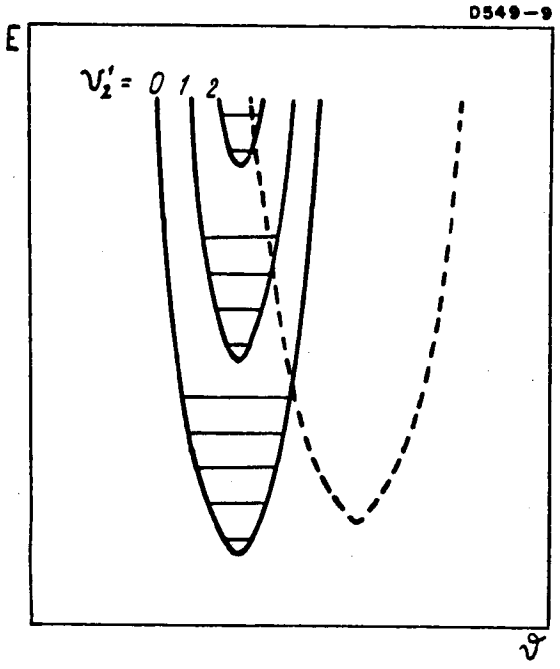

Fig. 30. Schematic representation of potential curves $V = F(\theta)$ for the A_2 and dissociative state of $CO(CN)_2$ (from Prochorow[60]).

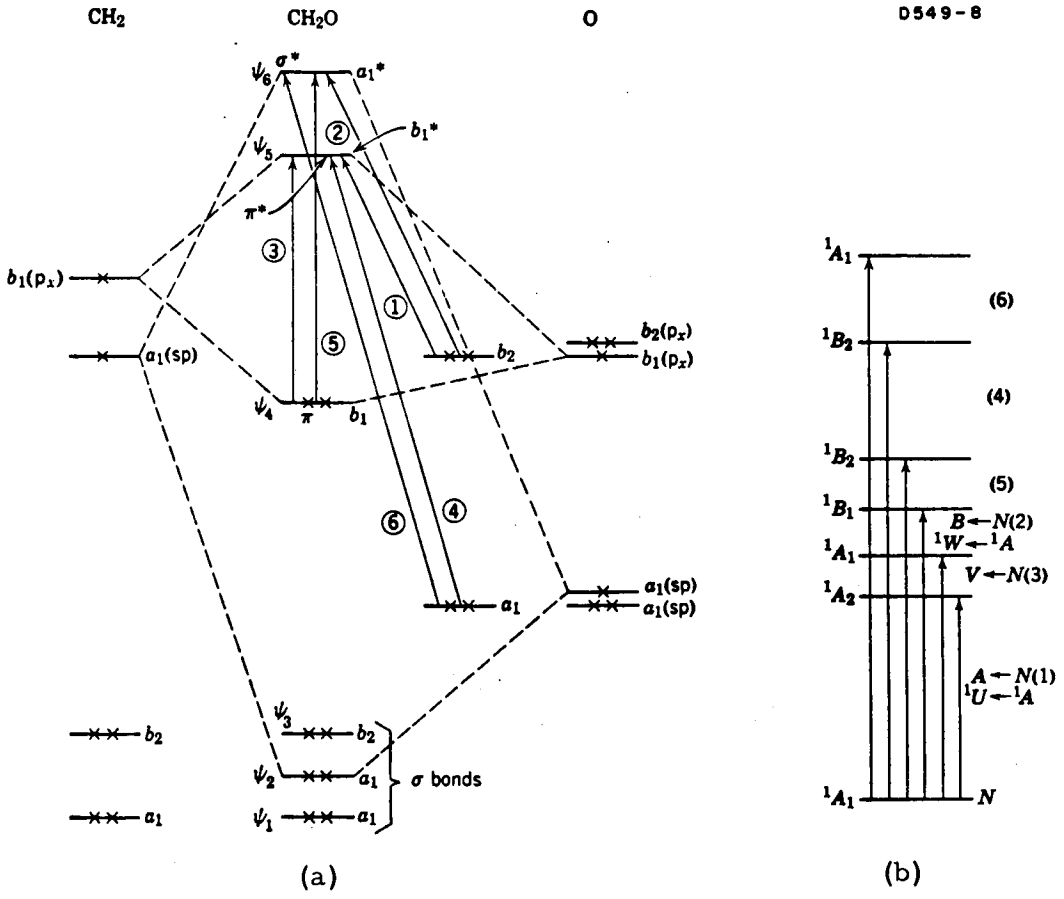

Fig. 31. The energy level diagram (a), and the term-level diagram (b), of formaldehyde (from Jaffé and Orchin[31]).

the vibrational analysis indicates that the first excited state corresponds to a planar configuration.[60] Kemula and Wierzchowski[65] have shown that carbonyl cyanide is photodecomposed by ultraviolet radiation with CO and $(CN)_2$ as the final products of reaction. Formation of $(CNCO)\cdot$ and $(CN)\cdot$ radicals is thought to be the primary photochemical process.

The absorption spectrum of $CO(CN)_2$ shows predissociation effects quite clearly; however, the predissociation limit depends strongly on the quantum number of the carbon skeleton bending frequency. This dependence of the dissociation limit is related to the difference in equilibrium values of the valence angles in the A_2 and dissociative states. It can be seen from Fig. 30 that intersection points depend on the vibrational numbers of the A_2 state and the bending vibration. The predissociation limits deduced from the spectra are 30,000; 27,030; 28,110; and 29,050 cm^{-1}, corresponding to the combinations ($v'_2 = 4$, $v'_5 \geq 0$); ($v'_2 = 1$, $v'_5 = 3$); ($v'_2 = 2$, $v'_5 = 2$); and ($v'_2 = 3$, $v'_5 = 1$).[1] The normal vibrations are indicated in Fig. 32.

J. METAL CARBONYLS

Absorption spectra for the carbonyl compounds of iron, vanadium, chromium, and nickel [$Fe(CO)_5$, $V(CO)_6$, $Cr(CO)_6$, and $Ni(CO)_4$] are shown in Figs. 33-36. The metal carbonyl compounds are expected to photodecompose to carbon monoxide. This has been demonstrated in the case of iron pentacarbonyl which photodecomposes in the gas phase with a quantum efficiency of two for carbon monoxide formation.[68] On the other hand, nickel tetracarbonyl exhibits great stability toward photodecomposition in the gas phase. The gas phase photochemistry of vanadium and chromium hexacarbonyl has not been investigated, although the photochromic behavior of chromium hexacarbonyl has been studied in liquid solutions, low temperature glasses, and polymer matrices.[69,70] Under these conditions the primary process is thought to be photodissociation of $Cr(CO)_6$ to $Cr(CO)_5$ and CO. Therefore, photodissociation of this metal carbonyl is also anticipated in the gas phase. Because of the weak absorption of these compounds in the

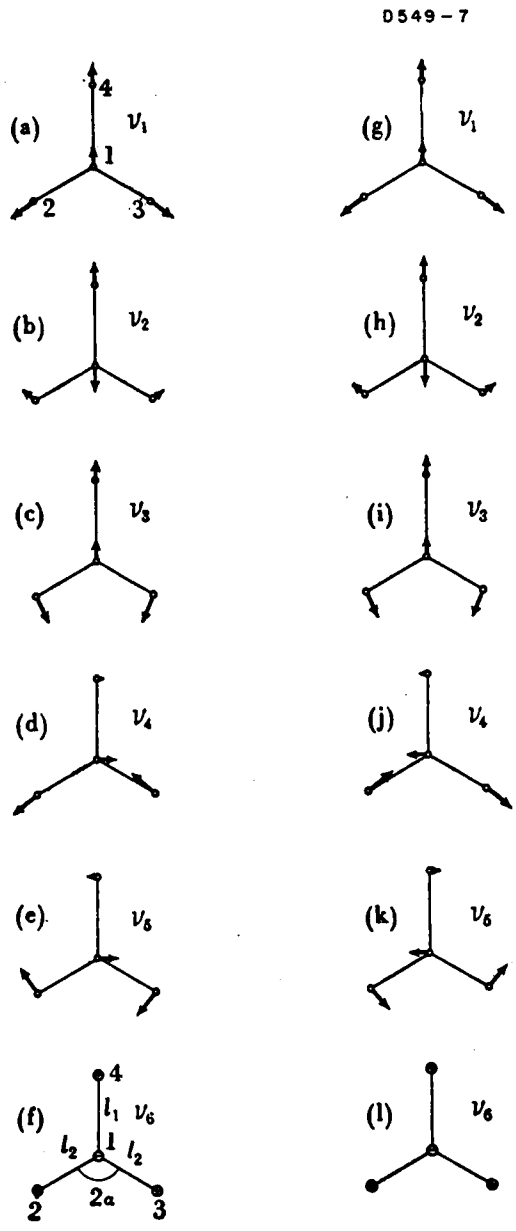

Fig. 32.
Normal vibrations of an XYZ_2 molecule and their behavior for a reflection at the plane of symmetry through XY perpendicular to the plane of the molecule (from Herzberg[32]).

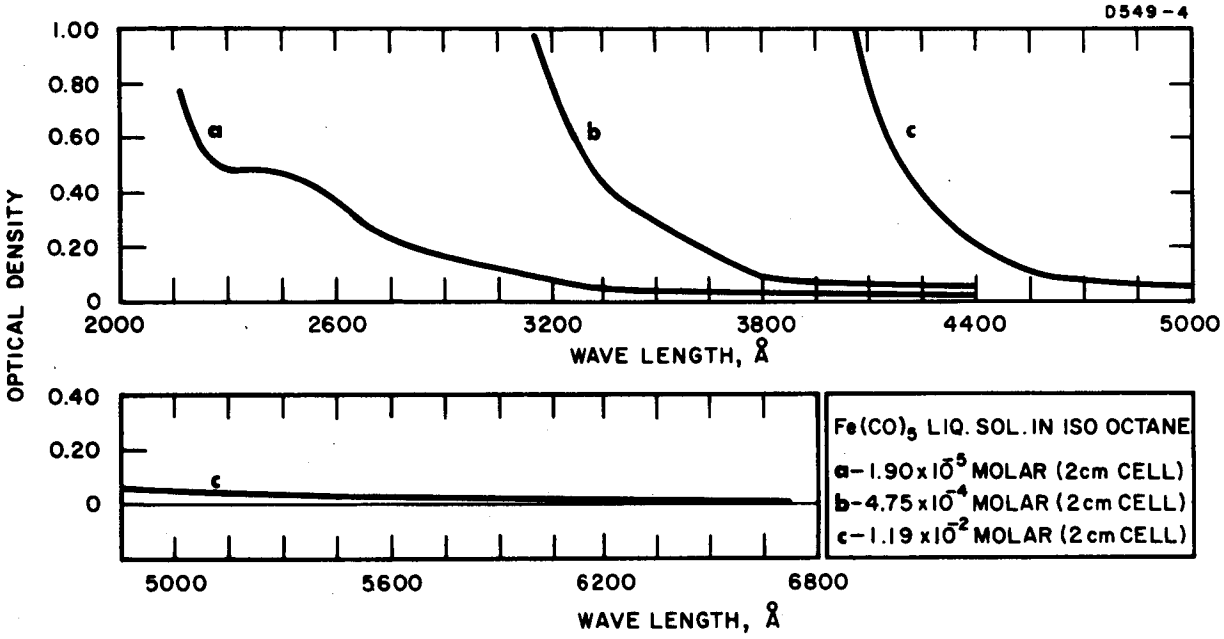

Fig. 33. The visible and ultraviolet spectrum of $Fe(CO)_5$ (from Sheline[66]).

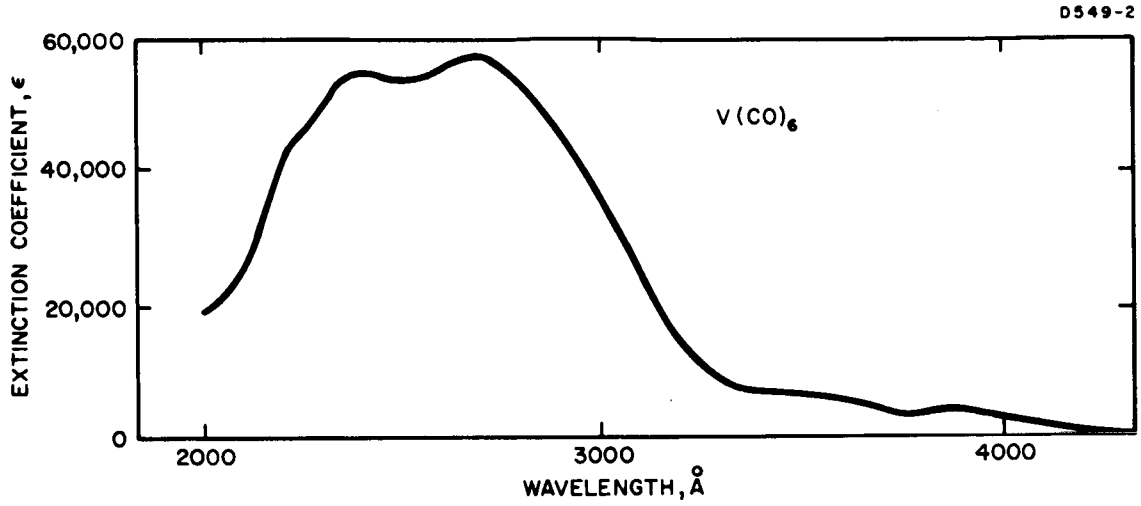

Fig. 34. Absorption spectrum of gaseous $V(CO)_6$ (from Haas[67]).

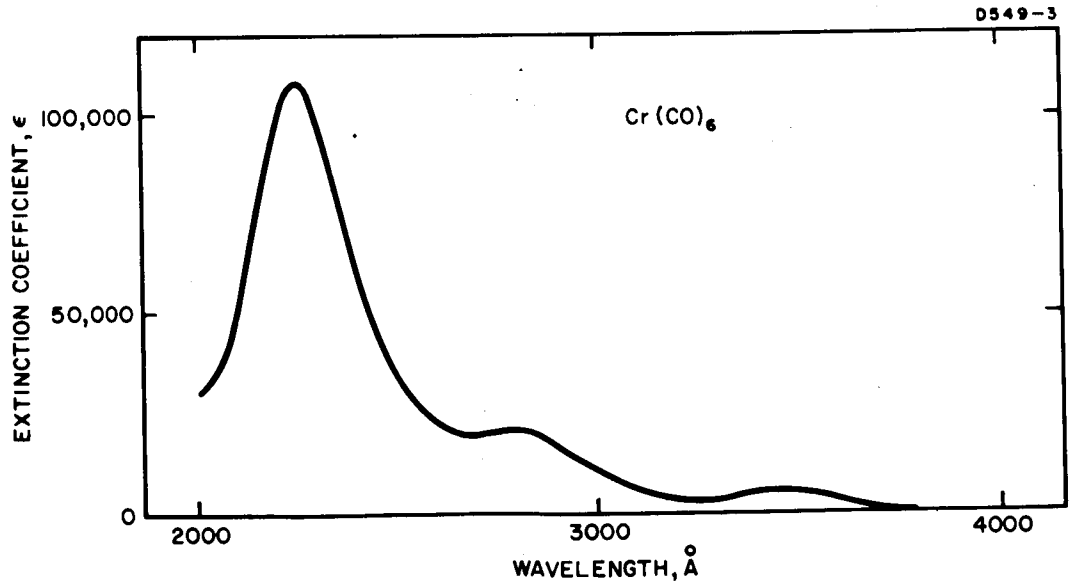

Fig. 35. The ultraviolet spectrum of gaseous $Cr(CO)_6$ (from Haas[67]).

visible portion of the spectrum, solar operation is likely to be marginal unless chain processes can be set up. Polanyi[71] has detected infrared emission from high vibrational levels of carbon monoxide in mercury quenching experiments. Hence laser action may be possible from systems such as the metal carbonyls, which can produce CO photochemically.

K. SULFUR, SELENIUM, AND TELLURIUM COMPOUNDS

The spectra of various sulfur chlorides are shown in Fig. 37, while spectra of sulfur monochloride (S_2Cl_2) and thionyl chloride ($SOCl_2$) are shown in Fig. 38. Sulfur dichloride (SCl_2) in cyclohexane[74] absorbs in the visible range with a maximum at 3950 Å and an inflection point near 5250 Å. Sulfur monochloride absorbs more strongly,[75] but in the short wavelength region; it has maxima at 2640 Å and 3050 Å. Solutions of S_2Cl_2 undergo photochemical decomposition,[76] but the reaction has not been studied in detail.

The spectra of carbon disulfide (CS_2), carbon oxysulfide (COS), and carbon diselenide (CSe_2) are given in Fig. 39. In heptane solution the last has absorption maxima[77] at 3760 Å and 2430 Å. Flash photolysis studies[78,79] indicate that ultraviolet light in the 2300 Å band gives partial decomposition into an electronically excited selenium atom and a vibrationally excited CSe radical.

$$CSe_2 + h\nu \rightarrow CSe\ (X^1\Sigma,\ v \leq 3) + Se\ (4^3P_{2,1,0}) \quad .$$

Although carbonyl sulfide COS is likely to operate as a photodissociative laser on the CO vibrational levels and possibly the atomic $^1D \rightarrow {}^3P$ transition of sulfur, solar pumping probably will not be feasible since the onset of absorption occurs at 2550 Å, with maxima at 2300 and 1510 Å (Ref. 80). The longest wavelength bands of COS are very diffuse, indicating that predissociation is operative; photochemical studies by Gunning, et al.,[81] show that dissociation occurs in the spectral region from 2290 to 2550 Å and that ^1D sulfur atoms

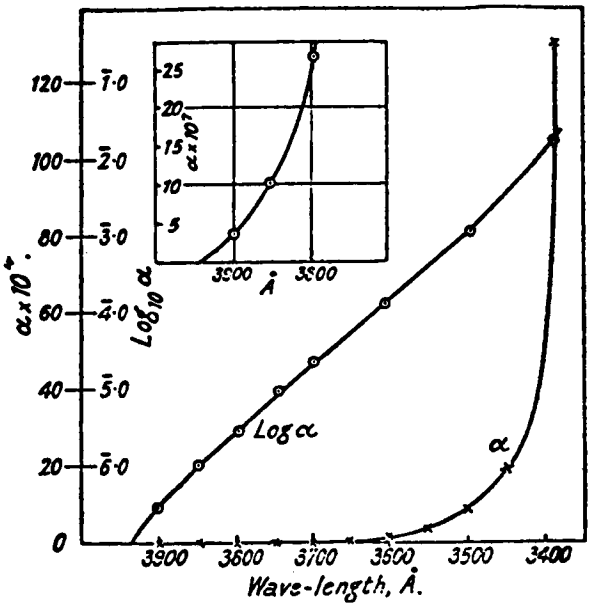

Fig. 36.
Values of extinction coefficient and of log α as a function of wavelength for $Ni(CO)_4$ (from Thompson and Garratt[68]).

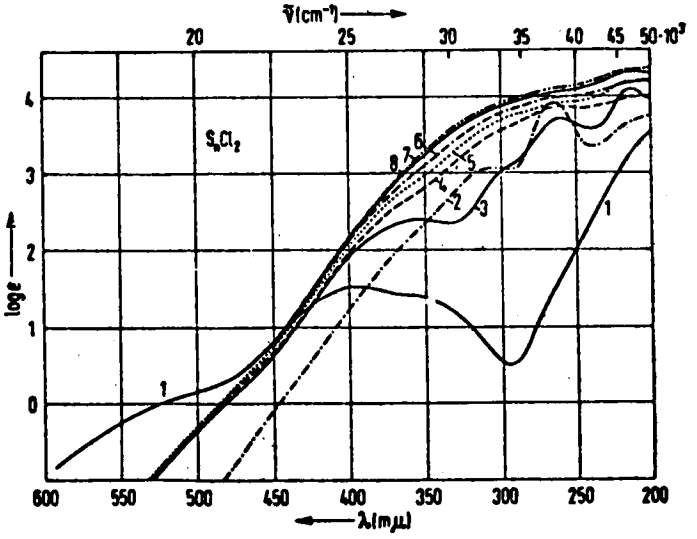

Fig. 37.
Absorption spectra of various sulfur chlorides (from Feher and Muenzner[72]).

are produced. Laser action has been obtained from pulsed discharges through pure COS and COS-N_2, COS-He, COS-CO, and COS-CO-He mixtures by Deutsch.[82] Emission at 31 wavelengths near 8.39 μ and 8.25 μ and at 29 wavelengths between 5.1 and 5.7 μ was observed. The latter set of lines is thought to result from the formation of vibrationally excited CO by decomposition of COS.

The spectra of the Group VI hydrides, H_2S, H_2Se and H_2Te, are given in Fig. 40, which shows that they have appreciable absorption only in the ultraviolet region.

Thiophosgene ($CSCl_2$) has a weak $n - \pi^*$ absorption band system in the visible region[83] out as far as 6000 Å. The organization of the spectrum of the 5340 Å band system is similar to that of the corresponding band system of formaldehyde.

L. OTHER COMPOUNDS

Ozone (O_3) absorbs strongly in the ultraviolet but only very weakly in the visible region, as shown in Fig. 41. In both regions it photodissociates into oxygen atoms and oxygen molecules. The visible band of ozone is considered to be a singlet-triplet excitation followed by formation of ground state products[25]:

$$O_3(S_o) + h\nu \rightarrow O_3(T_1) \rightarrow O_2(^3\Sigma_g^-) + O(^3P) \quad .$$

The strong ultraviolet band is probably an allowed singlet-singlet transition followed by decomposition into singlet products:

$$O_3(S_o) + h\nu \rightarrow O_3(S_1) \rightarrow \begin{cases} O_2(^1\Delta g) + O(^1D) \\ O_2(^1\Sigma g^+) + O(^1D) \end{cases} \quad .$$

Biacetyl ($CH_3COCOCH_3$) absorbs in the solar region, λ_{max} = 4100 Å (see Fig. 42), and photodissociates to CO, but not appreciably at room temperature.[25] The quantum yield of CO, Φ_{CO},

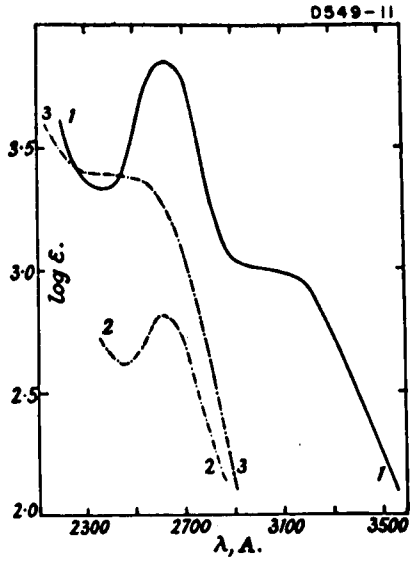

Fig. 38.
Ultraviolet absorption spectrum of S_2Cl_2 (from Koch[73]).

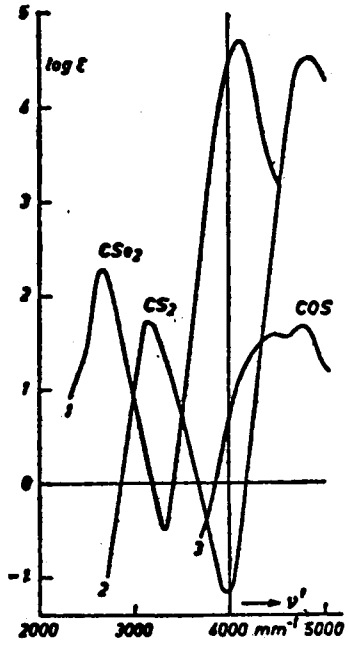

Fig. 39.
Ultraviolet absorption spectra. (1) CSe_2. (2) CS_2. (3) COS. (From Tzeiber, et al.,[77])

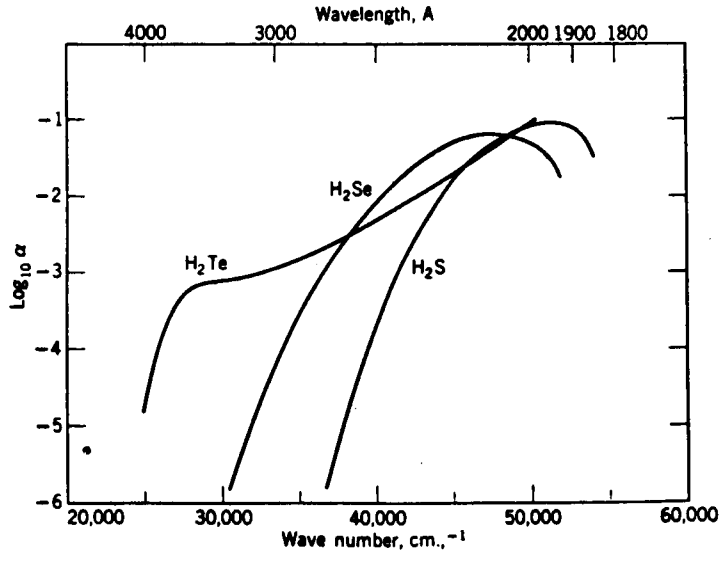

Fig. 40. The absorption spectrum of H_2S, H_2Se, and H_2Te; the absorption coefficient $a = \log (I_o/I)/\rho(atm)/cm$ (from Calvert and Pitts[25]).

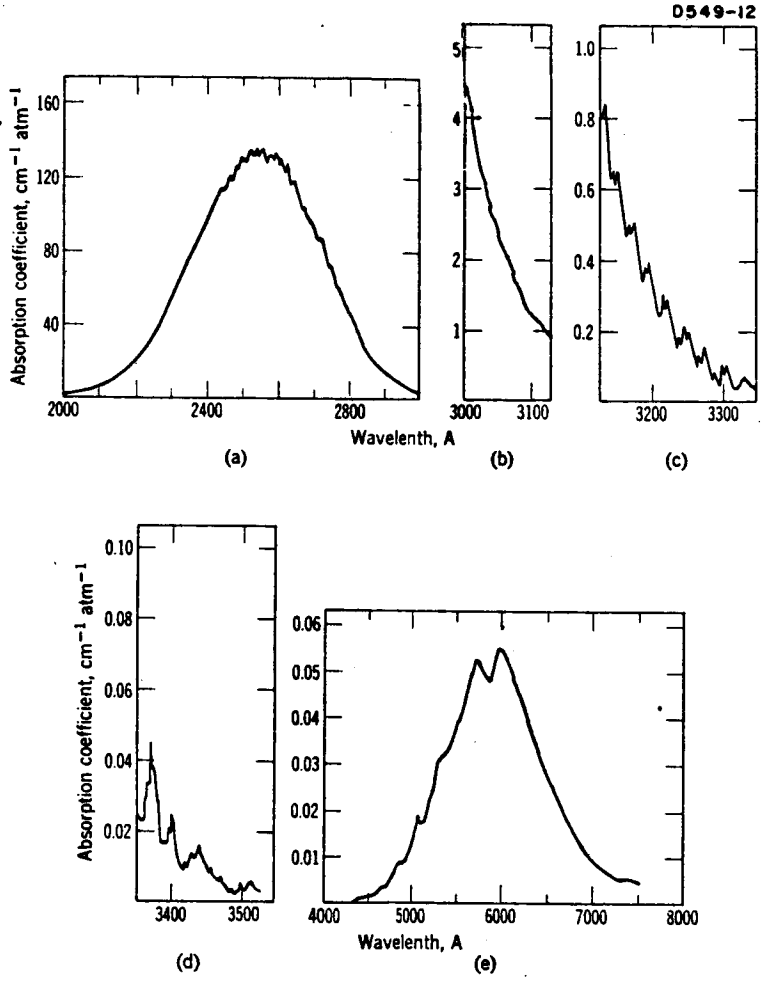

Fig. 41. Absorption spectrum of O_3 (from Calvert and Pitts[25]).

is 0.001 at 28°C, 0.04 at 100°C and 0.4 at 198°C with light of wavelength 4358 Å. Dissociation increases at shorter wavelengths; Φ_{CO} = 0.03 (28°), 0.2 (75°) at 3660 Å, and 0.5 (150°) at 2500 Å.

The absorption spectrum[84] and potential energy diagram for hydrogen iodide (HI) are shown in Figs. 43 and 44. Although the primary photochemical split of HI into atoms occurs with a quantum yield of near unity, the absorption of light is restricted to the short ultraviolet. The extent of excited iodine atom formation is wavelength dependent, as both of the following processes occur.[25]

$$HI + h\nu \rightarrow H(^2S_{1/2}) + I(^2P_{3/2})$$
$$\searrow H(^2S_{1/2}) + I(^2P_{1/2}) \quad .$$

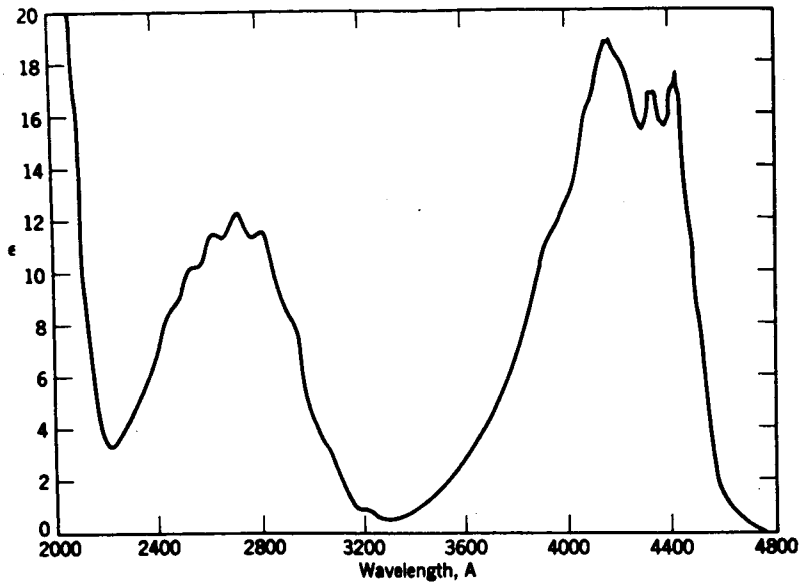

Fig. 42. Absorption spectrum for biacetyl [$CH_3COCOCH_3$(g)], 25°C (from Calvert and Pitts[25]).

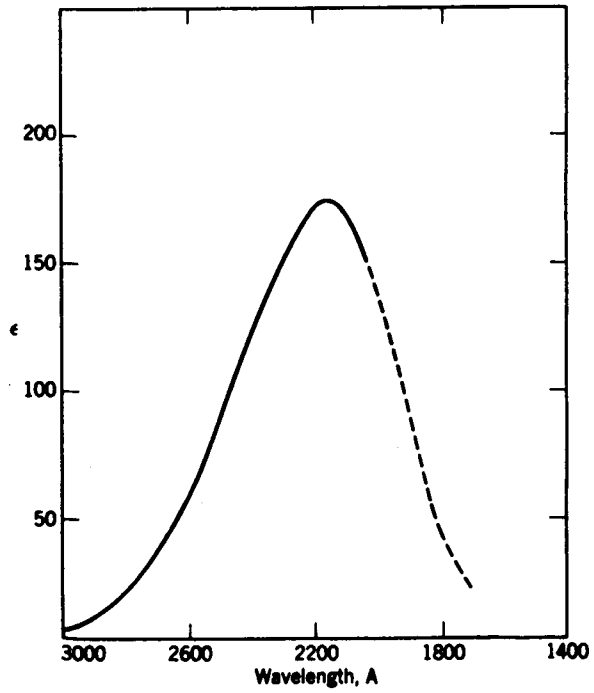

Fig. 43.
Absorption spectrum of HI (from Calvert and Pitts[25]).

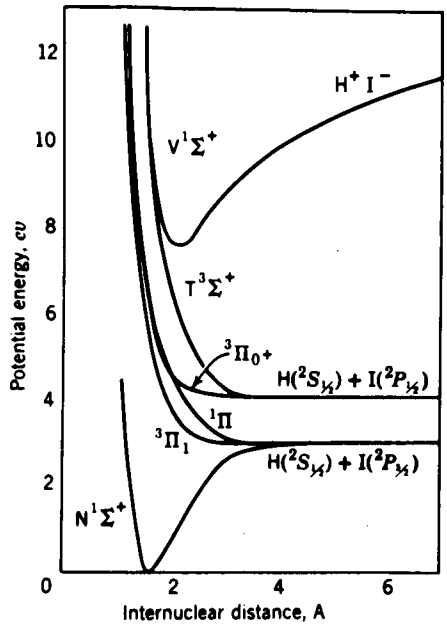

Fig. 44.
Potential energy curves for the lowest electronic states of HI (from Calvert and Pitts[25]).

SECTION IV

PHOTOCHEMISTRY

A. INTRODUCTION

The primary photochemical and secondary thermal processes which molecules undergo are of prime concern in a study of solar pumped photodissociative lasers. In this section we discuss the photochemistry and kinetics of several molecules in more detail with regard to their use as laser materials. The multitude of possible processes available to a molecule after absorption of a light quantum have recently been summarized by Calvert and Pitts[25]; they are shown in Table II. Which competitive reaction is undergone by the excited molecule is determined by such factors as the radiative lifetime of the molecule, the nature of the potential energy surfaces, the number of collisions, and the nature of the collision partner. Stepwise vibrational deactivation, differing intrinsic chemical reactivities of states of different multiplicity at each vibrational level, and energy transfer by intra- and intermolecular processes add to the complexity of molecular systems.

B. RATE OF TERMOLECULAR ATOMIC RECOMBINATIONS

Atomic recombination reactions are expected to be of importance in most of the photodissociative systems which we have suggested. This class of reactions was recently discussed by Kim[85]; calculations of the rate coefficient for the recombination of atomic halogens, oxygen, nitrogen, and hydrogen in the presence of an excess of various third bodies were carried out and compared with experimental values. Thus it is of interest to examine the method of calculation, the agreement with experiment, and the applicability of the results to gas mixtures employed in laser systems.

TABLE II

The Reaction Paths of an Electronically Excited Simple Molecule

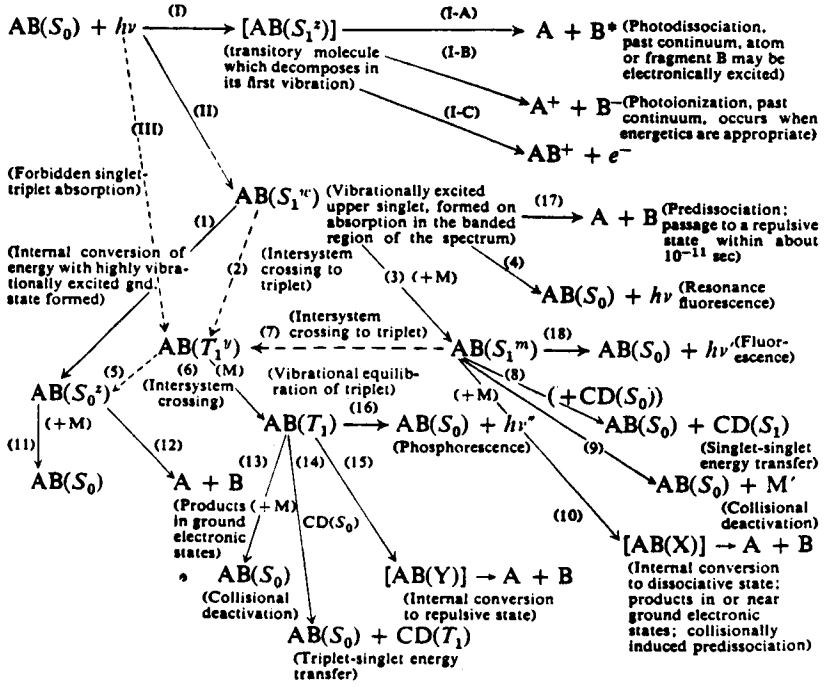

1. Formulation of the Rate Constant

The over-all reaction to be considered is

$$X + X + M \rightarrow X_2 + M \quad , \tag{36}$$

and the assumed mechanism which was originally suggested by Bunker and Davidson[86] involves an equilibrium

$$X + M \rightleftharpoons MX \tag{37}$$

and the elementary reaction

$$MX + X \rightarrow X_2 + M \quad . \tag{38}$$

MX is defined as a complex whose lifetime is longer than the average time of a collision. This includes the "bound" dimers of Bunker and Davidson,[86]

"metastable" dimers considered by Stogryn and Hirschfelder,[87] and "orbiting pairs" introduced earlier by Kim and Ross.[88] It is further assumed that the atom X and the dimer complex MX are rigid spheres. The equilibrium constant for reaction (37) is derived by using the Lennard-Jones potential for interaction between X and M and the above conditions.[88]

$$K = \frac{N_{MX}}{N_M N_X} = \frac{16}{15} \sigma_{MX}^3 (\pi T^{*3})^{-1/2} Qr \qquad (39)$$

where

$$Qr = 14.1 (1 - 0.245 T^{*-1} + 0.086 T^{*-2} - \ldots) . \qquad (40)$$

N_{MX}, N_M, N_X are the number densities, T^* is a reduced temperature (kT/ϵ_{MX}), and σ_{MX} and ϵ_{MX} are molecular parameters of the intermolecular potential function. The number of collisions between X and MX per unit time consistent with the spherical model is

$$Z = (8 RT/\pi\mu)^{1/2} \pi\sigma_c^2 N_X N_{MX} \qquad (41)$$

where $\pi\sigma_c^2$ is the collision cross section and μ is the reduced mass, $M_X M_{MX}/(M_X + M_{MX})$. The rate of disappearance of X is given by

$$- \frac{dN_X}{dt} = k_1 N_X^2 N_M = 2k_3 N_X N_{MX} \qquad (42)$$

N_{MX} is given by (39) as

$$N_{MX} = K N_M N_X . \qquad (43)$$

Thus

$$k_1 = 2k_3 K . \qquad (44)$$

It is then assumed that reaction (38) occurs at every collision with zero activation energy (i.e., $k_3 = (Z/N_X N_{MX})$). By combining equations (39), (41), and (44) and allowing for the electronic degeneracies g_x and g_{x_2} and a steric factor P, k_1 is given in terms of the molecular parameters discussed above.

$$k_1 = P(g_{x_2}/g_x^2)\,(64\pi N_A^2/15)\,(2R/\mu)^{1/2}\,(\epsilon_{MX}/k)^{3/2}\,\sigma_{MX}^3\,\sigma_c^2 T^{-1} Q_r \tag{45}$$

where N_A is Avogadro's number. If Q_r is approximated by its high temperature limit (14.1), eq. (45) becomes

$$k_1 = 8.84 \times 10^{13}\, P(g_{x_2}/g_x^2)\,\mu^{-1/2}\,(\epsilon_{MX}/k)^{3/2}\,[\sigma_{MX}(\text{Å})]^3\,[\sigma_c(\text{Å})]^2 T^{-1} \quad \text{cm}^6\text{-mole}^{-2}\text{-sec}^{-1} . \tag{46}$$

The (1/T) dependence of k_1 is in satisfactory agreement with the experimental work of Kiefer and Lutz[49] and Rink.[90, 91]

2. Halogen Atom Recombination

The polarizability of halogen atoms is approximated by that of the nearest inert gas atom. In this way the Lennard-Jones potential parameters (ϵ_{MX} and σ_{MX}) between the halogen atom and the third body molecule are obtained from the mixture rules.[86, 92]

$$\epsilon_{MX} = (\epsilon_M \epsilon_X)^{1/2} \tag{47}$$

$$\sigma_{MX} = (\sigma_M + \sigma_X)^{1/2} \tag{48}$$

where ϵ_M and σ_M are parameters of the third body molecule M, and ϵ_X and σ_X are assumed to be equal to the parameters of the inert gas corresponding to the halogen atom X (e.g., $\epsilon_I = \epsilon_{Xe}$, $\sigma_I = \sigma_{Xe}$, etc.).

To find the collision radius σ_c, the average distance between two centers of the molecule M and X in the dimer is assumed to be equal to σ_{MX} given by the mixture rules; then σ_c is calculated from

$$\sigma_c = \sigma_{MX} \frac{M_X}{\mu} \tag{49}$$

which is the maximum distance from X to the center of mass MX at contact provided that

$$\frac{M_X - M_M}{M_X + M_M} \geq \frac{\sigma_X/\sigma_M}{\sigma_X + \sigma_M} \quad . \tag{50}$$

The degeneracies of a halogen molecule and atom in their ground states $^1\sum$ and $^2P_{3/2}$ are $g_{x_2} = 1$ and $g_x = 4$. Neglecting steric hindrance (P = 1), k_1 is given by

$$k_1 = \frac{5.53 \times 10^{12}}{M_X^{1/2}} \left(\frac{2M_X + M_M}{M_X + M_M}\right)^{5/2} \left(\frac{\epsilon_{MX}}{k}\right)^{3/2} \left[\sigma_{MX}(\text{Å})\right]^5 T^{-1}$$

$$\text{cm}^6\text{-mole}^{-2}\text{-sec}^{-1} \quad . \tag{51}$$

Insertion of the molecular parameters given by Hirschfelder, et al.,[92] gives the results in Tables III, IV, and V. Inspection of the table shows good agreement between theory and experiment in nearly all cases.

3. Recombination of Atomic Oxygen, Nitrogen, and Hydrogen

The experimental data available for comparison correspond to the reaction

$$O + O + O_2 \rightarrow O_2 + O_2 \tag{52}$$

$$N + N + N_2 \rightarrow N_2 + N_2 \tag{53}$$

$$H + H + H_2 \rightarrow H_2 + H_2 \tag{54}$$

TABLE III

The Rate Coefficient $k_1 \times 10^{-16}$ (cm^6-$mole^{-2}$-sec^{-1}) for Iodine Atom Recombinations at 20°C

Third Body	Calculated	Observed[a]	Observed[b]
He	0.10	0.34	0.24
Ne	0.28	0.36	0.33
Ar	1.1	0.73	0.67
Kr	1.4	1.2	0.82
Xe	1.7	1.3	1.1
H_2	0.43	0.95	
N_2	1.1	0.9	
O_2	0.98	1.3	
CO_2	2.2	2.7	
CH_4	1.9	1.8	
CCl_4	5.8	10.2	
C_3H_8	4.9	6.1	
n-C_5H_{12}	7.8	9.4	
cyclo-C_6H_{12}	8.2	11.	
C_2H_4	2.9	3.4	
C_6H_6	7.0	17.	

[a] Ref. 93

[b] Ref. 94

TABLE IV

The Rate Coefficient $k_1 \times 10^{-15}$ (cm^6 $mole^{-2}$ sec^{-1}) for Iodine Atom Recombinations at High Temperatures

Third Body	Temperature, °K	Calculated	Observed[a]
He	1400	0.21	0.36
Ar	1300	2.4	0.90
N_2	1300	2.4	0.88 or 1.4
O_2	1275	2.3	1.1
CO_2	1120	5.7	1.9

[a]Ref. 95

TABLE V

The Rate Coefficient $k_1 \times 10^{-15}$ ($cm^6 mole^{-2} sec^{-1}$) for Bromine Atom Recombination in Argon

Temperature, °K	Calculated	Observed
298°	2.4	7.4[a]
1600°	0.45	0.68[b]

[a]Ref. 96

[b]Ref. 97, 98

where the molecules of the type formed in the reaction are the third bodies. The following approximations are introduced for the molecular parameters.

$$\epsilon_{MX} = \epsilon_{X_2} \tag{55}$$

$$\sigma_{MX} = \sigma_{X_2} \tag{56}$$

$$\sigma_c = \sigma_{X_2} \tag{57}$$

which can be justified in the case of hydrogen.[99]

Again using the Hirschfelder parameters, evaluation of (46) gives

$$k_1(O) = 1.5 \times 10^{18}\ T^{-1} \tag{58}$$

$$k_1(N) = 0.9 \times 10^{18}\ T^{-1} \tag{59}$$

$$k_1(H) = 1.3 \times 10^{18}\ T^{-1} \tag{60}$$

in units of $cm^6\text{-mole}^{-2}\text{-sec}^{-1}$. P is assumed to be unity and the degeneracies used for the calculations are $(g_{O_2}/g_O^2) = 3/25$, $(g_{N_2}/g_N^2) = 1/16$ and $(g_{H_2}/g_H^2) = 1/4$ corresponding to the ground states $^3\Sigma_g^-(O_2)$, $^3P_2(O)$; $^1\Sigma_g^+(N_2)$, $^4S(N)$; $^1\Sigma_g^+(H_2)$, $^2S(H)$ for oxygen, nitrogen, and hydrogen, respectively. Measurements by Rink, et al.,[90] are accounted for by the expression

$$k_1(O) = 3.2 \times 10^{18}\ T^{-1}\ cm^6\text{-mole}^{-2}\text{-sec}^{-1}\ , \tag{61}$$

in excellent agreement with the calculated value (eq. (58)), over a wide temperature range (1800 to 2800°K). Calculated and observed values of k_1 for oxygen, nitrogen, and hydrogen at 300°K are compared in Table V. Agreement between theory and experiment is poor except for nitrogen. The

deviations for hydrogen and nitrogen can suitably be attributed to the approximations (55), (56), and (57), but the factor of 10 deviation for oxygen may be accounted for more reasonably by an activation barrier for decomposition of the metastable complex, ozone, i.e.,

$$O + O_2 \rightleftarrows O_3^* \tag{62}$$

$$O_3^* + O \rightarrow 2O_2 \quad . \tag{63}$$

In conclusion, it is apparent that termolecular rate constants for atomic recombinations can be calculated from a comparatively simple model. Agreement with experiment is good without introducing an arbitrary steric factor ($P < 1$) when electronic degeneracies and approximate Lennard-Jones molecular parameters are used. In the case of iodine recombination where a large number of third bodies have been studied, it is found that helium is the most inefficient, lowering the rate constant observed when hydrocarbons are the third body by more than a factor of 10. The results of the calculations and experiments given in the tables above are directly applicable to the experimental conditions normally employed in photodissociative laser systems; therefore, the method of calculation outlined above is expected to be useful for obtaining rate coefficients which have not been tabulated.

TABLE VI

Comparison of Calculated with Observed Recombination Rate Coefficients $k_r \times 10^{-15}$ ($cm^6 mole^{-2} sec^{-1}$) at $300^\circ K$

Atom	Calculated	Observed
O	5.0	<0.5
N	3.0	1.6
H	4.3	18

C. ALKYL HALIDES:IODINE ATOM LASER

The main photochemical reaction of alkyl halides (RX, where X is Cl, Br, or I) when irradiated within their first absorption band is the dissociative primary process: $RX + h\nu \rightarrow R + X$. At shorter wavelengths in the second absorption band a molecular elimination of hydrogen halide may also occur[25]: $R_2CHCH_2X + h\nu \rightarrow R_2C = CH_2 + HX$. Only the first of these processes is of importance when using solar irradiation. This dissociation reaction occurs with high efficiency; for example, primary process quantum yields of unity have been measured for all of the following reactions:

$$CH_3I + h\nu \rightarrow CH_3 + I$$
$$CH_3Br + h\nu \rightarrow CH_3 + Br$$
$$C_2H_5I + h\nu \rightarrow C_2H_5 + I$$
$$C_2H_5Br + h\nu \rightarrow C_2H_5 + Br \quad .$$

The alkyl radicals in these dissociation reactions are much lighter than the halide atoms, and the alkyl radicals are assumed to acquire a large share of the excess energy after bond fission. For example "hot" methyl radicals are expected from the photolysis of methyl iodide. The spectroscopic analysis of Goodeve and Porret in 1938 indicated the probability of also obtaining electronically excited iodine atoms ($^2P_{1/2}$). The photochemical iodine atom laser work[1] in 1964 was the first direct experimental evidence for this conclusion.

The iodine atom laser[1-3] involves a direct process in which excited $^2P_{1/2}$ iodine atoms are formed in the gas phase photochemical dissociation of alkyl iodides. The excited iodine atoms readily emit at 1.315 μ in returning to their $^2P_{3/2}$ ground state. Because the iodine atoms are formed by a dissociative process, the system acts as a four level laser in which population inversion is achieved by the photochemical primary process. Even equal formation of the $^2P_{1/2}$ and $^2P_{3/2}$ states by photolysis presumably would give a population inversion because of the greater degeneracy of the lower state.

Reports by several investigators[1, 2, 9-11] on the alkyl iodide photodissociative laser system indicate that temperature, pressure, molecular structure, and added gases are all important variables which determine its output at 1.3 μ. No studies of the laser output dependence on pumping wavelengths have been reported, although this is likely to be an important consideration. De Maria and Ultee[9] recently reported energy outputs up to 65 J and peak power outputs up to 10^5 W for a duration of 1.5 msec. Their experimental configuration is shown in Fig. 45. The CF_3I pressure for maximum output was found to vary with temperature. At room temperature, maximum energy output was obtained at a pressure of 15 mm Hg. The over-all efficiency under these conditions is 0.16%. Other workers[10, 11] report maximum output at room temperature from CF_3I at 100 mm Hg pressure; maximum output from CH_3I is less by a factor of four and is observed at a lower pressure, 20 mm Hg. The qualitative nature of the laser output dependence on substrate pressure is expected, since both output and depletion reactions depend on the concentration of atomic iodine. The role played by molecular iodine in quenching the output is not yet clear. It may act as a catalyst to enhance nonradiative decay of excited iodine atoms or be a highly effective third body for recombination of atomic iodine. Experimental evidence exists for both cases.[2, 10, 11] These processes will, of course, be important in the operation of other systems containing iodine atoms. Other difficulties with the alkyl iodides for solar operation are (1) high irreversibility and (2) the fact that absorption of pumping radiation occurs only in the ultraviolet region.

D. DEACTIVATION OF EXCITED IODINE ATOMS

1. Photolysis of I_2

The primary photochemical process for the iodine molecule is dissociation into iodine atoms. If absorption occurs in the continuum of the spectrum (< 4995 Å) dissociation occurs from the original state on the first vibration of the excited molecule with the formation of one normal and one excited iodine atom:

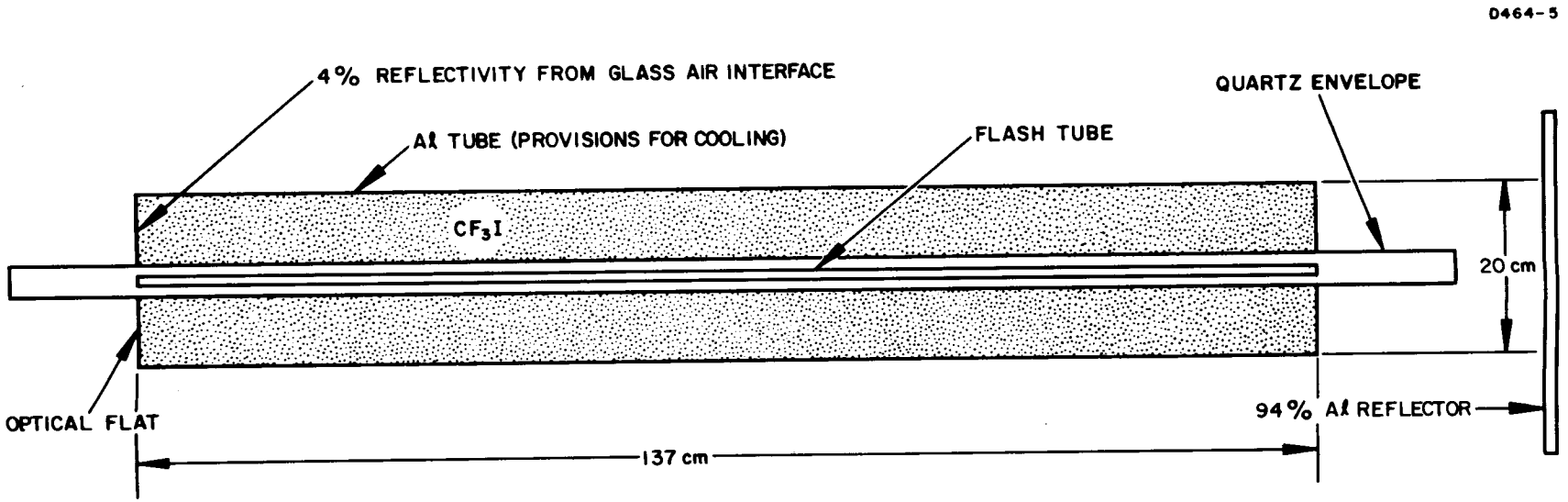

Fig. 45. Laser tube and cavity used by DeMaria and Ultee.[9]

$$I_2(^1\Sigma_g^+) + h\nu \rightarrow I_2(^3\Pi_{0u}^+) \rightarrow I(^2P_{3/2}) + I(^2P_{1/2}) \quad .$$

Although the excited and normal states are formed in equal population, the excited iodine atom is less degenerate than the ground state and stimulated emission is expected from photolysis for excitation wavelengths less than 4995 Å; however, laser action has not been observed. It was suggested that I_2 acts as a rapid quencher which catalyzes the deactivation or recombination of excited iodine atoms.[2]

The formation and decay of excited iodine atoms ($5p\ ^2P_{1/2}$) has been studied by a number of workers[100-106] using kinetic absorption spectroscopy and flash photolysis techniques.[107] Strong, et al.,[100] examined the rate of recombination of iodine atoms using light of different wavelength ranges for photodecomposition and obtained identical rate constants at all wavelengths. They concluded that excited atoms (formed when $\lambda < 4995$ Å) either recombine at the same rate as ground state atoms or are deactivated before measurements are made.

Donovan and Husain[108] studied the production and decay of $I(5p\ ^2P_{1/2})$ during the flash photolysis of iodine vapor in the presence of excess argon. Ground state and excited state atoms were observed in absorption by the transitions

$$5p(^2P_{3/2}) \rightarrow 6s(^2P_{3/2}) \qquad 1783 \text{ Å}$$
$$5p(^2P_{3/2}) \rightarrow 6s(^4P_{5/2}) \qquad 1830 \text{ Å}$$
$$5p(^2P_{1/2}) \rightarrow 6s(^2P_{1/2}) \qquad 1799 \text{ Å} \quad .$$

A first order kinetic decay of excited iodine atoms was observed when a mixture of 0.03 mm I_2 and 50 mm argon was photolyzed. Doubling the pressure of argon resulted in the same rate of decay; the excess argon apparently acts only to prevent the temperature from rising and to pressure broaden the atomic absorption lines rather than contributing significantly to the over-all relaxation processes. The mean radiative lifetime of the $5p(^2P_{1/2})$ state is ~0.1 sec[108,109]; therefore, non-chemical removal of excited atoms must be collisional. The molecular

iodine concentration during the atomic decay observation period remains constant to 1% under the conditions of the experiment. Donovan and Husain[108] postulate that deactivation occurs by conversion of the atomic electronic energy (21.7 kcal) to vibrational energy of the ground electronic state of molecular iodine.

$$I\ 5p\ (^2P_{1/2}) + I_2\ (X'\Sigma_g^+(\nu'' = 0)) \xrightarrow{k_1}$$

$$I\ 5p\ (^2P_{3/2}) + I_2\ (X'\Sigma_g^+(\nu'' = n))$$

The value of the first order rate constant for the decay of $I(^2P_{1/2})$ was found to be $k_1' = 3.6 \pm 0.5 \times 10^3$ sec^{-1}. This value, combined with the iodine concentration during the decay period determined by absorption, gives $k_1 = 3.0 \pm 0.5 \times 10^9$ liter-mole^{-1} sec^{-1}, which corresponds roughly to deactivation by one collision in fifteen. The value of the third order recombination rate constant measured at long delay times is $k_{Ar} = 6.8 \pm 0.7 \times 10^9$ liter^2-moles^{-2}-sec^{-1}, in agreement with other work.[100-106] However, determination of this coefficient by monitoring the population in the first vibrational level of I_2 up to 500 μsec after the flash results in a value two orders of magnitude larger, indicating vibrational nonequilibrium, although this could not be detected directly. The high rate of formation of I_2 ($\nu'' = 1$) may be the result of vibrational exchange after the relatively fast electronic-vibrational transfer between $I(^2P_{1/2})$ and $I_2(X'\Sigma_g'^+(\nu'' = 0))$ or from atomic recombination. Either of these processes may be favorable for attaining population inversion between other vibrational levels of I_2. The normal rate of formation of I_2 observed at long delay times ($t > 500$ μsec) by absorption from $\nu'' = 1$ suggests that vibrational exchange is comparable in rate to recombination and that energy transfer from $I(^2P_{1/2})$ may selectively excite certain vibrational levels of I_2.

2. Photolysis of CF_3I

Donovan and Husain[110] have made a detailed study of quenching of the $^2P_{1/2}$ state of iodine atoms by a variety of substances. The collision efficiencies of N_2, C_3H_8, and I_2 for deactivation of $I(^2P_{1/2})$ are 3.0×10^{-6}, 3.2×10^{-4}, and 7.2×10^{-2}, respectively.[110] Since molecular iodine is the most efficient quencher, another source of excited atoms was necessary for the studies with N_2 and C_3H_8. Mixtures of CF_3I, Ar, and N_2 or C_3H_8 were used. A long-lived (~6 msec) inversion was obtained by flash photolysis of 0.5 mm CF_3I and 50 mm argon. The decay of $I(^2P_{1/2})$ was found to increase with decreasing pressure of argon and not to be significantly dependent on the pressure of CF_3I. Measurements of the decay of $I(^2P_{1/2})$ were made by kinetic absorption spectroscopy in times during which the contribution from atomic recombination and subsequent relaxation by collision with I_2 is negligible. The simultaneous appearance of $I(^2P_{3/2})$ with the decay of $I(^2P_{1/2})$ indicates that the principal process in all cases studied is spin-orbit relaxation. These studies also show that the reaction

$$I(^2P_{3/2}) + I(^2P_{1/2}) + M \rightarrow I_2(B^3\pi^+_{ou}) + M$$

does not occur to a significant extent in the particular systems studied, since the decay of $I(^2P_{1/2})$ is observed to be first-order.

Methyl radicals produced by photolysis of CH_3I under similar conditions were found to be short-lived (~100 μsec); it was concluded, therefore, that CF_3 radicals do not affect the removal of $I(^2P_{1/2})$ atoms at times longer than 100 μsec after the photolysis flash. In addition, since molecular iodine is detected only at long delay times, quenching by the process $CF_3I + I(^2P_{1/2}) \rightarrow CF_3 + I_2$ does not occur to a significant extent. Because the decay of $I(^2P_{1/2})$ and the appearance of $I(^2P_{3/2})$ are in agreement and no HI could be detected, propane quenching by a hydrogen abstraction reaction can be ruled out.

No simple correlation was noted between the deactivating efficiencies of N_2, C_3H_8, and I_2 any molecular parameter, although there

is a decrease in efficiency with decreasing ionization potential for these three molecules. The high quenching efficiency of I_2 presumably results from the formation of a relatively stable I_3 complex. The low efficiency of argon quenching is in accordance with a general law proposed by Callear,[111] $\log P = -A\Delta E + B$, where P is the probability of energy transfer per collision, ΔE is the energy converted to translation, and B is a constant but has values for vibrational energy exchange only.

Deactivation of $I(^2P_{1/2})$ by H_2, D_2, and He was studied by photolysis of CF_3I mixtures. Quenching by H_2 and D_2 is similar, indicating that resonance quenching by a multivibrational transition of the energy acceptor is not rate determining. The energy discrepancies from energy matching between donor $(I^2P_{1/2})$ and acceptor (H_2 or D_2) for the $v'' = 2$ vibrational level are 479 and 1752 cm^{-1}. The latest studies include work with hydrides, paramagnetic molecules, and further investigations with inert gases (helium, argon, and xenon). As concluded earlier, the deactivation in inert gases takes place at the walls of the reaction vessel after diffusion. It is concluded that the probability of energy transfer by collisional deactivation is too low to be measured conveniently (more than 10^8 collisions are required for deactivation). Hydrides as a group deactivate $I(^2P_{1/2})$ relatively efficiently. The presence of a hydrogen atom in a molecule definitely enhances its deactivation efficiency. It has been suggested that formation of a loose hydrogen-bonded complex is involved in the energy transfer process.[112] Deactivation by the paramagnetic molecules NO and O_2 is relatively high (comparable to I_2, which deactivates $I(^2P_{1/2})$ in ~15 collisions). The ground state of $NO(^2\Pi_{1/2})$ is not paramagnetic; at 300°K, however, approximately 36% of the molecules are in the $^2\Pi_{3/2}$ state, which is paramagnetic. Nitric oxide in this state is ~2-1/2 times as effective as I_2. The probability for deactivation of $I(^2P_{1/2})$ by various gases is given in Table VII.

TABLE VII

Probability P of $I(^2P_{1/2})$ Deactivation by Collision

Deactivating Compound	P
He, Ar, Xe	Diffusion Controlled
CO_2	7.7×10^{-7}
CO	6.7×10^{-6}
N_2	3.0×10^{-6}
CF_3I	1.7×10^{-5}
CF_4	2.5×10^{-5}
H_2	1.8×10^{-4}
CF_3H	2.3×10^{-4}
CH_4	2.4×10^{-4}
D_2	3.1×10^{-4}
C_3H_8	3.2×10^{-4}
C_2H_5I	3.3×10^{-4}
D_2O	4.0×10^{-4}
DI	2.1×10^{-3}
HI	2.4×10^{-3}
H_2O	5.9×10^{-3}
O_2	5.6×10^{-2}
$NO(^2\Pi_{3/2})$, Paramagnetic	1.9×10^{-1}
$NO(^2\Pi_{1/2})$, Diamagnetic	6.7×10^{-2}
I_2	7.1×10^{-2}

3. Chemical Reactivity of $I(^2P_{1/2})$ with Propane

A photochemical investigation of the iodine propane system has been reported recently.[113] It was concluded from a kinetic analysis of i-propyl iodide formation that the $^2P_{1/2}$ state of iodine atoms is more reactive with respect to hydrogen abstraction than the $^2P_{3/2}$ state; it was noted that the reactivity of atomic chlorine is similar in this regard. The conclusion concerning iodine atom reactivity is based on quantum yield determinations of i-propyl iodide when molecular iodine was irradiated in both the continuum and banded region. The convergence limit of the $B\ ^3\Pi_{ou}^+ \leftarrow X\ ^1\Sigma_g^+$ transition of iodine is at 4995 Å (Quarterly Report No. 1, p. 15). Photolyses of mixtures of iodine (0.2 Torr), propane, and chemically inert gases (H_2, CO_2, Ar and N_2) were carried out at 4835, 5020, 5200, and 5480 Å. Even in the continuum region where the primary yield of iodine atoms is unity, the quantum yield of i-propyl iodide is very small, 1.5×10^{-4} at 4835 Å. Since the yield falls off at 5200 Å and is "very small" at 5480 Å, Callear and Wilson[113] conclude that only excited iodine atoms react with propane. However, it should be noted that the primary yield of iodine atoms from collision-induced predissociation in the banded region is considerably less than the value of unity in the continuum. The relative effect of other gases on the quantum yield of n-propyl iodide also indicates that only excited iodine atoms react with propane. It was found that the order of quenching efficiency of H_2, I_2, CO_2, Ar, and N_2 on i-propyl iodide formation is the same as that observed for deactivation of excited iodine atoms observed spectroscopically.[110] Although the observations are suitably interpreted as stated above, it is not clear that $I(^2P_{1/2})$ is generally more chemically reactive than $I(^2P_{3/2})$. This is of course an important consideration in the operation of photodissociative laser systems and assists in the choice of optimum gas mixtures. In contrast to the above chemical behavior it may be possible to find cases where the lower halogen level is more reactive than the upper level (e.g., recombination reactions).

E. INDIRECT FORMATION OF EXCITED IODINE ATOMS

A novel source of excited iodine atoms was suggested recently by Arnold, et al.[114] The $^1\Delta_g$ state of oxygen can be obtained in relatively large concentrations because of its long radiative lifetime (45 min) and resistance to collisional deactivation.[115] In addition to the interesting observation of emission in the visible region from a stream of $^1\Delta_g$ O_2 molecules, the following reactions were postulated to occur when iodine is added to the system:

$$O_2(^1\Delta_g) + I(^2P_{3/2}) \rightarrow O_2(^3\Sigma_g^-) + I(^2P_{1/2})$$

$$3O_2\,(^1\Delta_g) + I_2(^1\Sigma_g^+) \rightarrow 3O_2\,(^3\Sigma_g^-) + I_2(^3\pi_{0u}^+) \quad .$$

The $^3\pi_{ou}^+$ state of iodine can emit at wavelengths $\geq$ 5000 Å or dissociate to $I(^2P_{1/2})$ and $I(^2P_{3/2})$. These results indicate the possibility of enhancement of laser action in iodine systems by introducing oxygen molecules in the long-lived $^1\Delta_g$ state and the importance of "energy-pooling" processes in the formation of excited atomic and molecular states.

Evidence for the process

$$H\cdot + HI \xrightarrow{k_1} H_2 + I(^2P_{1/2})$$

in the flash photolysis of hydrogen iodide has been reported recently by Donovan and Husain.[116] Excited iodine atoms are also produced by photodissociation of HI, and ground state atoms are formed by a reaction analogous to that above and by photodissociation with light of wavelengths greater than 2600 Å. With quartz optics, about one-fifth of the iodine atoms produced by photolysis are in the upper state. The rate of molecular iodine formation is slow compared with that of relaxation in this system; therefore, I_2 does not contribute significantly to the quenching of $I(^2P_{1/2})$ although its deactivation efficiency is high.

F. IODINE MONOCHLORIDE

The vapor phase photolysis of ICl at 30 and 60°C in the presence of inert gases has been studied by Christie, Roy, and Thrush[117] using light from a tungsten source and filters to isolate the 4300 Å region. Previous photochemical work with ICl was concerned with mixtures of ICl and H_2.[118-120]

The following mechanism for the photochemical reaction between iodine monochloride and hydrogen at 28°C, with light of wavelength 4358 Å, resulted from these studies.[120]

1. $ICl + h\nu \rightarrow I\cdot + Cl\cdot$
2. $Cl\cdot + H_2 \rightarrow HCl + H\cdot$
3. $H\cdot + ICl \rightarrow HCl + I\cdot$
4. $Cl\cdot + ICl \rightarrow Cl_2 + I\cdot$
5. $I\cdot + I\cdot + M \rightarrow I_2 + M$.

The quantum yield of HCl formed in this system was found to be 1.5, indicating that reactions (2) and (4) compete for the chlorine atom. Reaction (4) is slightly favored over (2) because of a difference in activation energies of ~3 kcal.[120, 121] In the absence of (4), a quantum yield of two for HCl formation would be expected.

Christie, et al., have reported a value of two for the quantum yield of the initial photochemical decomposition of ICl in the presence of varying amounts of inert gases. The following mechanism was deduced.

1. $ICl + h\nu \rightarrow I\cdot + Cl\cdot$
2. $Cl\cdot + ICl \rightarrow I\cdot + Cl_2$
3. $I\cdot + I\cdot + M \rightarrow I_2 + M$

$$4. \quad I\cdot + Cl\cdot + M \rightarrow ICl + M$$

$$5. \quad Cl\cdot + Cl\cdot + M \rightarrow Cl_2 + M \quad .$$

Known values[100, 122] of k_3, k_4, and k_5 were used to calculate a value of k_2 ($k_2 = 5 \times 10^8 \exp(-4,500/RT)\ell$ - mole^{-1} - sec^{-1}). The rate constant for the analogous reaction

$$6. \quad Cl\cdot + BrCl \rightarrow Br\cdot + Cl_2$$

has also been reported[123] ($k_6 = 2 \times 10^9 \exp(-1,100/RT)\ell$ - mole^{-1} - sec).

The difference between k_2 and k_6 is somewhat surprising since the bond energies of ICl and BrCl are nearly equal; comparison of other mathematical reactions of three atom systems also indicates that the activation energy of (2) is anomalously high.[124] Christie, et al., suggest that the metastable $^2P_{1/2}$ state of the iodine atom may be involved in the transition state and thereby may account for the difference in k_2 and k_6. (The energies of this state for I, Br, and Cl are 21.7, 10.5, and 2.6 kcal/mole, respectively.) Thus, although, spectroscopic analysis indicates that only excited Br and Cl atoms are formed from photodissociation of IBr and ICl by visible and near ultraviolet light, kinetic studies suggest that excited iodine atoms may be produced as well.

G. NITROSYL CHLORIDE:NITRIC OXIDE LASER

In a recent flash photolysis study of nitrosyl chloride and bromide, Basco and Norrish[47] have observed vibrationally excited nitric oxide in all levels from v'' = 0 to v'' = 11 by absorption from the ground electronic states in the β, γ, δ, and ϵ systems. (The upper states of these systems are indicated in Fig. 46.) The decomposition mechanism may include both of the primary processes

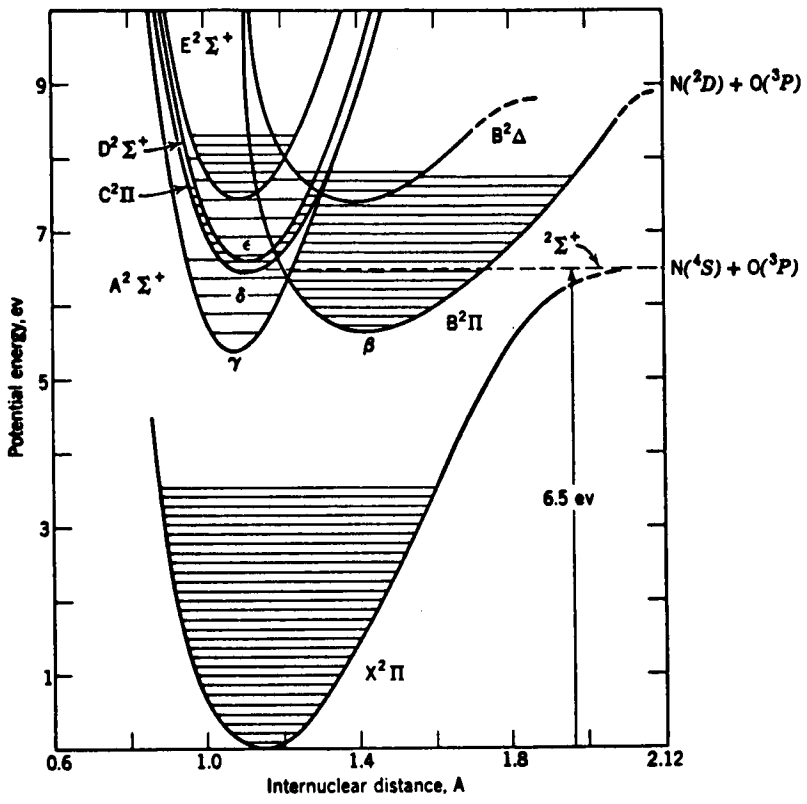

Fig. 46. Potential energy diagram for nitric oxide, NO (from Calvert and Pitts[25]).

$$NOCl + h\nu \rightarrow NO(X\,^2\pi,\ v \leqq 11) + Cl\left(^2P_{3/2,\,1/2}\right) \quad .$$

$$NOCl + h\nu \rightarrow NO(^4\pi) + Cl\left(^2P_{3/2,\,1/2}\right)$$

$$NO(^4\pi) + M \rightarrow NO(X\,^2\pi,\ v > 0) + M \quad .$$

The excitation of the halogen atom to the $^2P_{1/2}$ state is uncertain but may be expected as indicated in the spectroscopy section.

Kistiakowsky[125] found the quantum yield for decomposition to be two and constant over the wavelength range 3650 to 6350 Å and pressures from 87 to 685 mm Hg. He postulated formation of an excited molecule in the primary process rather than direct dissociation on the basis of line structure observed in the absorption spectrum and an inaccurate heat of dissociation, ΔH (46.4 kcal/mole). Later work with high pressures of inert gas,[126] an accurate value of ΔH (38 kcal/mole)(Ref. 127, 128), and absorption spectra[46, 129] of pure material established that the excited state mechanism is inconsistent with experiment, whereas all evidence points to the direct dissociation mechanism.

Basco and Norrish[47] found that the amount of $NO(v > 0)$ produced with wavelengths greater than 3000 Å (pyrex filter) is small relative to that produced at shorter wavelengths. (This is, of course, expected from a consideration of the relative values of the extinction coefficients in these two regions. Whether vibrationally excited nitric oxide can be formed by photolysis of NOCl in the visible and near ultraviolet regions is still an open question. The absence of $NO(v > 0)$ from the photolysis of NOCl at long wavelengths when the excitation rate is comparable to that in the ultraviolet would certainly be a significant observation.) The absence of excited NO in Basco and Norrish's system when pyrex filtering was used, together with results obtained from flash studies of Cl_2 - NOCl mixtures in a pyrex reaction vessel, enabled them to conclude that the reaction

$$Cl + NOCl \rightarrow Cl_2 + NO(v > 0)$$

does not proceed to a significant extent. Previous work by McGrath and Norrish[130] also indicates that in the general reaction

$$A + BCD \rightarrow AB + CD,$$

only AB is excited, not CD.

Although the mechanism involving the $^4\pi$ state of NO cannot be definitely excluded, the work of Basco and Norrish[47] favors formation of vibrationally excited NO in the primary process. From the dissociation energy of the ON-Cl bond (37 kcal/mole), dissociation of NOCl at 4000 Å could leave the NO fragment with as much as 30 kcal/mole ($v \simeq 5$) as well as producing an excited chlorine atom. The degree of excitation observed by Basco and Norrish[47] (2500 Å) is 55 kcal/mole ($v = 11$), but they indicate that higher vibrational levels may have been undetected by their apparatus.

From the rapid decay of NO ($v > 0$) they conclude that resonance transfer reactions are probably rate determining. Near-resonant transfer to the parent molecule NOCl or NOBr is possible, as well as to NO itself. The vibrational spacing of NO for $v'' = 0$ to $v'' = 11$ is 1900 to 1600 cm^{-1} and the frequency associated with the NO bond in NOCl or NOBr is 1800 cm^{-1}. Thus, transfer from the lower levels of NO is likely to be faster because of closer approach to the resonance situation, and this may be the reason for the low amount of excited NO produced with light in the visible region. The effect of excess NO in the photolysis tube, quenching of highly excited NO, and formation of large amounts of NO ($v = 1$), indicates that transfer occurs in a stepwise resonance manner. When NO ($v \geq 8$) participates with NOCl in a collision, it is conceivable that dissociation could occur. However, this would increase ϕ, the quantum yield of decomposition. Thus, the limiting value of two for ϕ is additional evidence for stepwise vibrational energy transfer.

In view of these results we expected to observe laser action from vibrational levels of NO and/or NOCl as well as from electronically excited clorine atoms. Another possibility is vibrationally excited chlorine formed in the secondary reaction

$$Cl + NOCl \rightarrow Cl_2(v > 0) + NO \quad .$$

Vibrationally excited NOCl may be formed by quenching of NO ($v > 0$) formed in the primary photochemical step or under certain conditions by the recombination reactions,

$$NO + Cl \rightarrow NOCl\ (v > 0)$$

$$2NO + Cl_2 \rightarrow 2NOCl \cdot$$

The rate of the latter termolecular reaction has been measured[131, 132] (see Fig. 47) and is 1.6×10^7 cm^6-$mole^{-2}$-sec^{-1} at room temperature. Rates of these reactions for NO($v > 0$) and $Cl(^2P_{1/2})$ as well as the reactions

$$Cl(^2P_{1/2}) + NOCl \rightarrow NO + Cl_2$$

$$2Cl(^2P_{1/2,\,3/2}) \rightarrow Cl_2$$

compared to their rates when the components are in ground states are not known but will be of considerable importance with regard to the degree of inversion attainable with either pulsed or continuous operation.

Although nitrosyl bromide has not been studied as extensively as the chloride it is expected to react in a very similar way. As discussed previously its absorption spectrum is similar to that of NOCl, and the results of Basco and Norrish[47] apply equally to NOBr and NOCl. The separation of the atomic doublet states ($^2P_{1/2}$ - $^2P_{3/2}$) of bromine is 3685 cm^{-1}; thus, laser action from this species would be expected at 2.7 μ, compared with 11.3 μ for atomic chlorine.

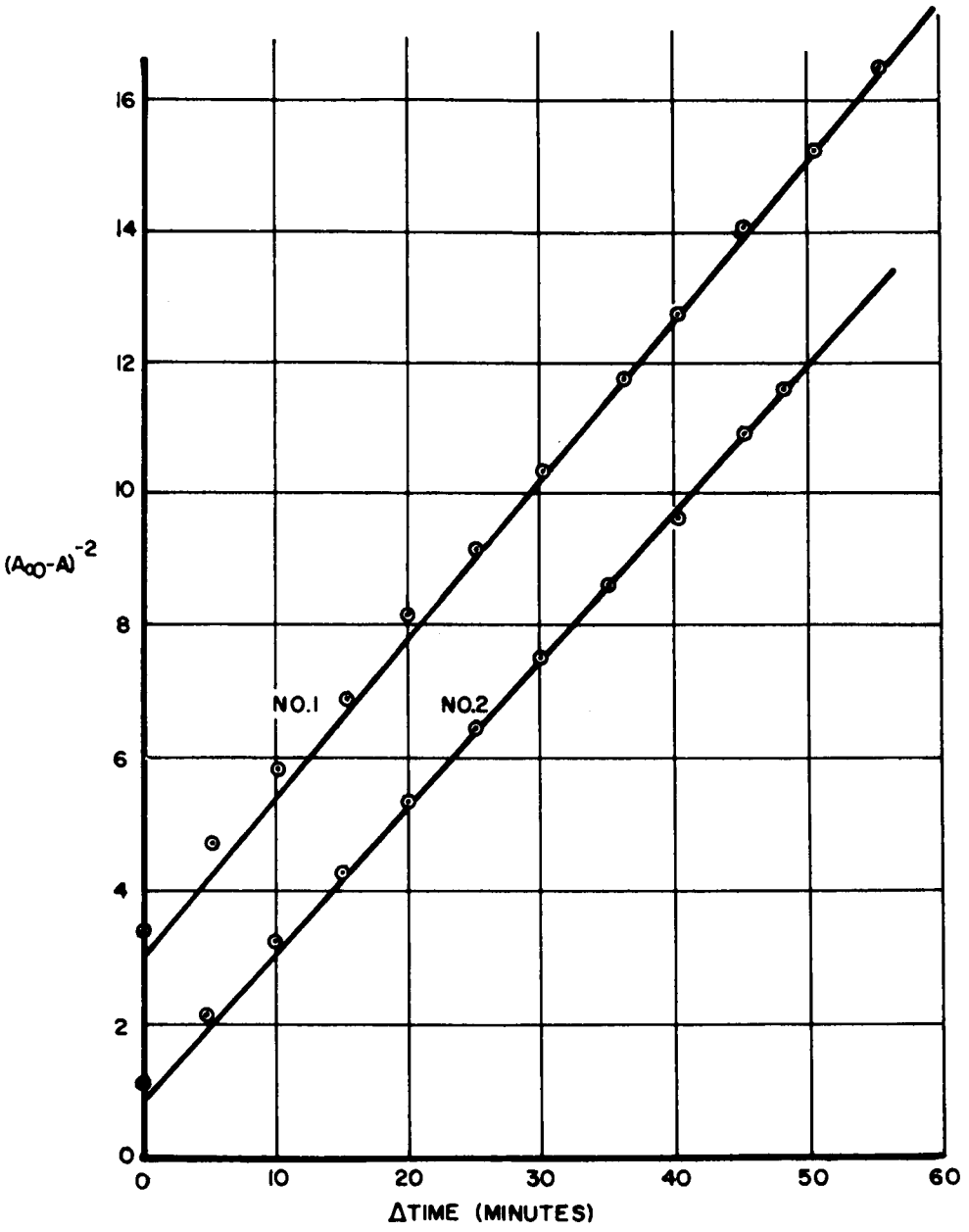

Fig. 47. Third order plot of photolysis back reaction $2NO(g) + Cl_2 \xrightarrow{k} 2NOCl(g)$. $A_\infty^{4750} = 1.186$, $\epsilon^{4750} = 5.3$ liter-mole^{-1}-cm^{-1} $k_{17}^{o} = 1.14 \times 10^{7}$ cm^{6}-mole^{-2}-sec^{-1}. (1) Mercury lamp exposure. (2) Sunlight exposure.

Successful operation of the nitrosyl chloride laser system by optical excitation was reported recently.[20] Fifteen spectral lines between 5.9 and 6.3 μ corresponding to vibrational-rotational transitions of NO were observed. Although threshold values were not reported, 10 W laser pulses were obtained with 1000 J input to a linear (50 cm) xenon flash lamp enclosed in an aluminum elliptical cavity. A pressure of 1 Torr of NOCl and 100 Torr of N_2 or He was used. Under these conditions laser action (~10 W peak pulses) occurred in the early portion (the first few microseconds) of the flash lamp temporal output. Less power was obtained upon repetitive excitation of the same gas mixture, although the time between flash lamp discharges was not reported. Addition of nitric oxide (NO) also reduced the laser power output. Another experimental feature reported is the use of a gold-doped germanium detector which was operated at liquid nitrogen temperature; the beam was coupled out of the laser cavity with a sodium chloride beam splitter which deflected approximately 4% of the beam. Potassium chloride windows were attached to the laser tube and two spherical silver mirrors formed the oscillator cavity.

We have also observed laser action from nitrosyl chloride; our experimental results on the stimulated emission of NO from the flash photolysis of NOCl are discussed in Part 2.

H. NITROGEN DIOXIDE

As shown in Fig. 21, nitrogen dioxide absorbs over a large portion of the visible and near ultraviolet spectral regions. The photodissociation of NO_2 by sunlight has been discussed in detail by Leighton[133] with regard to smog formation. Indeed, much of the interest in NO_2 photolysis has centered on establishing the maximum wavelength of light which induces dissociation. The limiting quantum yields of oxygen production in the photolysis of NO_2 at 25°C are 0.97 at 3130 Å, 0.92 at 3660 Å, 0.36 at 4047 Å, and 0.00 at 4358 Å (Ref. 133). At the shorter wavelengths (3660 and 3130 Å), the absorption spectrum is diffuse and fluorescence is very weak. In addition,

in this wavelength region it has been shown by isotopic techniques that oxygen atom exchange occurs when mixtures of NO_2 and $^{18-18}O_2$ are photolyzed.[134] From this evidence the primary process is deduced to be dissociation at 3130 Å and 3660 Å with nearly unit efficiency.

$$NO_2 + h\nu \rightarrow NO(X^2\pi) + O\ (^3P) \quad . \tag{64}$$

Recent work indicates that photodissociation occurs at 4047 Å but not at 4358 Å; isotopic exchange techniques were again employed.[134] An interesting temperature dependence of oxygen formation at 4047 Å was observed in the latter study. At a temperature of 293°C the photodecomposition of NO_2 proceeds with nearly unit quantum efficiency at 4047 Å, although the quantum yield is only 0.03 at 4358 Å. The isotopic exchange also increased with temperature at 4047 Å, but not at 4358 Å. This temperature dependence of the primary quantum yield was satisfactorily explained by taking into account the temperature dependent distribution of vibrational and rotational energies of the NO_2 molecule.[135]

In a similar study by Ford and Jaffé, it was proposed that oxygen atoms were produced in a secondary process when NO_2 is irradiated at 4047 Å (Ref. 136).

$$NO_2 + h\nu\,(4047\ \text{Å}) \rightarrow NO_2^* \tag{65}$$

$$NO_2^* + NO_2 \rightarrow N_2O_3 + O \quad . \tag{66}$$

Therefore, although the mechanism is not definitely established at all wavelengths, it is clear that efficient photodissociation of NO_2 occurs at wavelengths shorter than 4047 Å; even at this wavelength photodissociation occurs if there is sufficient internal energy in the molecule to make up the energy deficiency of the light. At longer wavelengths ($\lambda > 4047$ Å), excitationto the $^2B_1$ or $^2B_2$ states is followed by fluorescence, deactivation, or excited-molecule reactions, which do not lead to molecular dissociation.

Photolysis of NO_2 in the short wavelength region ($\lambda \sim 2500$ Å) produces oxygen atoms in the singlet D state.

$$NO_2 + h\nu\ (2500\ \text{Å}) \rightarrow NO\ (X^2\pi) + O\ (^1D) \quad . \tag{67}$$

It is significant that oxygen molecules with up to eight quanta of vibrational energy have been detected in the flash photolysis of NO_2 (Ref. 137). Further studies indicated population of levels up to $v = 12$ of O_2 and $v = 2$ of NO (Ref. 138). Thus photolysis of nitrogen dioxide by sunlight could result in significant populations of upper vibrational levels of NO_2 ($\lambda > 4047$ Å), NO, and O_2 ($\lambda > 4047$ Å). Since the solar pumping rate is relatively high because of spectral overlap, this molecule appears to be potentially useful with regard to obtaining coherent emission from solar pumped systems.

I. CYANOGEN:CYANYL RADICAL LASER

Pollack observed laser action from the flash photolysis of cyanogen, $(CN)_2$, whereas it was not obtained by excitation from an electrical discharge.[20] The following scheme was proposed to account for the results obtained from cyanogen.

$$(CN)_2 + h\nu \rightarrow 2CN\ (X^2\Sigma, v = 0)$$

$$CN\ (X^2\Sigma) + h\nu \rightarrow CN\ (B^2\Sigma, v = 0, 1, 2, 3, \ldots)$$

$$CN\ (B^2\Sigma) \rightarrow CN\ (X^2\Sigma, v = 0, 1, 2, 3, \ldots) \quad .$$

Laser action at 1921, 1925, and 1929 cm^{-1} was observed from 2 Torr of $(CN)_2$ with no buffer gas and 2000 J lamp input energy. This corresponds to laser action from the $X^2\Sigma'$, $v = 0, 1, 2, 3$ levels of CN. Cyanogen, is photodissociated to $CN(X^2\Sigma')$ radicals which are subsequently excited by the flash lamp. Laser action was obtained with $(CN)_2$ at 2 Torr with no buffer gas and an input of 2000 J into a 50 cm linear xenon flash lamp situated in an elliptical cavity. Thus the CN

radical system is another possibility for converting solar radiation to laser light since it has strong absorption in the visible and near infrared regions of the spectrum (3100 Å to 1.5 μ). The availability of sufficient concentrations of CN radicals would certainly be a problem; however, it possibly could be obtained by thermal decomposition of cyanogen compounds (XCN); it may be feasible to utilize solar radiation as the thermal source for this decomposition. Other disadvantages, such as irreversibility of the over-all reaction, may also make this system impractical. It is encouraging that laser action has been observed from molecular levels, however, since it has been thought that laser action is improbable in molecular systems because of the large number of possible transitions available to an excited molecular state. Experimental evidence is accumulating which indicates that in certain cases this apparent disadvantage[30] can be overcome.[139]

J. CARBON MONOXIDE LASER SYSTEMS

The reports of laser action from carbon monoxide[82] show that the energy levels of this molecule have suitable characteristics which allow population inversion and suggest that molecules which photodecompose to give CO as a product should be investigated. Several molecular systems, metal carbonyls, and ketones absorb in the solar spectral region and can be considered as sources of excited CO molecules.

Pollack[140] has reported laser oscillation on molecular transitions from flash photolysis of carbon disulfide, oxygen, and helium mixtures. A total peak power output of 0.5 W from 1 Torr CS_2, 1 Torr O_2, and 150 Torr He was obtained with 2000 J discharged into the flash lamp; the threshold input energy was below 200 J. Laser output frequencies corresponding to vibrational-rotational transitions of the ground electronic state of CO started 15 μsec after initiation of the excitation flash and had a duration of 10 to 20 μsec, much shorter than the flash lamp duration. Peak powers of 20 mW were observed on the

strongest of 31 lines from 1961 to 1761 cm^{-1}. The following reactions, suggested by the earlier flash photolysis studies by Wright[141] and Callear,[142] are thought to be responsible for production of excited CO.

$$CS_2 + h\nu \rightarrow CS + S$$

$$O_2 + S \rightarrow SO + O$$

$$SO + CS \rightarrow CO^* + S_2$$

$$O + CS_2 \rightarrow CO^* + S_2$$

$$O + CS_2 \rightarrow COS + S$$

$$COS + O \rightarrow CO^* + SO$$

Because the addition of CO decreased the output power, reactions of the type $M^* + CO \rightarrow CO^* + M$ are thought to be an unimportant source of CO^*. The output power was reduced by 50% when CO was substituted for helium. The observation that lines belonging to different vibrational transitions all start simultaneously was also used to support the hypothesis that CO is chemically produced in vibrationally excited states.

K. SOLAR AND CHEMICAL EXCITATION OF CARBON DIOXIDE

Since carbon dioxide is an efficient laser material, we have considered various excitation schemes for obtaining population inversion between its vibrational levels with the aid of photochemical processes or solar energy. Figure 48 illustrates the relevant vibrational levels of CO_2.

Three excitation mechanisms utilizing solar energy for population of the CO_2 (00^01) level can be visualized: (a) chemical reactions of atomic or molecular fragments produced by photodissociation;

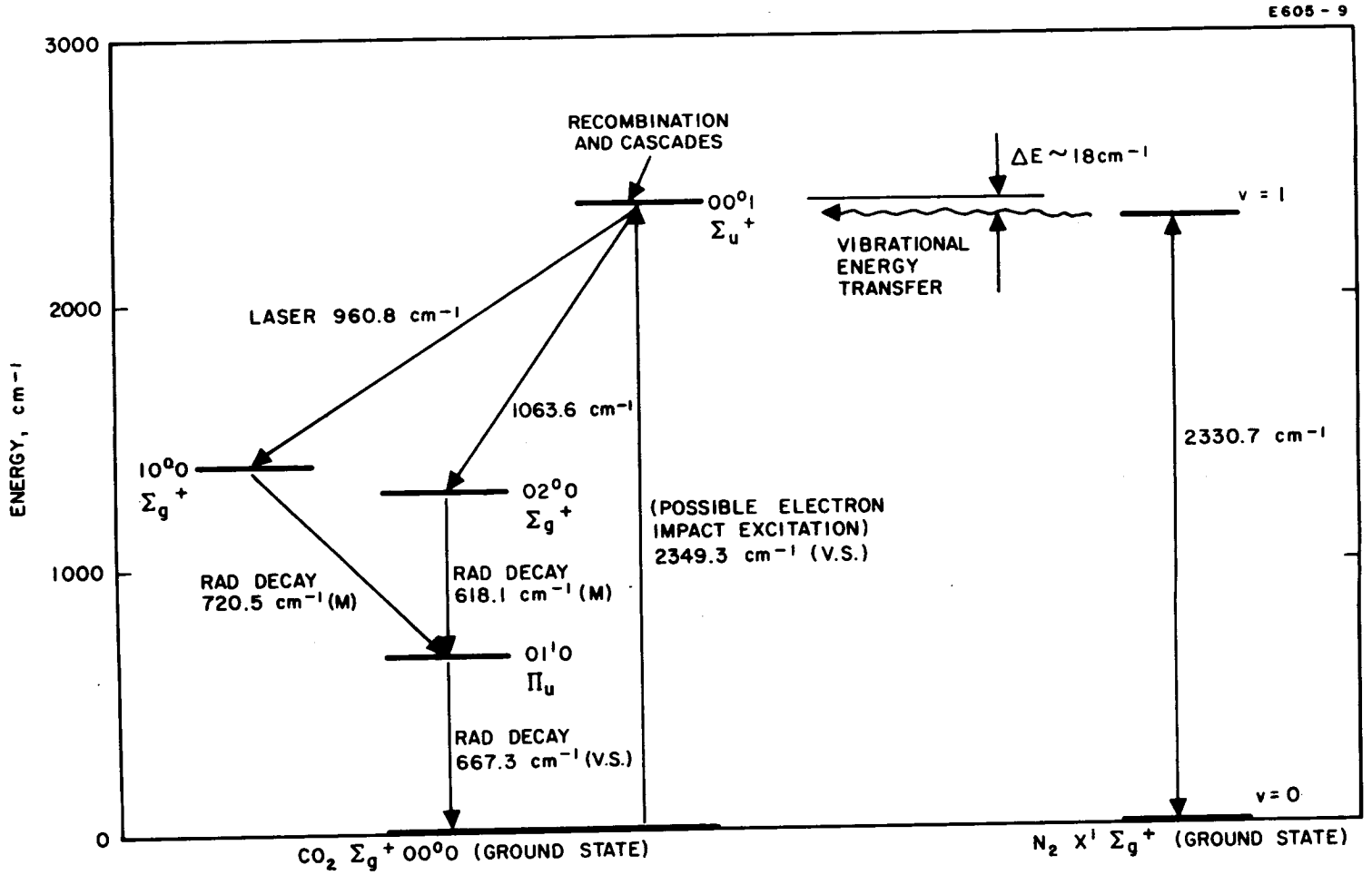

Fig. 48. Energy level diagram showing pertinent levels in CO_2 and N_2.

(b) formation of excited sensitizer molecules in photoinitiated chain reactions or direct photodissociation with subsequent transfer of vibrational energy to CO_2; (c) direct formation of CO_2 by photo and thermal decompositions. Of these possibilities, photoinitiated chain reactions with subsequent formation or sensitization of CO_2 $(00^0 1)$ seem most favorable since a major part of the excitation energy would be derived from chemical bonds. These excitation schemes are considered below. Because of the lack of extensive kinetic data of elementary reactions and nonradiative dissipation and energy transfer processes, it is not possible to predict the success or failure of these schemes.

1. Chemical Formation of CO_2 from Photodissociation Products

a. Nitrogen Dioxide-Carbon Monoxide

Nitrogen dioxide photodecomposes to oxygen atoms and nitric oxide when exposed to sunlight ($\lambda \leq 4050$ Å). Hence, mixtures of NO_2 and CO may produce excited CO_2 upon irradiation. Molecular oxygen could be used to convert NO back to NO_2. The pertinent reactions are

$$NO_2 + h\nu \rightarrow NO + O$$
$$O + CO \rightarrow CO_2^*$$
$$NO + O_2 \rightarrow NO_2 + O \quad .$$

b. Ozone-Carbon Monoxide

A similar situation exists for ozone, although its absorption coefficient is considerably lower than that for NO_2.

$$O_3 + h\nu \rightarrow O_2 + O$$
$$O + CO \rightarrow CO_2^* \quad .$$

c. Miscellaneous Systems

Additional secondary reactions which produce CO_2 from CO are listed below. In each case, the reactive species could be obtained from a photoinitiated process.

$$O + HCOOH \rightarrow CO_2^* + OH + H$$

$$H + O_2 + CO \rightarrow CO_2^* + OH$$

$$H + CH_3COO \rightarrow CH_4 + CO_2^*$$

$$OH + CO \rightarrow CO_2^* + H \quad .$$

Most of these reactions have been postulated as elementary processes occurring in high temperature flames. However, when light is used to form the reactive components, high temperatures are not necessary for the secondary reactions to proceed at reasonable rates. Chemiluminescence has been observed in some of these reactions, and the vibrational population distribution associated with a newly formed chemical bond is non-Boltzmann; however, experimental investigations are required to determine whether sufficient inversion density can be obtained to overcome cavity losses and allow laser oscillation.

2. Photochemical Formation of CO_2 (00^01) Sensitizers

Sensitization or energy transfer to the upper laser level of CO_2 is thought to be an important process in the operation of CO_2 lasers when excitation occurs by electrical discharge. Addition of either CO or N_2 enhances the power output; vibrational energy transfer is expected on the basis of close energy matching between the CO and N_2 fundamental vibrations and the CO_2 transition $00^00 \rightarrow 00^01$ which occurs at 2350 cm^{-1}. Thus it is of interest to consider photochemical formation of compounds which could transfer energy to the upper laser level of CO_2. Compounds whose fundamental vibrations occur at higher frequencies than 2350 cm^{-1} may be useful since anharmonicity

effects reduce the vibrational energy level separations of upper levels. Several possibilities are suggested below.

$$
\begin{aligned}
Cl_2 + h\nu &\rightarrow 2Cl \\
Cl + H_2 &\rightarrow HCl^* + H \\
H + Cl_2 &\rightarrow HCl^* + Cl \\
HCl^* + CO_2 &\rightarrow CO_2^* + HCl
\end{aligned}
$$

$$
\begin{aligned}
(CH_3)_2N_2 + h\nu &\rightarrow 2CH_3 + N_2^* \\
N_2^* + CO_2 &\rightarrow CO_2^* + N_2
\end{aligned}
$$

$$
\begin{aligned}
M(CO)_n + h\nu &\rightarrow M(CO)_{n-1} + CO^* \\
CO^* + CO_2 &\rightarrow CO_2^* + CO
\end{aligned}
$$

$$
\begin{aligned}
R_2C = C = O + h\nu &\rightarrow R_2C + CO^* \\
CO^* + CO_2 &\rightarrow CO_2^* + CO \quad .
\end{aligned}
$$

3. Photochemical and Thermal Decompositions

Direct formation of carbon dioxide is known to occur, but it usually requires ultraviolet rather than visible radiation. Organic acids and esters yield CO_2 in a photochemical primary process. However, compounds of this type which can be vaporized at room temperature ordinarily do not absorb appreciably beyond 3600 Å.

Solar energy might be utilized as a high temperature source to provide energy for thermal decomposition processes which produce either CO_2^* or CO_2^* sensitizers. Some possible examples are given below.

$$RN_3 \xrightarrow{\Delta} RN + N_2^*$$

$$(CH_3)_2N_2 \xrightarrow{\Delta} 2CH_3 + N_2^*$$

$$CH_3 + N_2O \rightarrow CH_3O + N_2^*$$

$$N_2^* + CO_2 \rightarrow CO_2^*$$

$$2CO + O_2 \xrightarrow{\Delta} 2\,CO_2^*$$

$$CH_3\overset{O}{\overset{\|}{C}}COOH + h\nu \rightarrow CH_3CHO + CO_2^*$$

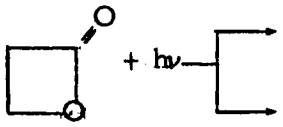

$$\rightarrow CO_2^* + C_2H_4$$

$$\rightarrow CO + CH_3CHO$$

SECTION V

EVALUATION OF SOLAR PUMPING

A. SOLAR EXCITATION RATES FOR PHOTODISSOCIATIVE SYSTEMS

We have attempted to obtain a rough measure of pumping rates for solar photodissociation of a number of molecules. This was accomplished by essentially overlapping the solar emission spectrum with the absorption spectrum of the molecule in question and performing an approximate numerical integration of the product of $\sigma(\lambda)\, I(\lambda)$ where $\sigma(\lambda)$ is the molecular cross section for absorption of a photon of wavelength λ, and $I(\lambda)$ is the number of photons/sec-cm^2 of wavelength λ within a given bandwidth reaching the earth from the sun.

Let us consider the photodissociation of the molecule AB

$$AB + h\nu \xrightarrow{\sigma I} A^* + B \text{ (excited fragment } A^* \text{ formed)} \tag{68}$$

$$A^* \xrightarrow{k_f} A + h\nu \text{ (fluorescence of } A^* \text{ to ground state)} \tag{69}$$

$$A^* + M \xrightarrow{k_d} A + M^* \text{ (collisional deactivation of } A^*) \tag{70}$$

$$A + B \xrightarrow{k_r} AB \text{ (recombination of AB)} \quad . \tag{71}$$

If the gas AB is subjected to photon flux $I(\lambda)$ (photons/sec-cm^2-unit wavelength interval) the rate of absorption of light by AB and hence the rate of dissociation is

$$R_d = \sigma(\lambda)\, I(\lambda)\, [AB] \text{ per cm}^3\text{-sec} \tag{72}$$

where [AB] is the concentration of AB in molecules per cubic centimeter. We see that $\sigma(\lambda)\, I(\lambda)$ in (72) is an effective rate constant for photodissociation of AB. The absorption cross section $\sigma(\lambda)$ is that which appears in the expression for the exponential attenuation of light passing through an absorbing medium

$$I/I_o = e^{-\sigma n \ell} = 10^{-\epsilon c \ell} \tag{73}$$

where ℓ is the length of the absorbing medium, n and c are concentrations in molecules per cubic centimeter and moles per liter, respectively, and ϵ is the molar extinction coefficient. Thus we have the connection between the absorption cross section and the molar extinction coefficient for a material ($\sigma = 3.82 \times 10^{-21}\, \epsilon$).

We have computed effective rate constants for photodissociation by taking the cross section, multiplying by the solar flux at a particular wavelength, and adding up the contributions of this product for all wavelengths.

$$\int_o^\infty \sigma(\lambda)\, I(\lambda)\, d\lambda = (\sigma I)_{eff} \quad . \tag{74}$$

In Fig. 49 we see first (Fig. 49(a)) a curve of $I(\lambda)$ versus λ showing the spectral flux arriving above the earth's atmosphere from the sun. The second curve (Fig. 49(b)) shows $\sigma(\lambda)$ versus λ for one of the molecules considered (ICl), and the third curve (Fig. 49(c)) shows the product $\sigma(\lambda)\, I(\lambda)$ plotted as a function of λ. The area under the third curve corresponds to the integral in (74). The integral in (74) is approximated by a sum for our computations.

$$\sum_{\lambda=0}^{\infty} \sigma(\lambda)\, I(\lambda)\, \Delta\lambda = (\sigma I)_{eff} \quad . \tag{75}$$

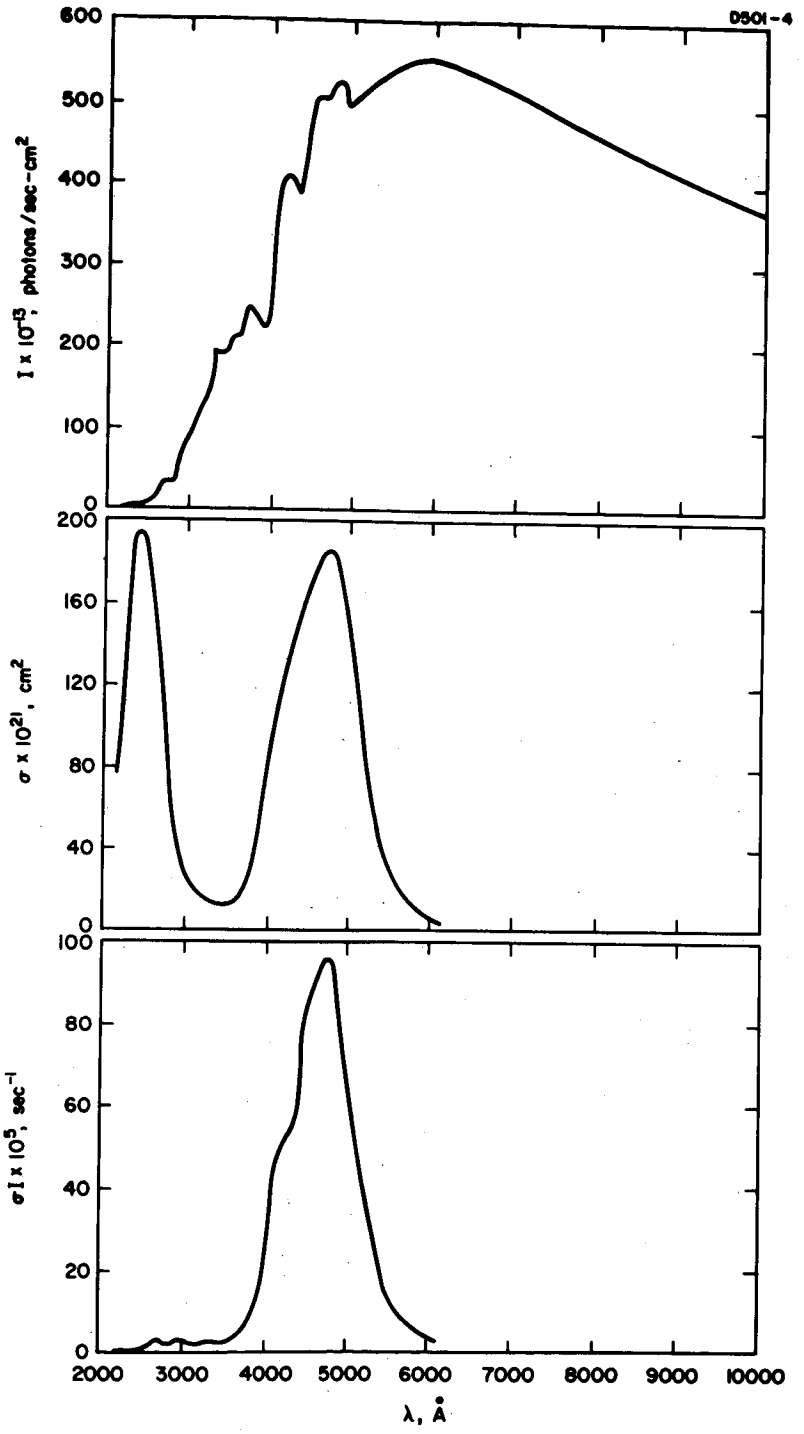

Fig. 49.
(a) Solar emission spectrum, (b) Absorption spectrum of iodine monochloride, (c) Solar pumping rate of ICl as derived from (a) and (b).

TABLE VIII

D638-1

Solar Pumping Rates

Compound	$(\sigma I)_{eff}$, sec^{-1}	Pumping Rate,[a] photons absorbed/sec-cm^3
IBr	6.7×10^{-2}	2.4×10^{15}
NO_2	3.0×10^{-2}	1.0×10^{15}
ICl	2.3×10^{-2}	8.1×10^{14}
N_2O_4	6.4×10^{-3}	2.3×10^{14}
Cl_2O	4.6×10^{-3}	1.6×10^{14}
NOCl	3.6×10^{-3}	1.3×10^{14}
CH_3I	8.8×10^{-4}	3.1×10^{13}

[a]For gas at 1 Torr, 278°K

In (75), $\Delta\lambda$ was taken to be 100 Å. Thus, the $(\sigma I)_{eff}$ were computed by taking the value of σ at a given wavelength, multiplying by the number of photons per second per square centimeter in a 100 Å bandwidth centered at that wavelength, and adding the products over the entire spectrum.

The results for a number of molecules are shown in Table VIII. In addition to the values of $(\sigma I)_{eff}$ we also include excitation (pumping) rates computed for gases at 1 Torr pressure and 278°K subjected to unconcentrated solar flux. The number of molecules contained in 1 cm^3 of an ideal gas under the above conditions is 3.5×10^{16} molecules/cm^3. We see that the initial pump rates given in Table VIII corresponds to a few tenths of a percent to a few percent per second of the total number of molecules present. Thus with a hundred-fold increase in intensity (a figure easily attainable), a substantial amount of photolysis can take place in a short time.

In order that the above numbers have meaning with regard to laser potential, the pump rates must be compared with those for deactivation processes of the excited fragments. However, in most cases, we have incomplete information on these processes.

B. EVALUATION OF SUN-PUMPED PHOTODISSOCIATIVE SYSTEMS

1. Energy Level Representation — Rate Equations

Photodissociative systems which produce excited fragments are expected to operate as four-level lasers. Therefore, it is of interest to determine semiquantitatively the dynamics of the processes responsible for achieving laser action. The parameters involved are A_{ij}, the rate coefficient which accounts for spontaneous radiation from level i to level j; W_{ij}, the probability per unit time that a molecule exposed to isotropic radiation of frequency ν_{ij} and intensity I_ν will absorb a quantum of energy $h\nu_{ij}$; S_{ij}, the transition probability per unit time for a spontaneous nonradiative transition; and k_{ij}, the rate coefficient for chemical processes. The general expression for the rate equations is given by

$$\frac{dN_i}{dt} = \sum_j W_{ij}(N_j - N_i) - \sum_j N_i A_{ij} + \sum_j (S_{ji}N_j - S_{ij}N_i)$$

$$+ \sum_j (k_{ji}N_j - k_{ij}N_i) \quad . \tag{76}$$

In order that a component of induced emission from level i may occur, N_j must be greater than N_i. This is a minimum requirement; the excess population or critical population density $(N_j - N_i)$ must be great enough to overcome cavity losses. A quantitative formulation of this quantity in terms of the cavity and emission parameters was developed in Section II. The condition for laser action is expressed by

$$\frac{\lambda_o^2}{4\pi^2 \tau \Delta\nu} \quad \frac{L}{\ln(1/R)} \left(\frac{m_j}{m_i} N_i - N_j \right) > 1 \qquad (77)$$

where λ_o, τ, $\Delta\nu$, and N have their usual significance. R is the reflectivity of the mirrors, m_j is the degeneracy of the j^{th} level, and L is the length of active material.

An estimate of $(N_i - N_j)$ can be obtained by consideration of the simplified energy level scheme given in Fig. 50. Processes such as fluorescence and nonradiative transitions from state 4 which terminate at levels other than 2 and 3 are omitted for simplicity and because they are considered to be of minor importance in the systems suggested. In most cases state 4 is very short lived, since W_{14} corresponds to excitation in the continuum; it is included in order to indicate the possibility of branching to the laser levels 2 and 3. The chemical and physical processes of potential photodissociative laser materials are conveniently analyzed systematically with reference to this type of schematic diagram; a few examples are indicated. The IBr case is straightforward; the situation for molecules such as NOCl and NO_2 requires explanation of what is intended by the diagram. After excitation of NOCl to state 4, process S_{43} may result in formation of vibrationally excited NO molecules, $Cl(^2P_{1/2})$ atoms or vibrationally excited NOCl molecules (not indicated) in the reversible part of the cycle. In the case of NO_2, process S_{43} indicates formation of vibrationally excited NO molecules and/or vibrationally excited O_2 formed in a chemical reaction between oxygen atoms produced in the primary process and ground state NO_2 molecules. Application of the generalized rate equation above for each level yields

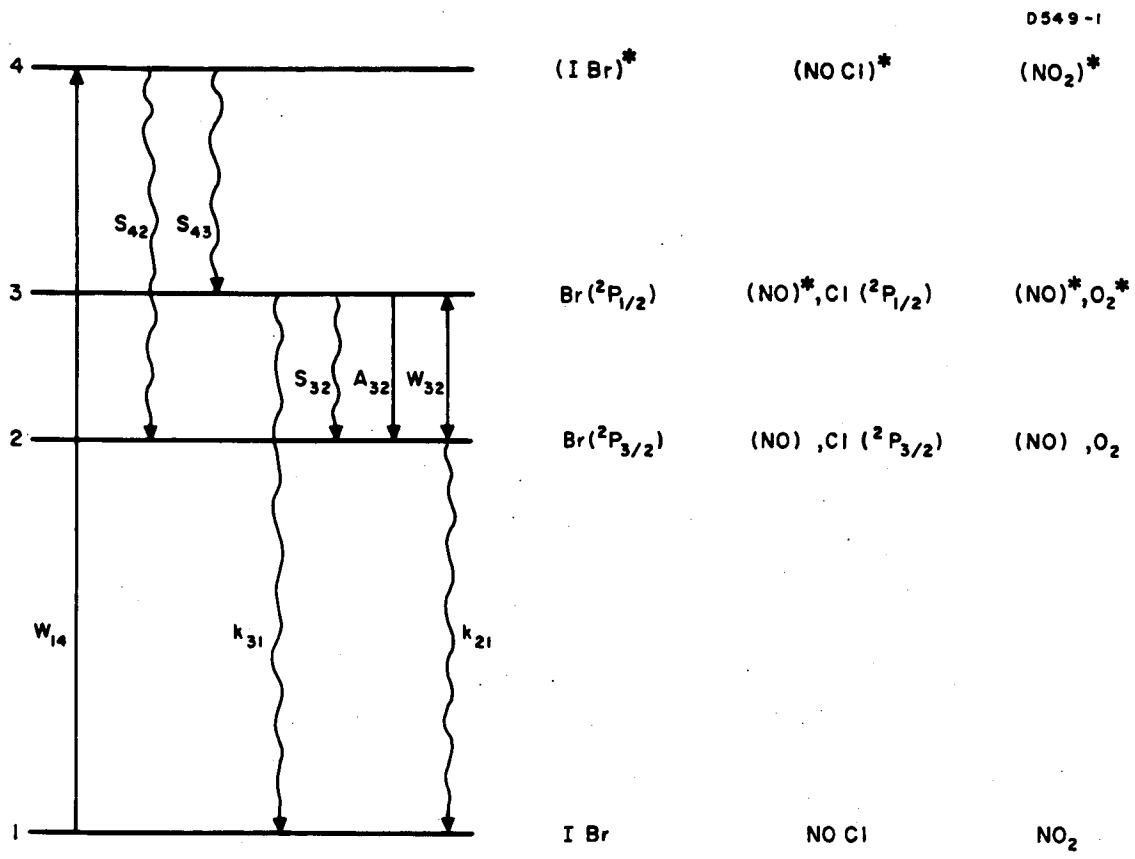

Fig. 50. Schematic diagram for photodissociative laser systems.

$$\frac{dN_1}{dt} = -W_{14}N_1 + k_{31}N_3 + k_{21}N_2 \tag{78}$$

$$\frac{dN_2}{dt} = S_{42}N_4 + (S_{32} + A_{32} + W_{32})N_3 - (k_{21} + W_{23})N_2 \tag{79}$$

$$\frac{dN_3}{dt} = W_{23}N_2 + S_{43}N_4 - (k_{31} + S_{32} + A_{32} + W_{32})N_3 \tag{80}$$

$$\frac{dN_4}{dt} = W_{14}N_1 - (S_{42} + S_{43})N_4 \quad . \tag{81}$$

These differential equations may be set equal to zero in the steady state approximation. This gives the following set of equations:

$$N_1 = \frac{k_{31}}{W_{14}} N_3 + \frac{k_{21}}{W_{14}} N_2 \tag{82}$$

$$N_2 = \frac{S_{42}}{k_{21} + W_{23}} N_4 + \frac{S_{32} + A_{32} + W_{32}}{k_{21} + W_{23}} N_3 \tag{83}$$

$$N_3 = \tau_3 S_{43} N_4 + \tau_3 W_{23} N_2 \tag{84}$$

$$N_4 = \frac{W_{14}}{S_{42} + S_{43}} N_1 \tag{85}$$

$$\tau_3 \equiv \frac{1}{k_{31} + S_{32} + A_{32} + W_{32}} \quad . \tag{86}$$

Rearranging (82) gives

$$N_2 = \frac{W_{14}}{k_{21}} N_1 - \frac{k_{31}}{k_{21}} N_3 \tag{87}$$

$$N_3 = \frac{W_{14}}{k_{31}} N_1 - \frac{k_{21}}{k_{31}} N_2 \quad . \tag{88}$$

Substitution of (85), (86), and (88), and into (83) and (84) gives

$$N_3 = \frac{\dfrac{S_{43}}{S_{42} + S_{43}} + \dfrac{W_{23}}{k_{21}}}{\dfrac{1}{\tau_3} + \dfrac{k_{31} W_{23}}{k_{21}}} W_{14} N_1 = \alpha N_1 \tag{89}$$

$$N_2 = \frac{\dfrac{S_{42}}{S_{42} + S_{43}} + \dfrac{S_{32} + A_{32} + W_{32}}{k_{31}}}{k_{21} + W_{23} + \dfrac{(S_{32} + A_{32} + W_{32})\, k_{21}}{k_{31}}} W_{14} N_1 = \beta N_1 \tag{90}$$

$$(N_3 - N_2) = (\alpha - \beta) N_1 \, . \tag{91}$$

When

$$S_{43} >> S_{42} \tag{92}$$

$$k_{21} >> k_{31}, \tag{93}$$

α and β simplify to

$$\alpha = \left(\frac{W_{23}}{k_{21}} + 1\right) \tau_3 W_{14} \tag{94}$$

$$\beta = \left(\frac{S_{32} + A_{32} + W_{32}}{k_{21}}\right) \tau_3 W_{14} \quad . \tag{95}$$

Equation (91) reduces to

$$(N_3 - N_2) = \frac{k_{21} - (S_{32} + A_{32})}{k_{21}} \tau_3 W_{14} N_1 \, . \tag{96}$$

If

$$k_{21} >> (S_{32} + A_{32}) \tag{97}$$

$$(N_3 - N_2) = \tau_3 W_{14} N_1 \, . \tag{98}$$

For photodissociative systems S_{4j} is very large ($\sim$ molecular vibration frequency). This implies the condition

$$N_4 << (N_1 + N_2 + N_3) \equiv N_o \, . \tag{99}$$

Combination of (89) and (90) gives

$$N_3 = \frac{\alpha}{\beta} N_2 \, . \tag{100}$$

Substitution of (89), (90), and (100) into (99) gives direct relationships between N_3, N_2, and N_o.

$$N_3 = \frac{\alpha}{\alpha + \beta + 1} N_o \tag{101}$$

$$N_2 = \frac{\beta}{\alpha + \beta + 1} N_o \tag{102}$$

$$(N_3 - N_2) = \frac{\alpha - \beta}{\alpha + \beta + 1} N_o . \tag{103}$$

Thus the inversion density available for laser action from a particular system can be expressed in terms of the parameters α, β, and N_o. N_o is a known quantity and α and β are calculable from a knowledge of molecular and atomic rate coefficients for radiative, nonradiative, and chemical processes. Although values for all of these coefficients may not be known, systems may be anticipated for which the conditions (92) and (93) hold and reduce the complexity of α and β.

Therefore, in order to obtain maximum efficiency from photodissociative laser systems, it is important to choose molecules for which the primary quantum yield of dissociation and the branching ratio (S_{43}/S_{42}) is high. The rate coefficient k_{21} for depletion of the lower laser level should be greater than the sum of the rate constant S_{32} for internal radiationless conversion between the laser levels, the reciprocal of the natural radiative lifetime τ_o of the upper laser level, and k_{31} (the coefficient for deactivation of the upper laser level by chemical processes).

2. Feasibility of Operation — Critical Inversion Density

An approximate estimate of the potentiality of solar pumped photodissociative systems for producing coherent emission can be made by calculating the concentration which can be produced in the upper laser level during the lifetime of this state. The extent by which this maximum concentration N_m of active species exceeds the minimum inversion density required for laser action (eq. (77)) is a measure of the capability of the system to operate. We have calculated N_m for several photodissociative systems using the values of solar pumping rates presented in Table VIII and estimated lifetimes for the excited species in a typical laser gas mixture (1 Torr substrate and 100 Torr buffer gas). These values are given in Table IX.

The required inversion density is given by rearrangement of (77) and substitution of the required parameters. A sample calculation is carried out below for the IBr system.

$$\left(\frac{m_2}{m_3} N_3 - N_2\right)_{min} = \frac{4\pi^2 \tau_3 \Delta\nu}{\lambda_o^2} \cdot \frac{\ln (1/R)}{L} \quad . \qquad (104)$$

The degeneracies $(2J + 1)$ of the appropriate levels of Br are $m_2 = 4$, $m_3 = 2$, and $\lambda_o = 2.7\ \mu$. R and L are taken as 0.99 and 100 cm respectively, and τ_3 is estimated from its radiative lifetime τ_o. For Br, τ_3 is assumed to be $10^{-2}\ \tau_o$ by analogy with iodine behavior under similar conditions. $\Delta\nu$ is calculated in the usual way for Doppler and collision broadening[145]:

$$\Delta\nu = \Delta\nu_D + \Delta\nu_c \qquad (105)$$

TABLE IX

Evaluation of Sun-Pumped Photodissociative Systems

Substrate (Parent Molecule)	Excited Species	Solar Pumping Rate[a]	Natural Radiative Lifetime τ_o, sec	Estimated Lifetime τ Under Laser Conditions	Estimated[f] Population of Active Species
CH_3I	I	3.1×10^{13}	0.13[b]	10^{-3}[d]	3.1×10^{10}
IBr	Br	2.4×10^{15}	1.1[b]	$10^{-2}\tau_o$	2.6×10^{13}
ICl	Cl	8.1×10^{14}	81[c]	$10^{-2}\tau_o$	6.5×10^{14}
Cl_2O	Cl	1.6×10^{14}	81[c]	$10^{-2}\tau_o$	1.3×10^{14}
NOCl	Cl	1.3×10^{14}	81[c]	$10^{-2}\tau_o$	1.0×10^{14}
NOCl	NO	1.3×10^{14}	—	10^{-4}[e]	1.3×10^{10}
N_2O_4	NO_2	2.3×10^{14}	—	10^{-4}	2.3×10^{10}
NO_2	NO	1.0×10^{15}	—	10^{-4}[e]	1.0×10^{11}
Cl_2O	ClO	1.6×10^{14}	—	10^{-4}[e]	1.6×10^{10}

[a] Photons absorbed per sec-cm^3 for gas at 1 Torr and 25°C; see Quarterly Report No. 2, p. 19.

[b] Ref. 109.

[c] Calculated from $A_m(J, J') = 35,320\ (\tilde{\nu}/R)^3 S_m(J, J')/2J + 1\ \text{sec}^{-1}$ given in Ref. 143. The value of $S_m(1/2, 3/2) = 4/3$ which we used is that calculated by Garstang[109] for np and np^5 atomic configurations.

[d] Ref. 108.

[e] Ref. 144.

[f] Product of the solar pumping rate and lifetime τ in units of active species per cubic centimeter.

where

$$\Delta\nu_D = 2\sqrt{2\ln 2}\ \frac{\nu_o}{c}\sqrt{\frac{kT}{M}} \tag{106}$$

$$\Delta\nu_c = \frac{Z_1}{\pi} = \sqrt{2}\ Nd^2\sqrt{\frac{8kT}{\pi M}} \tag{107}$$

Z_1 ≡ collision number

N ≡ number density

d ≡ diameter.

Substitution of the appropriate values for bromine gives

$$\Delta\nu = 2 \times 10^8\ \text{sec}^{-1}\ .$$

Thus

$$(2N_3 - N_2)_{min} = \frac{4\pi^2 \times 10^{-2} \times 2 \times 10^8}{(2.7 \times 10^{-4})^2} \cdot \frac{10^{-2}}{10^2} \cong 10^{11}\ \text{cm}^{-3}\ . \tag{108}$$

Comparison with the values listed in Table IX indicates that laser action is to be expected from the IBr system as well as from several of the other systems for which the above calculations are applicable (within an order of magnitude).

Note that since magnification of the solar flux was not assumed, a hundred-fold increase in intensity should be easily attainable with a collector. Therefore, it would be expected that many of the systems suggested to date might produce stimulated coherent emission when subjected to solar radiation, at least on a pulsed basis. Experimental investigations are required to determine optimum operating conditions and hence a maximum power output on either a pulsed or continuous

basis. However, as indicated in Part 2, preliminary experimental results with flash photolysis are disappointing because they suggest that high power pumping intensities may be necessary — apparently in order to overcome highly efficient collisional deactivation processes by parent molecules, as in the case of IBr. However the failure to observe laser action from IBr in preliminary experiments may be caused by effects other than pumping intensity. No attempt was made to filter the pumping light or to remove minor impurities. Both of these procedures could be quite important and must be considered before a complete evaluation of this material can be made.

C. SUN-PUMPED SOLID STATE LASERS

As a point of comparison, it must be noted that there are several solid state laser materials with which solar pumping is feasible. There are two reports of lasers actually operated with sunlight as the pumping source, although detailed information regarding power output and efficiency was not presented. Both lasers use solid phase materials (glass or crystals) that emit in the infrared. In one case,[146] Nd_2O_3-doped barium crown glass was pumped for 0.5 sec intervals with sunlight collected from a 61 cm diameter parabolic mirror. This was a 30 mm long fiber laser consisting of a 0.1 mm neodymium-glass core clad by a 1.0 mm diameter soda-lime silicate glass. Flash thresholds with a xenon flash lamp were on the order of 1 J for this laser, whose output is at 1.06 μ. The other[147] solar powered laser was a $CaF_2:Dy^{2+}$ system at liquid neon temperature; laser output was at 2.36 μ. Low pulsed laser threshold and the location of the pumping bands made it particularly suitable for sun-pumped operation. Simulated solar pumping has also been reported for a neodymium-doped calcium tungstate laser rod.[148] Continuous pumping of a 2 by 2 by 12 mm laser rod was achieved using a compact xenon arc lamp. The required spectral flux in the main pumping region from 5600 to 6000 Å was found to be 19.2 W. This system utilized a special water-cooled strontium titanate cone-sphere in which the laser rod was embedded. It was calculated that sufficient sunlight for this laser could be obtained using a collector with an area less than 1 m^2.

SECTION VI

SUMMARY OF PRELIMINARY EXPERIMENTAL STUDIES

The chief objectives of the experimental program, the details of which are given in Part 2 of this report, were to make a qualitative analysis of materials which absorb solar radiation and could potentially serve as useful laser materials. An exhaustive study was not made; factors which could be conveniently controlled (such as pressure, excitation energy, and intensity) were investigated briefly for six compounds: CF_3I, CF_3Br, IBr, BrCN, NO_2 and NOCl. The results of the experimental work are summarized here.

Laser action was not observed in the 1 to 7 μ region for CF_3Br, IBr, BrCN, and NO_2. Trifluoromethyl iodide and nitrosyl chloride were studied with regard to laser gain and pumping threshold. The former was used primarily to evaluate the experimental apparatus, although some new information on this system was obtained. The gain measurements at low pressures suggest that excited iodine atoms do not recombine as fast as gound state atoms. Furthermore, preliminary experiments with CF_3I using a pyrex filter indicate that excited iodine atoms are produced when CF_3I is photodissociated by radiation in the 3000 Å region. (This is a controversial and critical consideration in the interpretation of CF_3I photochemistry.)

Laser experiments with nitrosyl chloride have shown that chemical reversibility can be achieved by the addition of chlorine. The return reaction of chlorine and nitric oxide to form the starting material $Cl_2 + 2NO \rightarrow 2NOCl$ is very slow ($\tau_{1/2} \sim 39$ days) under the optimum conditions for laser action from NOCl-He mixtures. Although addition of NO causes a reduction of laser output, chlorine can be added in large excess with no ill effects. In this case, chlorine acts to replace helium as a buffer gas, in addition to increasing the rate of the back

reaction. Cycling times are reduced to five minutes when the gas mixture is condensed into a sidearm whose volume is one-tenth that of the laser tube, allowed to stand at room temperature, and reintroduced into the laser tube.

The maximum partial pressure of NOCl in NOCl-Cl_2 mixtures is ~ 6 Torr, and maximum laser output is achieved in the range of 3 to 5 Torr (same limits as for NOCl-He mixtures); the pumping rate from unconcentrated solar radiation is then $\sim 7 \times 10^{14}$ sec^{-1} - cm^{-3}. This is approximately four orders of magnitude lower than that used in our flash photolysis apparatus; however, magnification of the solar intensity by two or three orders of magnitude can be achieved with relatively simple collecting devices. Further investigation, especially with regard to the quenching processes, is required to determine whether a practical laser device based on this system can be achieved which is reversible and operates entirely from solar energy.

SECTION VII

CONCLUSIONS AND RECOMMENDATIONS

Several general excitation mechanisms are recommended for consideration in achieving solar pumped photochemical laser systems. Mechanisms for possible laser action include (1) photochemical dissociation to form electronically excited fragments, (2) photochemical dissociation to form vibrationally excited species, (3) stimulated emission from recombination reactions of fragments generated photochemically, (4) excitation by secondary chemical reactions resulting from species formed photochemically or thermally, (5) Franck-Condon pumping, and (6) expansion of a hot gas into a low pressure region where the equilibrium radiation temperature is much smaller than $\Delta E/k$.

Photodissociative processes provide the most direct photochemical laser excitation mechanism; this study has resulted in the selection of more than twenty compounds which absorb light in the solar region ($\lambda > 3000$ Å) and are potentially useful as solar-pumped photodissociative laser systems. Solar excitation pumping rates have been calculated for several of these gases at 1 Torr and compared with the approximate lifetime of the active excited species in order to estimate their population density. Favorable solar pumping estimates were obtained for molecules such as ICl, NOCl, Cl_2O, IBr and NO_2, but it is difficult to conclude from the known spectroscopic and photochemical properties of the compounds selected whether any of these will function in a solar pumped laser. Specific values for the rate processes which govern the population and depletion of their laser levels are not well known and must be determined experimentally. A preliminary flash photolysis survey did not show laser action for NO_2, IBr, BrCN, and CF_3Br in the 1 to 7 μ region. However, these and other compounds undergoing photodissociative processes should be studied experimentally in more detail.

The nitrosyl chloride photodissociative laser emits in the 6 μ region and our preliminary experimental studies show that it can be operated effectively as a chemically reversible system, particularly by using NOCl in the presence of excess Cl_2 with no other buffer gas. The results indicate that concentration of the solar flux by three or four orders of magnitude would provide excitation (pumping) rates sufficient for solar operation. However, our experimental investigations have been limited; we recommend an intensive experimental program designed to fully evaluate spontaneously reversible photochemical laser systems. Chemical reversibility should also be possible for the interhalogens and nitrosyl bromide by techniques similar to those used for nitrosyl chloride.

Experimental parameters such as gas pressures and pumping wavelengths must be studied in many of these photochemical systems because of their effect on the population inversion of the active species. Pressures should be low enough to avoid deleterious predissociation effects, such as may occur with I_2 and Br_2. In many of the photodissociative systems (such as the halogens, ICl, NOCl, and NO_2), pumping in the long wavelength absorption bands probably should be minimized in order to avoid direct formation of unexcited photodissociative species.

Although systems excited by the other mechanisms have been analyzed in less detail, several possible examples are suggested for experimental laser studies: excited ICl and IBr molecules formed by recombination of their atoms; excited NO_2, N_2O_4, ICN, and $CO(CN)_2$ molecules by Franck-Condon pumping; and excited CO_2, N_2O, and HCN molecules by expansion of hot gases into regions of lower temperature and pressure. Several processes of excitation by secondary chemical reactions have also been recommended for additional studies particularly in regard to the formation of excited CO_2 molecules (such as by the photolysis of NO_2 in the presence of CO and by the thermally activated reaction of CO and O_2).

A scheme for the kinetic analysis and evaluation of photochemical laser systems has been outlined, but detailed calculations on specific systems are limited by the paucity of information on excited state behavior. However, when laser action can be observed from a system under special circumstances, information of this nature can be obtained and used to modify experimental parameters so that operation may be achieved under more convenient conditions. Our general conclusion is that most of the selected compounds will produce laser action under specific laboratory conditions, but that solar operation can be achieved only after careful study of the low threshold materials and modification of solar collecting devices to provide sufficient pumping intensities.

The present studies also suggest that experimental investigations should be carried out with excitation radiation having shorter wavelengths and higher intensities than are available from solar radiation. Most of the compounds which we have proposed for solar pumped photodissociative systems absorb more strongly in the ultraviolet region ($\lambda < 3000$ Å) than at longer wavelengths, and the fragments produced are more energetic. Thus, if intense ultraviolet pumping radiation is utilizing the possibility for discovering new laser sources is increased and information fundamental to the understanding of all types of photodissociative laser systems may be obtained.

SECTION VIII

REFERENCES

1. J.V.V. Kasper and G.C. Pimentel, Appl. Phys. Letters 5, 231 (1964).

2. J.V.V. Kasper, J.H. Parker, and G.C. Pimentel, J. Chem. Phys. 43, 1827 (1965).

3. "A report on two chemical laser investigations," in Laser Focus, p. 12, October 15, 1965.

4. H. Neuimin and A. Terenin, Acta Physicochim URSS 5, 465 (1936).

5. A. Jakovleva, Acta Physicochim URSS 9, 665 (1938); 10, 433 (1939).

6. K. Butkow, Z. Physik 58, 232 (1929).

7. P.K. Sen-Gupta, Nature 136, 513 (1935).

8. D. Porret and C.F. Goodeve, Proc. Roy. Soc. (London) A165, 31 (1938).

9. A.J. DeMaria and C.J. Ultee, results reported at the 4th International Conference on Quantum Electronics, Phoenix, Arizona, April 1966.

10. T.L. Andreyva, V.A. Dudkin, V.I. Malyshev, G.V. Mikhailov, V.N. Sorokin, and L.A. Novikova, Zh. Eksperim. i Teor. Fiz. 49, 1408 (1965).

11. M.A. Pollack, Appl. Phys. Letters 8, 36 (1966).

12. J. Franck, H. Sponer, and E. Teller, Z. Phys. Chem. B18, 88 (1932).

13. G. Kornfield and M. McCaig, Trans. Faraday Soc. 30, 991 (1934).

14. G.M. Harris and J.E. Willard, J. Am. Chem. Soc. 76, 4678 (1954).

15. R.D. Doepker and P. Ausloos, J. Chem. Phys. 41, 1865 (1964).

16. H.M. Frey, Proc. Roy. Soc. (London) A250, 409 (1959); A251, 575 (1959).

17. G. Herzberg, Proc. Chem. Soc. 116 (1959).

18. N. Basco and R.G. W. Norrish, Can. J. Chem. 38, 1769 (1960).

19. A.B. Callear and R.G.W. Norrish, Nature 188, 53 (1960).

20. M.A. Pollack, Twenty-Fourth Conference on Electron Device Research, California Institute of Technology, Pasadena, Calfiornia, June 1966.

21. V.N. Kondrat'ev, Kinetics of Chemical Gas Reactions (Academy of Sciences, USSR, Moscow, 1958), p. 240.

22. R.A. Young and R.L. Sharpless, Discussions Faraday Soc. 33, 228 (1962); J. Chem. Phys. 39, 1071 (1963).

23. A.N. Terenin and N.A. Prizlezhaeva, Physik Z. Soviet Union 2, 337 (1932).

24. C. Zener, Phys. Rev. 37, 556 (1931).

25. J.G. Calvert and J.N. Pitts, Jr., Photochemistry (Wiley and Sons, New York, 1966).

26. N. Basco, J.E. Nicholas, R.G.W. Norrish, and W.H. J. Vickers, Proc. Roy. Soc. (London) A272, 147 (1963).

27. M.A. Pollack, Appl. Phys. Letters 9, 230 (1966).

28. K.E. Shuler, T. Carrington, and J.C. Light, Appl. Optics, Suppl. 2, p. 81 (1965).

29. J.V.V. Kasper and G.C. Pimentel, Phys. Rev. Letters 14, 352 (1965).

30. J.R. Henderson and M. Muramoto, Appl. Optics 5, 831 (1966).

31. N.G. Basov, A.I. Oraevskii, and V.A. Shcheglov, JETP Letters 4, 41 (1966).

32. G. Herzberg, Infrared and Raman Spectra (Van Nostrand, New York, 1945).

33. G. Herzberg, Spectra of Diatomic Molecules, 2nd ed. (Van Nostrand, New York, 1950).

34. H. Sponer, Radiation Res., Suppl. 1, 558 (1959).

35. L.A. Turner, Phys. Rev. 38, 574 (1931).

36. L.A. Turner, Phys. Rev. 31, 983 (1926).

37. D.J. Seery and D. Britton, J. Phys. Chem. 68, 2263 (1964).

38. W.G. Brown and G.E. Gibson, Phys. Rev. 40, 529 (1932).

39. D.M. Yost and J. McMorris, J. Am. Chem. Soc. 54, 2247 (1932).

40. W.G. Brown, Phys. Rev. 42, 355 (1932).

41. H. Cordes, Z. Physik. 74, 34 (1932).

42. D.M. Yost and J. McMorris, J. Am. Chem. Soc. 53, 2625 (1931).

43. H. Cordes and H. Sponer, Z. Physik. 63, 338 (1930).

44. G. Herzberg and P. Scheibe, Physik Chem. B7, 390 (1930).

45. D. Porret and C.F. Goodeve, Trans. Faraday Soc. 33, 690 (1937).

46. C.F. Goodeve and S. Katz, Proc. Roy. Soc. (London) A172, 436 (1939).

47. N. Basco and R.G.W. Norrish, Proc. Roy. Soc. (London) A268, 291 (1962).

48. J. Mason, J. Chem. Soc. 4537 (1963).

49. M. Green and J.W. Linnett, Trans. Faraday Soc. 57, 1 (1961).

50. C.F. Goodeve and J.I. Wallace, Trans. Faraday Soc. 26, 254 (1930).

51. W. Finkelnburg, H.J. Schumacher, and G. Stiefer, Z. Physik. Chem. B15, 127 (1931).

52. F.J. Lifscomb, R.G.W. Norrish, and G. Porter, Nature 174, 785 (1954).

53. R.M. Badger and S. Woo, J. Am. Chem. Soc. 53, 2572 (1931).

54. K.D. Bayes, Can. J. Chem. 39, 1074 (1961).

55. R.A. Young, J. Chem. Phys. 40, 1848 (1964).

56. N. Basco, J.E. Nicholas, R.G.W. Norrish, and W.H.J. Vickers, Proc. Roy. Soc. (London) A272, 147 (1963).

57. A. Neuimin and A. Terenin, J. Chem. Phys. 3, 436 (1935).

58. A.V. Jakovleva, Acta Physicochim URSS 9, 665 (1938); 10, 433 (1939).

59. A.V. Jakovleva, Soviet Phys.—JETP 9, 10 (1939).

60. J. Prochorow, A. Tramer, and K.L. Wierzchowski, J. Mol. Spectry. 19, 45 (1966).

61. H.H. Jaffé and M. Orchin, Theory and Applications of Ultraviolet Spectroscopy (Wiley and Sons, New York, 1962).

62. J.C.D. Brand, J. Chem. Soc. 858 (1956).

63. G.W. Robinson, Can. J. Phys. 34, 699 (1956).

64. A.D. Cohen and C. Reid, J. Chem. Phys. 24, 85 (1956).

65. W. Kemula and K.L. Wierzchowski, Roczniki Chem. 27, 524 (1953).

66. R.K. Sheline, J. Am. Chem. Soc. 73, 1615 (1951).

67. H. Haas and R.K. Sheline, J. Am. Chem. Soc. 88, 3219 (1966).

68. H.W. Thompson and H.P. Garratt, J. Chem. Soc. (London) 524, 8 (1934).

69. A.G. Massey and L.E. Orgel, Nature 191, 1387 (1961).

70. M.A. El-Sayed, J. Phys. Chem. 68, 433 (1964).

71. G. Karl and J.C. Polanyi, J. Chem. Phys. 38, 271 (1963).

72. F. Feher and H. Muenzner, Chem. Ber. 96, 1131 (1963).

73. H.P. Koch, J. Chem. Soc. 394 (1949).

74. Feher and Muenzner, op. cit.

75. L. Lorenz and R. Samuel, Z. Physik Chem. (Leipzig) B14, 219 (1931).

76. R.G. Sowden and N. Davidson, J. Chem. Soc. 78, 1291 (1956).

77. E. Treiber, J. Gierer, J. Rehnstrom, and K.E. Almin, Acta Chem. Scand. 11, 752 (1957).

78. A.B. Callear and W.J.R. Tyerman, Trans. Faraday Soc. 61, 2395 (1965).

79. A.B. Callear and W.J.R. Tyerman, Trans. Faraday Soc. 62, 73 (1966).

80. W.C. Price and D.M. Simpson, Proc. Roy. Soc. (London) A169, 501 (1939).

81. A.R. Knight, O.P. Strauz, S.M. Malm, and H.E. Gunning, J. Am. Chem. Soc. 86, 4243 (1964).

82. T.F. Deutsch, Appl. Phys. Letters 8, 334 (1966).

83. J.C.D. Brand, J.H. Callomon, D.C. Moule, J. Tyrrell, and T.H. Goodwin, Trans. Faraday Soc. 61, 2365 (1965).

84. J. Romand, Ann. Phys. (Paris) 4, 529 (1949).

85. S.S. Kim, Technical Report BRN-18-P, Project Squid, Contract Nonr 3623(00), NR-098-038, January 1966.

86. D.L Bunker and N. Davidson, J. Am. Chem. Soc. 80, 5090 (1958).

87. D.E. Stogryn and J.O. Hirschfelder, J. Chem. Phys. 31, 1531, 1545 (1959); 33, 942 (1960).

88. S.K. Kim and J. Ross, J. Chem. Phys. 42, 263 (1965).

89. H. Kiefer and R.W. Lutz, J. Chem. Phys. 42, 1709 (1965).

90. J.P. Rink, H.T. Knight, and R.E. Duff, J. Chem. Phys. 34, 1942 (1961).

91. J.P. Rink, J. Chem. Phys. 36, 572 (1962).

92. J.O. Hirschfelder, C.F. Curtiss, and R.B. Bird, Molecular Theory of Gases and Liquids (Wiley, New York, 1954).

93. K.E. Russell and J. Simon, Proc. Roy. Soc. (London) A217, 271 (1953).

94. M.I. Christie, A.J. Harrison, R.G.W. Norrish, and G. Porter, Proc. Roy. Soc. (London) A231, 446 (1955).

95. D. Britton, N. Davidson, W. Gehman, and G. Schott, J. Chem. Phys. 25, 804 (1956).

96. R.L. Strong, J.C. Chien, P.E. Graf, and G. Porter, Proc. Roy. Soc. (London) A231, 446 (1955).

97. D. Britton and N. Davidson, J. Chem. Phys. 25, 8101 (1956).

98. H.B. Palmer and D.F. Hornig, J. Chem. Phys. 26, 98 (1957).

99. H. Margenau, Phys. Rev. 66, 303 (1944); 64, 131 (1943).

100. R.L. Strong, J.C.W. Chien, P.E. Graf, and J.E. Willard, J. Chem. Phys. 26, 1287 (1957).

101. M.I. Christie, A.J. Harrison, R.G.W. Norrish, and G. Porter, Proc. Roy. Soc. (London) A231, 446 (1955).

102. D.L. Bunker and N. Davidson, J. Am. Chem. Soc. 80, 5088 (1958).

103. G. Porter and J.A. Smith, Proc. Roy. Soc. (London) A261, 28 (1961).

104. J. Engleman and N. Davidson, J. Am. Chem. Soc. 82, 4770 (1960).

105. G. Porter, Z.G. Szabo, and M.G. Townsend, Proc. Roy. Soc. (London) A270, 493 (1962).

106. G. Porter, Discussions Faraday Soc. 33, 198 (1962).

107. R.G.W. Norrish and G. Porter, Nature 164, 658 (1949).

108. R.J. Donovan and D. Husain, Nature 206, 171 (1965).

109. R.H. Garstang, J. Res. Natl. Bur. Std. (U.S.) A68, 61 (1964).

110. R.J. Donovan and D. Husain, Trans. Faraday Soc. 62, 2023 (1966).

111. A.B. Callear, Appl. Optics, Suppl. 2, 145 (1965).

112. G.C. Pimentel, private communication.

113. A.B. Callear and J.F. Wilson, Nature 211, 517 (1966).

114. S.J. Arnold, N. Finlayson, and E.A. Ogryzlo, J. Chem. Phys. 44, 2529 (1966).

115. S.J. Arnold, E.A. Ogryzlo, and H. Witzke, J. Chem. Phys. 40, 1769 (1964)

116. R.J. Donovan and D. Husain, Trans. Faraday Soc. 62, 1050 (1966).

117. M.I. Christie, R.S. Roy, and B.A. Thrush, Trans. Faraday Soc. 55, 1149 (1959).

118. G.K. Rollefson and F.E. Lindquist, J. Am. Chem. Soc. 52, 2793 (1930).

119. G.K. Rollefson and J.C. Potts, J. Chem. Phys. 1, 400 (1933).

120. L.J.E. Hofer and E.O. Wiig, J. Am. Chem. Soc. 67, 1441 (1945).

121. W.H. Rodebush and W.C. Klingelhofer, J.Am. Chem. Soc. 55, 130 (1933).

122. K.E. Russell and J. Simons, Proc. Roy. Soc. (London) A217, 271 (1953).

123. M.I. Christie, R.S. Roy, and B.A. Thrush, Trans. Faraday Soc. 55, 1139 (1959).

124. A.G. Sykes, Kinetics of Inorganic Reactions (Pergamon Press, New York, 1966).

125. G.B. Kistiakowsky, J. Am. Chem. Soc. 52, 102 (1930).

126. A.J. Allmand, Chem. Soc. Disc. 34 (1931).

127. C.R. Bailey and A.B.D. Cassie, Proc. Roy. Soc. (London) A145, 336 (1934)

128. P.G. Ashmore and J. Chanmugam, Trans. Faraday Soc. 49, 263 (1953).

129. G.L. Natanson, Acta Physicochim URSS 11, 521 (1939).

130. W.D. McGrath and R.G.W. Norrish, Z. Phys. Chem. 15, 245 (1958).

131. I. Welinsky and H.A. Taylor, J. Chem. Phys. 6, 466 (1938).

132. J.N. Pitts, Jr., J.D. Margerum, and W.E. McKee, ARS J. 1, 895 (1961).

133. P.A. Leighton, Photochemistry of Air Pollution (Academic Press, New York, 1961).

134. F.E. Blacet, T.C. Hall, Jr., and P.A. Leighton, J. Am. Chem. Soc. 84, 4011 (1962).

135. J.N. Pitts, Jr., J.H. Sharp, and S.I. Chan, J. Chem. Phys. 39, 238 (1963); 40, 3665 (1964).

136. H.W. Ford and S. Jaffe, J. Chem. Phys. 38, 2935 (1963).

137. F.J. Lipscomb, R.G.W. Norrish, and B.A. Thrush, Proc. Roy. Soc. (London) A233, 455 (1956).

138. N. Basco and R.G.W. Norrish, Can. J. Chem. 38, 1769 (1960).

139. P.P. Sorokin and J.R. Lankard, IBM J. Res. Develop. 10, 162 (1966).

140. M.A. Pollack, Appl. Phys. Letters 8, 237 (1966).

141. F.J. Wright, J. Phys. Chem. 64, 1648 (1960).

142. A.B. Callear, Proc. Roy. Soc. (London) A276, 401 (1963).

143. E.U. Condon and H. Odishaw, Handbook of Physics (McGraw-Hill, New York, 1958), pp. 7-52.

144. R.G.W. Norrish, Solvay Institute 12th Chemistry Conference, Energy Transfer in Gases, R. Stoops, Ed. (Interscience, New York, 1962), p. 99.

145. A.C.G. Mitchell and M.W. Zemansky, Resonance Radiation and Excited Atoms (Cambridge University Press, New York, 1961), pp. 99 and 160.

146. G.R. Simpson, Appl. Optics 3, 783 (1964).

147. R.C. Duncan, Z.J. Kiss, and H.R. Lewis, NASA Report N64-12567, 1963.

148. P.H. Kech, J.J. Redmann, C.E. White, and R.E. DeKinder, Appl. Optics 2, 827 (1963).